

Aus der Medizinischen Klinik und Poliklinik IV  
(Direktor: Prof. Dr. med. Reincke)  
Ludwig-Maximilians-Universität München  
Sektion für Rheumatologie und Klinische Immunologie  
Leiter: Prof. Dr. med. Hendrik Schulze-Koops

**Analysis of molecular mechanisms contributing to  
regulatory T cell phenotype: implications for  
rheumatoid arthritis**

Dissertation  
zum Erwerb des Doktorgrades der Naturwissenschaften (Dr. rer. nat.)  
an der Medizinischen Fakultät  
der Ludwig-Maximilians-Universität München

vorgelegt von  
**Sonja Haupt**  
aus Stuttgart – Bad Cannstatt

2015

**Gedruckt mit Genehmigung der Medizinischen Fakultät der Ludwig-  
Maximilians-Universität München**

Betreuerin:	PD Dr. rer. nat. Alla Skapenko
Zweitgutachter:	Prof. Dr. rer. nat. Ludger Klein
Dekan:	Prof. Dr. med. dent. Reinhard Hickel
Tag der mündlichen Prüfung:	13.04.2016

Teile dieser Arbeit wurden in folgenden Originalpublikationen veröffentlicht:

1. Qihui Zhou\*, **Sonja Haupt**\*, Johannes T. Kreuzer, Ariane Hammitzsch, Fabian Proft, Carla Neumann, Jan Leipe, Matthias Witt, Henrik Schulze-Koops, and Alla Skapenko

Decreased expression of miR-146a and miR-155 contributes to an abnormal Treg phenotype in patients with rheumatoid arthritis.

\*These authors contributed equally to this work

Ann Rheum Dis (2015) 74(6): 1265-74 (Zhou et al. 2015)

2. **Sonja Haupt**, Viktoria S. A. Söntgerath, Jan Leipe, Hendrik Schulze-Koops, and Alla Skapenko

Alternative promoter methylation regulates in a tight junction with Foxp3 transcription of *GARP*.

submitted

## Eidesstattliche Versicherung

Haupt, Sonja

---

Name, Vorname

Ich erkläre hiermit an Eides statt, dass ich die vorliegende Dissertation mit dem Thema

**Analysis of molecular mechanisms contributing to regulatory T cell phenotype:  
implications for rheumatoid arthritis**

selbständig verfasst, mich außer der angegebenen keiner weiteren Hilfsmittel bedient und alle Erkenntnisse, die aus dem Schrifttum ganz oder annähernd übernommen sind, als solche kenntlich gemacht und nach ihrer Herkunft unter Bezeichnung der Fundstelle einzeln nachgewiesen habe.

Ich erkläre des Weiteren, dass die hier vorgelegte Dissertation nicht in gleicher oder in ähnlicher Form bei einer anderen Stelle zur Erlangung eines akademischen Grades eingereicht wurde.

---

Ort, Datum

---

Unterschrift Doktorandin

---

## CONTENTS

<b>ABBREVIATIONS .....</b>	<b>3</b>
<b>SUMMARY .....</b>	<b>6</b>
<b>ZUSAMMENFASSUNG .....</b>	<b>8</b>
<b>1 INTRODUCTION .....</b>	<b>10</b>
1.1 T cells in the immune system.....	10
1.2 Regulatory T cells.....	12
1.3 Glycoprotein A repetitions predominant.....	14
1.4 Transcriptional regulation of gene expression in T cells .....	15
1.4.1 Foxp3 .....	16
1.4.2 NFAT family.....	17
1.4.3 NF- $\kappa$ B family .....	17
1.4.4 STAT family .....	18
1.4.5 MafF.....	18
1.5 Chromatin structure and chromatin remodeling.....	18
1.6 DNA methylation.....	19
1.7 Alternative promoter usage.....	20
1.8 MicroRNAs in regulation of gene expression.....	20
1.9 Rheumatoid arthritis.....	21
1.9.1 Disease characteristics, diagnostic criteria, and scoring of disease activity.....	21
1.9.2 RA pathogenesis.....	22
1.10 Objective of the thesis.....	25
<b>2 MATERIALS AND METHODS .....</b>	<b>26</b>
2.1 Materials .....	26
2.1.1 Reagents and cytokines .....	26
2.1.2 Antibodies .....	28
2.1.3 Ladders/Markers .....	30
2.1.4 Serum .....	31
2.1.5 Enzymes .....	31
2.1.6 Single nucleotide polymorphism (SNP) genotyping assays.....	31
2.1.7 TaqMan Gene Expression assays .....	32
2.1.8 Oligonucleotides .....	32
2.1.9 Kits, devices, and software.....	35
2.1.10 Buffers and solutions.....	37
2.2 Methods .....	40
2.2.1 Cell purification .....	40
2.2.2 Cell culture.....	43
2.2.3 Flow cytometry .....	44
2.2.4 Isolation of nucleic acids.....	45
2.2.5 Complementary DNA (cDNA) synthesis.....	46
2.2.6 Real-time PCR .....	46
2.2.7 5'Rapid Amplification of cDNA Ends (RACE).....	48
2.2.8 DNA amplification and purification.....	49
2.2.9 Cloning.....	50
2.2.10 Luciferase reporter assays .....	54
2.2.11 ChIP.....	57
2.2.12 Bisulfite DNA sequencing.....	60
2.2.13 DNA-protein binding assay.....	61
2.2.14 SDS-PAGE and Western blotting.....	63
2.2.15 Enzyme-linked immunosorbent assay (ELISA) .....	64
<b>3 RESULTS.....</b>	<b>65</b>
3.1 Characterization of molecular mechanisms contributing to the characteristic phenotype of Tregs .....	65

---

3.1.1	Analysis of GARP transcription.....	65
3.1.2	Analysis of MafF expression in Tconvs and MafF-mediated regulation of Foxp3.....	79
3.2	Characterization of molecular mechanisms regulating GARP expression and Treg function in RA.....	81
3.2.1	Influence of DNA methylation on GARP expression in RA.....	81
3.2.2	SNP frequencies in the GARP gene locus in patients with RA and HCs.....	84
3.2.3	Haplotype distribution in patients with RA and HCs.....	86
3.2.4	NF- $\kappa$ B activity and STAT1 expression and phosphorylation in Tregs from patients with RA.....	88
3.2.5	Increased expression of pro-inflammatory cytokines in Tregs from patients with RA.....	89
<b>4</b>	<b>DISCUSSION.....</b>	<b>91</b>
4.1	DNA methylation of alternative promoters and Foxp3 regulate GARP expression.....	91
4.1.1	Molecular mechanisms underlying GARP transcriptional regulation.....	91
4.1.2	Effect of TGF- $\beta$ on GARP expression.....	95
4.2	MafF expression in Tconvs and iTregs.....	96
4.3	GARP in RA.....	97
4.3.1	Diminished GARP expression in RA-Tregs correlates with DNA demethylation.....	97
4.3.2	SNP alleles in the GARP gene locus are associated with RA.....	98
4.4	Decreased expression of miR-146a in Tregs from patients with RA.....	99
	<b>BIBLIOGRAPHY.....</b>	<b>102</b>
	<b>ACKNOWLEDGEMENTS.....</b>	<b>121</b>

**ABBREVIATIONS**

ACPA	Anti-citrullinated protein antibodies
ACR	American College of Rheumatology
AMOTL2	Angiomotin like 2
Anti-CCP	Anti-cyclic citrullinated protein
APC	Antigen presenting cell
APS	Ammonium persulfate
bHLH	Basic helix-loop-helix
BLK	B lymphoid tyrosine kinase
bp	Base pair
BSA	Bovine serum albumin
bZIP	Basic leucine zipper
cAMP	Cyclic adenosine monophosphate
can	Canonical
CD	Cluster of differentiation
cDNA	Complementary DNA
cds	Coding sequence
ChIP	Chromatin Immunoprecipitation
CIA	Collagen-induced arthritis
CNS	Conserved non-coding sequence
Com	Complementary
CRP	C-reactive protein
CsA	Cyclosporin A
CTLA-4	Cytotoxic T lymphocyte-associated antigen 4
DAS28	Disease activity score in 28 joints
DC	Dendritic cell
DMEM	Dulbecco's Modified Eagle Medium
DMSO	Dimethyl sulfoxide
DNA	Deoxyribonucleic acid
DNMT	DNA methyltransferases
dNTP	Deoxyribonucleotide triphosphate
ds	Double-stranded
DTT	Dithiothreitol
<i>E.coli</i>	<i>Escherichia coli</i>
EDTA	Ethylenediaminetetraacetic acid
ELISA	Enzyme-linked immunosorbent assay
ESR	Erythrocyte sedimentation rate
EULAR	European League Against Rheumatism
FACS	Fluorescence activated cell sorting
FAM	Fluorescein amidite
FCS	Fetal calf serum
FITC	Fluorescein isothiocyanate
FLS	Fibroblast-like type B synoviocyte
For	Forward
Foxp3	Forkhead box P3
GARP	Glycoprotein A repetitions predominant

---

GATA	GATA-binding factor
gDNA	Genomic DNA
GSP	Gene specific primer
H3ac	Pan-acetylated histone H3
H3K4me3	Trimethylated lysine 4 at histone H3
H3K27me3	Trimethylated lysine 27 at histone H3
HC	Healthy control
HEPES	4-(2-hydroxyethyl)piperazin-1-ethanesulfonic acid
HLA	Human leukocyte antigen
IDO	Indoleamine 2,3-dioxygenase
IFN	Interferon
Ig	Immunoglobulin
I $\kappa$ B	Inhibitor of NF- $\kappa$ B proteins
IKK	I $\kappa$ B kinase
IL	Interleukin
Ion	Ionomycin
IPEX	Immunodeficiency, polyendocrinopathy, and enteropathy, X-linked syndrome
IPTG	Isopropyl $\beta$ -D-1-thiogalactopyranoside
IRAK	IL-1 receptor associated kinase
iTreg	Induced regulatory T cell
JAK	Janus kinase
kDa	Kilo Dalton
KDM5B	Lysine-specific demethylase 5B
KMT2A	Lysine N-methyltransferase 2A
LAG3	Lymphocyte activation protein 3
LB	Lysogeny broth
LD	Linkage disequilibrium
LRR	Leucine rich repeat
LTBP	Latent TGF- $\beta$ binding protein
MACS	Magnetic activated cell sorting
MafF	V-maf musculoaponeurotic fibrosarcoma oncogene homolog F
MBD	Methyl-CpG binding domain
MFI	Mean fluorescence intensity
MGB	Minor groove binder
MHC	Major histocompatibility complex
MLL	Mixed-lineage leukemia
miRNA	Micro RNA
mRNA	Messenger RNA
n.a.	Not applicable
n.d.	Not determined
NFAT	Nuclear factor of activated T cells
NF- $\kappa$ B	Nuclear factor kappa B
NFQ	Non-fluorescent quencher
NHS	Normal human serum
NK cells	Natural killer cells
nt	Nucleotide
PAGE	Polyacrylamide gel electrophoresis

---

PCR	Polymerase chain reaction
PBMC	Peripheral blood mononuclear cells
PBS	Phosphate buffered saline
PE	Phycoerythrin
PFA	Paraformaldehyde
PIC	Protease inhibitor cocktail
PIPES	Piperazine-N,N'-bis-2-ethanesulfonic acid
PMA	Phorbol myristate acetate
PMSF	Phenylmethylsulfonylfluorid
pTreg	Peripheral regulatory T cell
RA	Rheumatoid arthritis
RACE	Rapid amplification of cDNA ends
Rb1	Retinoblastoma 1
RbBP5	Retinoblastoma binding protein 5
Rev	Reverse
RF	Rheumatoid factor
RISC	RNA-induced silencing complex
RNA	Ribonucleic acid
RPMI	Roswell Park Memorial Institute
RXR	Retinoic X receptor
SAM	S-Adenosylmethionine
scr	Scrambled
SD	Standard deviation
SDS	Sodium dodecyl sulfate
SEM	Standard error of the mean
SH2	Src-homology 2
SJC28	Swollen joint count on 28 joints
SLE	Systemic lupus erythematosus
SNP	Single nucleotide polymorphism
S.O.C medium	Super Optimal Broth medium
STAT	Signal transducer and activator of transcription
TAE	Tris-Acetate-EDTA
Taq	<i>Thermus aquaticus</i>
Tconv	Conventional T cell
TCR	T cell receptor
TEMED	Tetramethylethylenediamine
TGF	Transforming growth factor
Th cell	T helper cell
TJC28	Tender joint count on 28 joints
TLR	Toll-like receptor
TNF	Tumor necrosis factor
TRAF	TNF receptor associated factor
Treg	Regulatory T cell
TSS	Transcription start site
tTreg	thymic regulatory T cell
UTR	Untranslated region
wt	wildtype
X-Gal	5-bromo-4-chloro-indolyl- $\beta$ -D-galactopyranoside

## SUMMARY

Regulatory T cells (Tregs) contribute to peripheral tolerance and prevent autoimmune diseases, such as rheumatoid arthritis (RA). Understanding the molecular mechanisms underlying Treg phenotype and function and delineating the factors that might lead to failure of Treg suppressive capacity may disclose important therapeutic strategies for autoimmune diseases.

In the first part of my thesis, I focused on the characterization of molecular mechanisms regulating expression of a Treg-specific surface molecule, glycoprotein A repetitions predominant (*GARP*). Two alternative promoters regulate *GARP* expression. I could show that transcription from the strong up-stream promoter was attenuated by binding of transcription factors to the intragenic down-stream promoter. DNA demethylation of several CpGs in the intragenic promoter ensured Treg-specific binding of the transcription factors, Foxp3, NFAT, and NF- $\kappa$ B. *GARP* expression upon T cell receptor stimulation was regulated by permissive histone modifications caused by replacement of the H3K4-specific demethylase, PLU-1, by Foxp3. *GARP* serves as a transporter of latent TGF- $\beta$ . TGF- $\beta$  together with retinoic acid is a critical factor for the generation of induced Tregs (iTregs). Recently, the transcription factor *MafF* was reported to be specifically downregulated during iTreg generation and upregulated during effector T cell differentiation. In this regard, I could demonstrate that overexpression of MafF during Treg induction attenuated TGF- $\beta$ /retinoic acid-mediated Foxp3 expression suggesting a negative function of MafF on the induction of iTregs.

In the second part of my thesis, molecular mechanisms underlying impaired function of Tregs in RA were analyzed. In collaborative work with my colleagues, we found that *GARP* expression was decreased in Tregs from RA patients. Interestingly, the down-stream promoter was demethylated in Tregs from RA patients compared to healthy controls suggesting that attenuation of the up-stream promoter might be a mechanism leading to the decreased *GARP* expression in RA. In addition, I found that three nucleotides in the *GARP* gene locus are highly polymorphic in patients with RA as compared to healthy controls. Thus, polymorphisms in the *GARP* gene locus might also contribute to decreased *GARP* expression in RA. Considering *GARP* function as a TGF- $\beta$  transporter, changes in the transcriptional control of the Treg-specific molecule, *GARP*, might contribute to the altered phenotype of Tregs in RA.

Beside Treg-specific *GARP* expression, miRNA has been reported to influence the Treg phenotype and function. It has been previously shown that miR-146a is highly expressed in

---

Tregs. We found that in Tregs from RA patients miR-146a expression was decreased. Decreased miR-146a expression coincided with altered expression of its target genes, STAT1, TRAF6, and IRAK1 which are involved in regulation of cytokine expression. When we analyzed the production of several cytokines by Tregs from RA patients we found an increase in the production of pro-inflammatory cytokines indicating a pro-inflammatory phenotype of Tregs in patients with RA. Thus, decreased miR-146a expression might also contribute to the altered phenotype of Tregs in RA.

In summary, in my PhD thesis I characterized Treg-specific *GARP* expression, as well as the effect of the transcription factor MafF on iTreg induction. Furthermore, I described several molecular mechanisms that might contribute to the impaired Treg phenotype and function in RA. These data might have important implications for understanding the pathogenesis of autoimmune diseases and might provide potential therapeutic targets.

## ZUSAMMENFASSUNG

Regulatorische T-Zellen (Tregs) haben eine entscheidende Rolle bei der peripheren Toleranz und bei der Unterdrückung von Autoimmunerkrankungen, wie rheumatoide Arthritis (RA). Analyse der molekularen Mechanismen, welche dem Phänotyp und der Funktion von Tregs zugrunde liegen und die eventuell zur Beeinträchtigung der Suppressivität von Tregs führen, könnten neue Therapieansätze für Autoimmunerkrankungen offenbaren.

Im ersten Teil meiner Doktorarbeit habe ich molekulare Mechanismen charakterisiert, welche die Expression des Treg-spezifische Oberflächenmoleküls glycoprotein A repetitions predominant (*GARP*) regulieren. Zwei alternative Promotoren regulieren die Expression von *GARP*. Ich konnte zeigen, dass die Transkription des starken vorgeschalteten Promotors, durch die Bindung von Transkriptionsfaktoren an den intragenischen Promotor, abgeschwächt wird. Die Demethylierung mehrerer CpGs im intragenischen Promotor gewährleistet die Treg-spezifische Bindung der Transkriptionsfaktoren Foxp3, NFAT und NF- $\kappa$ B. Der Austausch der H3K4-spezifischen Demethylase PLU-1 durch Foxp3 führte vermehrt zu permissiven Histonmodifikationen nach Aktivierung des T-Zell Rezeptors und zur Expression von *GARP*. *GARP* wurde als ein Transporter für latentes TGF- $\beta$  beschrieben. TGF- $\beta$  und Retinolsäure sind wichtige Faktoren zur Erzeugung von „induced“ Tregs (iTregs). Der Transkriptionsfaktor *MafF* wurde kürzlich untersucht und ist spezifisch während der Entwicklung von iTregs herunterreguliert und während der Effektor-T-Zell-Differenzierung hochreguliert. In diesem Zusammenhang konnte ich zeigen, dass die Überexpression von *MafF* während der iTreg-Induktion die TGF- $\beta$ /Retinolsäure-vermittelte Foxp3-Expression hemmt. Diese Ergebnisse lassen vermuten, dass *MafF* die Differenzierung von iTregs negativ beeinflusst.

Im zweiten Teil meiner Doktorarbeit habe ich molekulare Mechanismen untersucht, die zu einer Beeinträchtigung der Funktionalität von Tregs in RA führen. In Zusammenarbeit mit meinen Kollegen konnten wir zeigen, dass die Expression von *GARP* in Tregs von RA-Patienten vermindert ist. Der nachgeschaltete Promotor war interessanterweise in Tregs von RA-Patienten im Vergleich zu Tregs von gesunden Spendern demethyliert. Das deutet darauf hin, dass die Hemmung des vorgeschalteten Promotors eventuell einen Mechanismus darstellt, der zur Reduktion von *GARP* in RA führt. Außerdem habe ich drei Nukleotide im *GARP*-Genlokus gefunden, die hoch polymorph in Patienten mit RA im Vergleich zu gesunden Spendern sind. Diese Ergebnisse weisen darauf hin, dass Polymorphismen möglicherweise zur Verminderung

---

der *GARP*-Expression in RA beitragen. Da *GARP* ein TGF- $\beta$ -Transporter ist, könnten Veränderungen in der Expression des Treg-spezifischen Moleküls am abgeänderten Treg-Phänotyp in RA mitwirken.

Außer der Expression von *GARP* beeinflusst auch die Regulation durch miRNAs den Phänotyp und die Funktion der Tregs. Für miR-146a konnte bereits gezeigt werden, dass sie in Tregs hochreguliert ist. In diesem Zusammenhang konnten wir zeigen, dass die Expression von miR-146a in Tregs von RA-Patienten vermindert ist. Die Reduktion von miR-146a traten zusammen mit einer veränderten Expression ihrer Zielgene *STAT1*, *TRAF6* und *IRAK1* auf, welche alle in die Expression von Zytokinen involviert sind. Wir konnten zeigen, dass Tregs von RA-Patienten mehr Zytokine produzierten als die von gesunden Spendern. Tregs von RA-Patienten wiesen somit einen pro-inflammatorischen Phänotyp auf. Folglich beeinflusst die verminderte Expression von miR-146a auch den Phänotyp von Tregs in RA.

Zusammenfassend konnte ich in meiner Doktorarbeit die Treg-spezifische *GARP*-Expression charakterisieren, sowie den Effekt des Transkriptionsfaktors MafF auf die iTreg-Induktion beschreiben. Außerdem habe ich mehrere molekulare Mechanismen beschrieben, die eventuell eine Rolle für die verminderte Funktion und den veränderten Phänotyp von Tregs in RA spielen. Diese Daten sind wichtige Erkenntnisse für das Verständnis der Pathogenese von Autoimmunerkrankungen und bieten möglicherweise neue therapeutische Ansätze.

## 1 INTRODUCTION

### 1.1 T cells in the immune system

The immune system has evolved to provide rapid and specific means for protecting hosts against viral, bacterial, fungal, or parasitic pathogens experienced over a lifetime (Alberts et al. 2002). Two types of immune response, innate and adaptive, interact cooperatively to assure host defense. The innate immunity establishes the first line of defense that is based on the action of macrophages and granulocytes. It is non-specific and short-lasting, but acts immediately after pathogen invasion and activates the later-acting adaptive immune response mainly executed by lymphocytes providing specific and long-lasting protection against pathogens (Janeway et al. 2001). Lymphocytes are found in the circulation, in central lymphoid organs and tissues, such as spleen, tonsils, and lymph nodes. Thymus-derived lymphocytes (T cells) react directly against a foreign antigen that is presented to them on the surface of antigen-presenting cells (APCs). Dendritic cells (DCs) are the most effective APCs that can activate naïve T cells. In addition, macrophages are not as effective in presenting antigens to naïve T cells, but they are able to activate memory T cells. Upon antigen recognition, naïve T cells mature into effector cells and induce either cell-mediated immune responses initiated by cytotoxic T cells or humoral immune responses mediated by bone marrow-derived lymphocytes (B cells). The primary lymphoid organ indispensable for T cell development is the thymus. It provides the suitable microenvironment with specific combination of stromal cells, cytokines and chemokines to generate functional T cells from precursor cells (thymocytes) (Luckheeram et al. 2012). The T cell receptor (TCR) gene rearrangement and thymocyte selection are the critical steps in the development of mature T cells capable of recognizing an infinite range of antigens. First, T cells that are capable of interacting with major histocompatibility complex (MHC) molecules are selected by positive selection. Only those thymocytes that interact with MHC appropriately (i.e. not too strongly or too weakly) will receive a "survival signal". Subsequently, negative selection removes thymocytes that are capable of strongly binding with "self" MHC peptides thereby removing potential autoreactive T cells (Daniels et al. 2006; Klein et al. 2009).

TCR constitutes of  $\alpha\beta$ - or  $\gamma\delta$ -chains bonded with five CD3 (CD, cluster of differentiation) subunits ( $\gamma$ ,  $\delta$ ,  $\mu$ ,  $\pi$ , and  $\epsilon$ ). The TCR interacts with antigen-MHC complexes and mediates T cell activation signals, such as nuclear factor of activated T cells (NFAT) signaling or nuclear factor kappa B (NF- $\kappa$ B) activation (Shaw et al. 1988; Thaker et al. 2015). T cells can be distinguished

according to specific surface molecules. The precursors are CD4 and CD8 double-positive and differentiate into mature T cell subtypes (Luckheeram et al. 2012). Based on the interaction of the TCR of double-positive cells with MHC class I or II molecules, two subtypes of T cells can develop. CD8 T cells recognize endogenously synthesized antigens (such as viruses or tumor peptides) presented by MHC class I molecules and differentiate into cytotoxic effector T cells that can kill infected cells.

CD4 T helper (Th) cells interact with MHC class II molecules presenting extracellular antigen peptides captured by professional APCs. CD4 Th cells carry out a variety of functions, ranging from activation of the cells of the innate immune system, B cells, cytotoxic T cells, as well as non-immune cells, and also play a critical role in the suppression of the immune reaction (Zhu et al. 2010). Continuing studies identified several subtypes of CD4 Th cells, such as conventional T cells (Tconvs) and regulatory T cells (Tregs). The differentiation of the lineages depends on the complex network of cytokine milieu of the microenvironment, concentration of antigens, type of APCs, costimulatory molecules, and consequent transcription factor production and epigenetic modifications. The main co-stimulatory receptor is CD28 which is expressed on all naïve T cells. Ligands of CD28 on DCs are CD80 (B7-1) and CD86 (B7-2) which are upregulated upon activation (Acuto et al. 2003). The initial source of cytokines is from APCs and innate immune cells. Subsequently, some cytokines are produced by T cells in an autocrine or paracrine manner. Tconvs can be further subdivided. Th1 and Th2 cells are known since 1986 when they were firstly described by Coffman and Mosmann (Mosmann et al. 1986). Th1 cells play a critical role in the defense against intracellular pathogens such as bacteria or protozoa (Annunziato et al. 2009). Th1 cells mainly produce high amounts of interferon (IFN)- $\gamma$ , interleukin (IL)-2, lymphotoxin- $\alpha$ , and tumor necrosis factor (TNF). The master regulator of Th1 differentiation, the T-box transcription factor, was found to be mainly dependent on signal transducer and activator of transcription (STAT)-1, which is activated by IFN- $\gamma$  (Afkarian et al. 2002; Lighvani et al. 2001). Th2 cell function is important for humoral immune responses to infections with helminthes (Annunziato et al. 2009). Signature cytokines are IL-4, IL-5, and IL-13 (Abbas et al. 1996; Annunziato et al. 2009; Mosmann et al. 1986). IL-4 upregulates the Th2 master transcription factor, GATA binding factor (GATA)-3 (Kaplan et al. 1996; Zhu et al. 2001). IL-6 plays a role in Th2 differentiation by inhibiting the Th1 lineage through IL-6-induced upregulation of suppressor of cytokine signaling 1 expression which interferes with STAT-1 activation downstream to IFN- $\gamma$  signaling (Diehl et al. 2000; Diehl et al. 2002). Th17 cells are

characterized by the production of the signature cytokines IL-17A and IL-17F (Wei et al. 2007; Wilson et al. 2007). IL-1 $\beta$ , IL-6, IL-21, IL-23, and transforming growth factor (TGF)- $\beta$  are the major signaling cytokines involved in Th17 differentiation, and retinoic acid receptor-related orphan receptor gamma-t is the master regulator (Acosta-Rodriguez et al. 2007; Bettelli et al. 2006; Volpe et al. 2009; Yang et al. 2008).

## 1.2 Regulatory T cells

Positive and negative selection of T cells in the thymus is necessary to eliminate harmful autoreactive T cells however this process is not error-free. Some cells escape selection in the thymus. Evading autoreactive cells in the periphery have the potential to induce autoimmune diseases, such as rheumatoid arthritis (RA). To circumvent autoimmune reactions, several additional mechanisms for peripheral tolerance developed, such as Treg-mediated suppression.

In the eighties, Shimon Sakaguchi firstly demonstrated the existence of Tregs and described their pivotal role in maintaining peripheral tolerance and preventing autoimmune diseases (Sakaguchi et al. 1985). Tregs constitute 5-10% of the CD4 Th cell population in the peripheral blood of healthy individuals. They express several Treg-specific molecules, like the alpha-chain of the IL-2 receptor (CD25) or the master transcription factor forkhead box P3 (Foxp3). *Scurfy* mice or patients with the immunodeficiency, polyendocrinopathy, and enteropathy, X-linked (IPEX) syndrome lack detectable Tregs. Both have mutations in the *Foxp3* gene. Because *Foxp3* is encoded on the X-chromosome, the affected population is mainly males. It was shown that the *scurfy* phenotype can be rescued by the transfer of CD25+ Tregs (Fontenot et al. 2003). Thus, they can ameliorate the symptoms of autoimmune or inflammatory reactions (Frey et al. 2005; Read et al. 2000). Furthermore, Treg suppress immune responses against allergens, tumor cells, and infections (Belkaid 2008; Chatila 2005; Knutson et al. 2007). Tregs can be discriminated according to the anatomical location of their differentiation (Abbas et al. 2013). Foxp3+ Tregs that differentiate in the thymus are called tTregs. They can differentiate in the periphery and are named pTregs. Additionally, Tregs that are induced *in vitro* are referred to induced Tregs (iTregs). In this regard, TGF- $\beta$  plays an important role in inducing Tregs (Huter et al. 2008).

Tregs can exert their suppressive function mainly on CD4 and CD8 T cells, but are also able to control B cells, natural killer (NK) cells, DCs and other APCs (Schmidt et al. 2012). Treg-mediated suppression involves cell contact and soluble factors. For instance, the co-inhibitory molecule cytotoxic T lymphocyte-associated antigen 4 (CTLA-4) is widely expressed on Tregs

and leads to downregulation of CD80/CD86 on APCs, thereby inhibiting Tconv activation by APCs (Takahashi et al. 2000; Wing et al. 2008). Additionally, Tregs can target DCs via CTLA-4 or lymphocyte activation protein 3 (LAG3). CTLA-4-CD80/CD86 interaction increases indolamine 2,3-dioxygenase (IDO) expression in DCs (Puccetti et al. 2007). This enzyme catalyzes the degradation of tryptophan to kynurenine, leading to starvation of Tconvs and to direct cell cycle arrest.

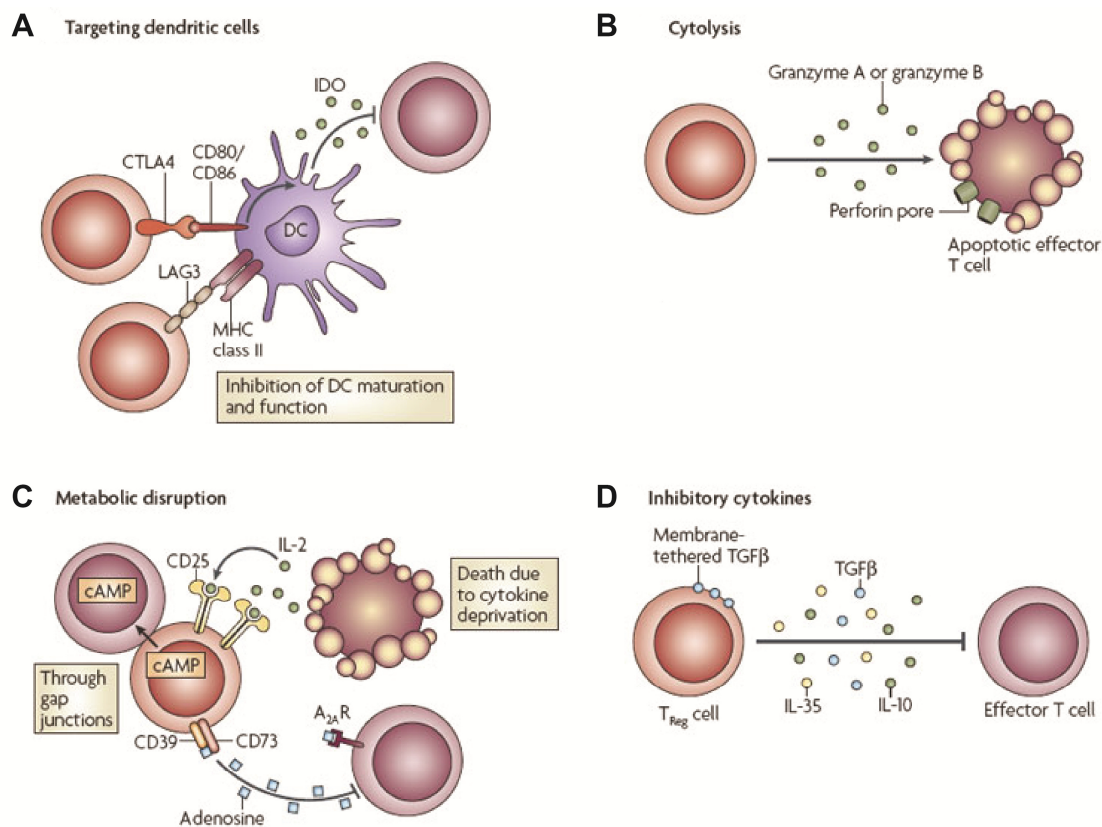


**Figure 1 Mechanisms of Treg suppression.** (A) CTLA-4 or LAG3 on Treg can bind to CD80/CD86 or MHCII on DCs, respectively. Thereby, the enzyme IDO gets expressed which upregulates immunosuppressive substances. (B) Expression of perforin and granzyme A or B by Tregs leads to cell lysis and apoptosis of the target cell. (C) Tregs express CD39/CD73 on the surface. This results in the production of extracellular adenosine. Gap junctions can transport cyclic adenosine monophosphate (cAMP) directly into the target cell. This disrupts the metabolism. Furthermore, CD25 can capture IL-2 on the surface of Tregs making it unavailable to other T cells. (D) Tregs can produce inhibitory cytokines like IL-35, IL-10, and TGF- $\beta$ . Adapted from (Vignali et al. 2008).

Moreover, Tregs can induce apoptosis of target cells by a cell-contact dependent mechanism. Upon activation, Tregs are able to induce the serine protease granzyme A or B and kill target cells in a perforin-dependent manner (Grossman et al. 2004). Additionally, granzyme B-deficient Tregs have impaired suppressive activity *in vitro* (Gondek et al. 2005). Furthermore, metabolic disruption of effector T cells is mediated by the expression of the ectoenzymes CD39 and CD73.

Those factors enable Tregs to catalyze pericellular adenosine triphosphate and adenosine diphosphate to anti-inflammatory adenosine (Bopp et al. 2007; Borsellino et al. 2007; Kobie et al. 2006). In contrast, importance of IL-2 deprivation by Tregs via their high CD25 expression remains controversial (Fontenot et al. 2005; Pandiyan et al. 2007).

Another mechanism is the suppression via inhibitory cytokines, like IL-35, IL-10, and TGF $\beta$ . IL-35 was recently implicated in Treg suppression and was shown to directly inhibit proliferation of Tconvs (Collison et al. 2007). There are several lines of evidence that IL-10 plays a role in Treg-mediated suppression of intestinal and pulmonary inflammation (Asseman et al. 1999; Asseman et al. 2003; Rubtsov et al. 2008). Blocking IL-10 or usage of IL-10-deficient Tregs abrogates the protective effect *in vivo*. In contrast to this, *in vitro* studies using neutralizing antibodies to IL-10 or TGF- $\beta$  suggested that these cytokines may not be essential for Treg suppression (Jonuleit et al. 2001). Interestingly, TGF- $\beta$  receptor-deficient mice developed T cell-mediated autoimmunity within several weeks after birth (Li et al. 2006). The relevance of TGF- $\beta$ -mediated suppression can be illustrated by different diseases. For instance, Tregs can inhibit NK cells and Tconvs via TGF- $\beta$  in the tumor microenvironment (Li et al. 2007; Strauss et al. 2007). In addition, TGF- $\beta$  is critical for Treg-mediated suppression of CD8 T cells in a model of type 1 diabetes (Green et al. 2003). If TGF- $\beta$  plays a pivotal role in Treg suppression, it is surprising that Treg function relies on cell-cell contact. TGF- $\beta$  as a soluble and secreted cytokine should not depend on cell-cell contact. Remarkably, Th clones that were inhibited by Tregs showed the same transcriptional signature as those that were treated with recombinant TGF- $\beta$  (Stockis et al. 2009b). However, it was not possible to detect active, soluble TGF- $\beta$  in the supernatant of the co-cultures. One explanation is that TGF- $\beta$  is secreted in a latent form from Tregs and is bound to the Treg membrane by the glycoprotein A repetitions predominant (GARP) (Stockis et al. 2009a). Interestingly, GARP is another Treg-specific surface molecule that is required for the expression of the TGF- $\beta$  latency-associated peptide and both molecules bind to each other on the Treg surface (Stockis et al. 2009a; Tran et al. 2009). Furthermore, it represents a latent TGF- $\beta$  binding protein (LTBP) that provides a cell surface platform for  $\alpha_v$  integrin-dependent TGF- $\beta$  activation (Wang et al. 2012a).

### 1.3 Glycoprotein A repetitions predominant

Recently, a novel Treg-characteristic surface molecule, *GARP* or *leucine rich repeat containing protein 32 (LRRC32)*, has been described (Tran et al. 2009). GARP was firstly defined in several

genetic alterations associated with different malignancies (Ollendorff et al. 1994; Ollendorff et al. 1992). The human *GARP* gene was mapped to the chromosomal region *11q13.5-14* and consists of three exons. The homologous mouse gene has been found in the *7F* chromosomal region (Ollendorff et al. 1992; Roubin et al. 1996). The *GARP* gene locus possesses two alternative promoters which lead to the production of two different transcript variants. The protein is encoded in the last two exons and the coding sequence is highly conserved between species. The 80 kDa transmembrane protein consists of 662 amino acids and shares over 80% identity between human and mouse. The extracellular region contains 20 leucine rich repeats (LRRs), followed by a hydrophobic transmembrane domain and a 15-residue C-terminal cytoplasmic domain (Ollendorff et al. 1994). The extracellular LRRs form a horseshoe-like domain. The N-terminal signal peptide of the protein needs to be cleaved for efficient translocation of the mature protein to the cell surface (Chan et al. 2011). The LRR-family of proteins exhibits evolutionary similarities to Toll-like receptors (TLRs) (Bottcher et al. 2004). Expression of *Garp* was detected in various areas in the mid-gestation mouse embryo and in several adult tissues. More recently, GARP protein expression was detected in human megakaryocytes/platelets and activated Foxp3+ Tregs (Macaulay et al. 2007; Tran et al. 2009). The regulatory mechanisms controlling restricted *GARP* expression in Tregs are still not completely understood. *GARP* is upregulated in response to TCR stimulation on Tregs and lasts only a short time (Tran et al. 2009; Wang et al. 2009; Zhou et al. 2013b). Interestingly, murine *Garp* expression can also be induced by culture of Tregs only in the presence of IL-2 or IL-4 (Edwards et al. 2013). Expression of *GARP* is not dependent on TGF- $\beta$  since TGF- $\beta$ -deficient Tregs retain their *GARP* expression. Furthermore, *GARP* expression is post-transcriptionally down-regulated by miR-142-3p despite sustained TCR signaling (Zhou et al. 2013b). It was shown that Foxp3 expression is necessary, but not sufficient to drive *GARP* expression (Tran et al. 2009; Wang et al. 2009). Moreover, epigenetic regulation was implicated in *GARP* expression since a Treg-specific hypomethylated region in intron 1 was identified (Schmidl et al. 2009).

#### **1.4 Transcriptional regulation of gene expression in T cells**

DNA is normally wrapped around a set of eight histone molecules in the nucleosome (Kornberg 2007). Coiling of DNA into condensed chromatin leads to transcriptionally inactive chromatin. For active gene transcription, nucleosomes have to be removed from promoter regions to allow the binding of the components of the transcriptional machinery. The RNA polymerase II

transcriptional complex is responsible for all messenger RNA (mRNA) synthesis in eukaryotes (Kornberg 2007). This complex comprises six proteins: polymerase II and five general transcription factors known as transcription factor IIB, -D, -E, -F, and -H. Polymerase II is capable of unwinding DNA, synthesizing RNA, and rewinding DNA. However, it cannot recognize promoter regions or initiate transcription. Thus, general transcription factors are essential to fulfill these functions. Promoter-specific activator proteins are generally sequence-specific DNA binding proteins that regulate specific gene expression by directing the pre-initiation complex to the transcription start site (TSS) of the gene (Green 2005). RNA polymerase II is recruited and moves along DNA producing the RNA transcript (elongation). In addition, post-transcriptional events can regulate the abundance of transcripts.

Transcription factors are specific transcriptional activators or repressors. Binding of transcription factors is often cell type specific and modulates the transcription levels of the genes they act on. In this regard, the master transcription factor of Tregs, Foxp3, is necessary to develop the Treg-specific gene expression signature. Additionally, changes in gene expression represent the culmination of the TCR signaling pathway which is necessary for differentiation and proliferation of the T cells and the ability to produce effector cytokines. Furthermore, interaction of cytokines with the respective receptor can induce gene expression in T cells. Transcription factors that have a particular role in TCR- or cytokine-stimulated changes in gene expression belong to the NFAT, NF- $\kappa$ B, or STAT families. Moreover, the V-maf musculoaponeurotic fibrosarcoma oncogene homolog F (MafF) was also recently implicated in T cell signaling.

#### 1.4.1 Foxp3

Foxp3 is known as the “master regulator” of the Treg lineage. Induction of the Foxp3 gene in normal naïve T cells converts them to Treg-like cells with some suppressive functions, indicating that Foxp3 is likely to play a key role in controlling expression of critical suppression-mediating molecules (Hori et al. 2003). Thus, Foxp3 was often described as the lineage-specification factor for Treg development. The *Foxp3* gene consists of 11 coding and three non-coding exons (Lozano et al. 2013). Foxp3 can act as transcriptional repressor or activator. This dual function is possible mainly through interaction of Foxp3 with a variety of binding partners. The N-terminal domain with two proline-rich regions interacts with factors that are involved in transcriptional suppression. Factors that bind to this region are the Ikaros family member Eos, chromatin remodeling factors, and c-Rel. Foxp3 also contains a Zinc finger and a leucine zipper motif. The

latter can form homodimers or binds to histone H1.5 that is located in the *IL-2* or *CTLA-4* gene loci. The C-terminus of the protein contains a forkhead domain that is responsible for nuclear localization, DNA binding, and interaction with NFAT. It is plausible that the ability of Foxp3 to bind to this vast quantity of factors might guarantee its multifaceted way of regulation.

#### 1.4.2 NFAT family

The NFAT family of transcription factors comprises five proteins that are evolutionary related to the Rel/NF- $\kappa$ B family, namely NFAT1, -2, -3, -4, and -5 (Chytil et al. 1996). The phosphorylated form of NFAT is usually localized in the cytoplasm (Hogan et al. 2003). Upon TCR stimulation intracellular calcium stores are depleted and calmodulin-dependent enzymes like calcineurin get activated. Calcineurin dephosphorylates NFAT proteins leading to their nuclear translocation and target gene transcription. Target genes of NFAT include *Foxp3*, *CD25*, and *Ctla-4* (Wu et al. 2006). Interestingly, NFAT can regulate the transcription of Foxp3 in Tregs however it has also been identified as interaction partner of Foxp3 (Bettelli et al. 2005; Tone et al. 2008; Wu et al. 2006).

#### 1.4.3 NF- $\kappa$ B family

The NF- $\kappa$ B family of proteins encompasses five members: p65, RelB, c-Rel, p50, and p52. They can form a variety of homo- and heterodimers that activate different genes (Li et al. 2002b). The most prevalent form is the heterodimer p65 and p50. Normally, NF- $\kappa$ B resides in its inactive form in the cytoplasm bound to the inhibitor of NF- $\kappa$ B proteins (I $\kappa$ B). Besides TCR stimulation, TNF, IL-17 or IL-1 $\beta$  can activate the I $\kappa$ B kinase (IKK) complex that phosphorylates I $\kappa$ B and leads to the degradation of I $\kappa$ B. Subsequently, NF- $\kappa$ B can translocate to the nucleus leading to the transcription of genes containing the consensus  $\kappa$ B sequence. Genes with  $\kappa$ B sites include cytokines and chemokines (TNF, IL-1 $\beta$ , IL-2, IL-6, macrophage inflammatory proteins), adhesion molecules, anti-apoptosis genes, cell proliferation associated genes, matrix metalloproteinases (Pahl 1999). The NF- $\kappa$ B subunit p65 can be inhibited by the NF- $\kappa$ B activation inhibitor, JSH-23, which prevents the binding to DNA (Shin et al. 2004). NF- $\kappa$ B is important for thymic Foxp3 induction and the subunit c-Rel directly binds to the *Foxp3* locus thereby initiating chromatin opening (Isomura et al. 2009; Long et al. 2009). Furthermore, NF- $\kappa$ B was found to interact with Foxp3 to regulate the transcriptional program of Tregs (Bettelli et al. 2005).

#### 1.4.4 STAT family

The STAT family of proteins includes STAT1, -2, -3, -4, -5, and -6. It has critical roles in cellular responses to cytokines. STAT proteins exhibit preference for specific cytokine receptors, for example STAT1 shows preference for interferons. Signaling through the cytokine receptor leads to activation of receptor-associated Janus kinases (JAKs) and the phosphorylation of residues on the receptor. This creates sites for interaction with proteins that contain phosphotyrosine-binding src-homology 2 (SH2) domains. STAT proteins contain SH2 domains and bind to the receptor and are themselves tyrosine-phosphorylated by JAKs. Thus, STAT proteins can dimerize and translocate to the nucleus where they can activate target genes. STAT1-deficient mice showed reduced numbers and functional impairment of Tregs (Nishibori et al. 2004). In addition, STAT1-deficient Tregs failed to control allograft rejection *in vivo* (Wei et al. 2010).

#### 1.4.5 MafF

The basic leucine zipper (bZIP) transcription factors of the Maf oncogene family have a variety of functions in T cell processes. The C-terminal bZIP domain mediates DNA binding and dimerization (Kataoka et al. 1996). Small Maf proteins include MafF, MafG, and MafK and they lack the N-terminal transactivation domain. Expression of *MafF*, has been recently reported to be down-regulated during the development of iTregs (Prots et al. 2011). Recent studies could show that pro-inflammatory cytokines like TNF and IL-1 $\beta$  induce *MafF* transcript levels (Massrieh et al. 2006). These results might suggest a role for MafF during effector T cell differentiation whereas it seems to negatively influence Treg induction. In addition, MafF was linked to type-1 diabetes mellitus pathology suggesting that MafF could be a useful target for autoimmune therapy (Menegazzo et al. 2012).

### 1.5 Chromatin structure and chromatin remodeling

Apart from their role in DNA packaging, tightly condensed chromatin structures provide a barrier to active gene transcription (Roeder 2005). Histone modifications include acetylation, methylation, ubiquitination, and phosphorylation at different amino acids on the N-terminal histone tails. Histone tail modifications act dynamically and in combination to open up regions for active gene transcription by permitting binding of transcription factors or condensing chromatin to an inactive state (Grunstein 1997). Histone acetylases generally activate, whereas

histone deacetylases repress gene expression. In addition, histone methyltransferases or -demethylases can be associated with both, repressive and permissive marks. Examples for permissive modifications are trimethylated lysine 4 at histone H3 (H3K4me3) or pan-acetylated histone H3 (H3ac) (Cervoni et al. 2001; Ooi et al. 2007). In contrast, trimethylated lysine 27 at histone H3 (H3K27me3) is often enriched at inactive chromatin regions (Wei et al. 2009).

In humans there are at least eight histone lysine methyltransferases with specificity for H3K4. These include the *mixed-lineage leukemia (MLL)* genes, *MLL1-5*, *hSET1a/b*, and *ASH1*. One member, the MLL1 which is also called lysine N-methyltransferase 2A (KMT2A) mediates H3K4me3 and associates with histone acetyltransferases, thereby marking sites of active gene transcription (Milne et al. 2002; Zhao et al. 2013). Recently, MLL1 was found to associate with Foxp3 and regulates Foxp3-activated genes by inducing H3K4me3 (Kato et al. 2011). Interestingly, Foxp3-binding sites were decorated with MLL1 and other complex members, such as retinoblastoma binding protein 5 (RbBP5), before Foxp3 induction. The JARID family member PLU-1, or lysine-specific demethylase 5B (KDM5B) is associated with MLL1 and facilitates steady-state demethylation of H3K4. It was demonstrated that Foxp3 replaces PLU-1, thereby shifting the balance in favor of H3K4 methylation. Another interesting aspect of MLL1 is the fact that it contains a CpG-interacting CXXC domain that may couple the H3K4 methylation reaction to un-methylated DNA (Cierpicki et al. 2010).

## 1.6 DNA methylation

DNA methylation is a process that involves the addition of a methyl group to the fifth carbon of a cytosine residue. DNA methylation represses transcription directly by inhibiting binding of transcription factors and indirectly by recruiting methyl-CpG-binding domain (MBD) protein family members with chromatin remodeling activities. Thus, the MBD protein family is the linkage between histone modifications and DNA methylation (Hashimoto et al. 2010). DNA methylation is established and maintained by two DNA methyltransferase (DNMT) families, the so-called ‘*de novo*’ methyltransferases of the Dnmt3 family and the ‘maintenance’ methyltransferase Dnmt1. Several lines of evidence indicate that members of the Dnmt3 family can act as a sensor for H3K4 methylation and induce *de novo* DNA methylation when H3K4 methylation is absent. Genome-wide methylation analyses revealed hypomethylated regions in Treg-signature genes in Tregs. Additionally, those regions were associated with Foxp3 binding (Zhang et al. 2013). The Treg-specific hypomethylation pattern is involved in Treg-specific gene

expression, lineage stability, and full suppressive activity (Morikawa et al. 2014; Ohkura et al. 2012).

### **1.7 Alternative promoter usage**

The usage of alternative promoters is a mechanism to create flexibility and diversity in the complex patterns of gene expression. Multiple promoters or TSS are apparently frequently used to influence transcription in diverse ways. The level of transcription initiation can vary between alternative promoters. Additionally, the turnover or translation efficiency of mRNA isoforms with different leader exons can differ. Alternative promoters were reported to have different tissue specificity and react differently to some signals. Finally, alternative promoter usage can lead to the generation of protein isoforms differing at the amino terminus (Ayoubi et al. 1996). Characteristic features of alternative promoters are CpG islands which are short genomic regions with approximately 10 times higher CpG frequencies and higher GC content than the genomic average (Bird 2011). Since CpG islands are associated with regulation of gene expression, it could be expected that they display tissue-specific DNA methylation patterns. Interestingly, CpG islands associated with TSS rarely show methylation (Maunakea et al. 2010). The gene body which is defined as the region past the first exon plays an important role in tissue- or cell-specific gene expression (Laurent et al. 2010). DNA methylation of intragenic promoters was found to be associated with higher levels of gene expression in rapid dividing cells such as hematopoietic cells (Aran et al. 2011; Ball et al. 2009). Most gene bodies are CpG-poor and alternative TSS located down-stream of the main promoter frequently lack CpG islands. However, methylation of CpGs of an intragenic, alternative TSS blocks initiation at this element, whereas it allows the transcriptional elongation of the transcript initiated by the up-stream promoter. Therefore, DNA methylation was suggested to be a mechanism for controlling alternative promoter usage (Maunakea et al. 2010).

### **1.8 MicroRNAs in regulation of gene expression**

In contrast to the 5' transcriptional regulation of expression, microRNAs (miRNAs) that bind to the 3' untranslated region (UTR) represent a mechanism of post-transcriptional modulation. MiRNAs are endogenous approximately 22 nucleotide (nt) long RNAs that are involved in the posttranscriptional cleavage of mRNAs or translational repression (Bartel 2004). They are complementary to sites in the 3' UTR of the respective mRNA. Moreover, about a quarter of all

miRNAs are encoded in introns, suggesting that they are not transcribed from their own promoters but are instead processed from the introns. This mechanism is a convenient system for coordinate expression of a miRNA and a protein. Other miRNAs are clustered and are transcribed as a multi-cistronic primary transcript. MiRNA maturation involves nuclear cleavage of the pri-miRNA, which liberates the 60-70 nt long pre-miRNA by the Drosha RNase III endonuclease. Next, the miRNA is processed in the cytoplasm by the RNase III endonuclease Dicer into around 22 nt long double-stranded (ds) fragments. After separation via helicases, the single-stranded RNAs become incorporated into the RNA-induced silencing complex (RISC). Subsequently, the RISC/miRNA complex can down-regulate gene expression by either mRNA cleavage or translational repression depending on the degree of complementarity of the miRNA and the mRNA. Furthermore, the involvement of miRNAs in fine-tuning of gene expression makes them promising new targets for disease treatment.

## **1.9 Rheumatoid arthritis**

### **1.9.1 Disease characteristics, diagnostic criteria, and scoring of disease activity**

RA is a systemic autoimmune disease affecting approximately 1% of people in the developed world (Alamanos et al. 2005). The incidence is higher in women than in men, the ratio varies between 2:1 and 3:1. The age of disease onset peaks around the fifth decade of life. Furthermore, RA is described by synovial inflammation leading to joint damage and bone destruction. It can cause severe disability and increases mortality. Inflammatory cells such as T cells, B cells, and macrophages accumulate in the inflamed joints which can lead to persistent synovitis and cartilage destruction (Bettelli et al. 2007). The autoantigens are still not identified for RA however the main cause of the autoimmune condition seems to be the failure in the maintenance of immunological self-tolerance. Plasmatic cells infiltrating the joint produce autoantibodies recognizing the Fc portion of Immunoglobulin G (IgG). Those autoantibodies are named rheumatoid factor (RF). In some RA patients, lymphocytes infiltrating the synovial tissue can accumulate in follicular structures and form germinal centers (Weyand et al 2003). In addition, RF has been detected in germinal center cells (Mellors et al 1959). The IgM class is the most significant type of RF in regards to RA that emerges in around 70-80% of patients. It has been demonstrated that RA-specific autoantibodies recognize citrulline-containing peptides/proteins as common antigenic entity, and they are collectively termed as anti-citrullinated protein antibodies (ACPAs) (Girbal-Neuhauser et al. 1999; Schellekens et al. 1998; Sebbag et al. 1995).

In 2010, new classification criteria for patients with early RA were introduced by the American College of Rheumatology (ACR) and the European League Against Rheumatism (EULAR) (Aletaha et al. 2010). This classification aimed to allow earlier diagnosis, treatment and inclusion in clinical trials. Patients with at least one swollen joint and the presence of synovitis that cannot be explained by any other disorder such as systemic lupus erythematosus (SLE), psoriatic arthritis, gout etc., can be included. The 2010 criteria include tender and swollen joint count, acute phase reactants, ACPA, RF, and symptom duration. Acute phase reactants refer to the level of C-reactive protein (CRP) and erythrocyte sedimentation rate (ESR). The clinical and diagnostic parameters are then combined into a score ranging from zero to ten. Classification as definite RA is based on the achievement of a total score of at least six.

The disease activity score in 28 joints (DAS28) has been developed as a quantitative index for the measurement of RA disease activity (Fransen et al. 2006; van Riel 2014). The DAS28 combines information from tender and swollen joints, acute phase reactant, and patient self-report of general health. The final score is calculated from all four parameters and can range from zero to ten. Cut points were developed to classify patients in remission, as well as low, moderate and high disease activity. A DAS28 < 2.6 corresponds with being in remission. Additionally, patients with low disease activity reached a DAS28 between 2.6 and 3.2. Patients who reached a score between 3.2 and 5.1 are termed as patients with moderate activity and a DAS28 higher than 5.1 indicates high disease activity.

### 1.9.2 RA pathogenesis

The etiology of RA is unknown, however many studies suggest that a combination of environmental and genetic factors is responsible. The structure of class II MHC molecules in APCs is associated with increased risk of RA. More than 80% of patients carry the epitope of the *human leukocyte antigen (HLA)-DRB1\*04* cluster (Smolen et al. 2007). Other RA-associated loci include *protein tyrosine phosphatase non-receptor type 22*, *CD28*, *CTLA-4*, *REL*, and *B lymphoid tyrosine kinase (BLK)*. Despite genetic predisposition, smoking and infection might influence the development, rate of progression and severity of the disease (Getts et al. 2010; Klareskog et al. 2007). Epigenetic influences such as DNA hypomethylation or dysregulation of histone marks, abnormal signal transduction, as well as miRNA expression can increase pro-inflammatory genes and contribute to the disease pathogenesis (Bottini et al. 2013). H3K4me3 peaks were previously shown to overlap with RA risk loci in Tregs (Okada et al. 2014). In

addition, NFAT inhibitors such as Cyclosporin A (CsA) and tacrolimus have been studied for their efficacy as treatment for RA (Furst et al. 2002; Yocum et al. 2003).

Several studies observed a variety of abnormalities in function and phenotype of Tregs in RA (Zhou and Haupt et al. 2015). CD25<sup>+</sup> Tregs isolated from the peripheral blood of patients with RA are unable to control the production of inflammatory cytokines, such as TNF and IFN- $\gamma$ , by effector cells while they are still capable of controlling Tconv cell proliferation (Ehrenstein et al. 2004). Interestingly, TNF is able to down-modulate Treg function (Valencia et al. 2006). Anti-TNF therapy can reverse impaired control of cytokine production (Ehrenstein et al. 2004). Furthermore, TNF inhibits the phosphorylation and function of Foxp3, indicating a critical role of TNF in the hampered Treg suppression (Nie et al. 2013). Another mechanism for defective Tregs in RA might be the reduction of CTLA-4 (Flores-Borja et al. 2008). In mice, CTLA-4-deficient Tregs have impaired suppressive activity on Tconvs (Tivol et al. 1995). Interestingly, an altered DNA methylome was described for peripheral blood mononuclear cells (PBMCs) from patients with RA (Liu et al. 2011). One prominent example is the methylation of one CpG in the CTLA-4 promoter in Tregs from RA patients which lead to diminished binding of NFAT2 thereby decreasing CTLA-4 expression and Treg function (Cribbs et al. 2014). In the context of RA two miRNAs, miR-146a and miR-155, have been reported to be associated with the disease and are highly expressed in Tregs (Leah 2011; Nakasa et al. 2008; Pauley et al. 2008). Several studies indicate that miR-155 deficiency does not lead to dysfunction of Tregs under non-inflammatory conditions. However, in an inflammatory setting, the miR-155 deficient Tregs fail to respond correctly (Leng et al. 2011). MiR-146a limits TNF receptor associated factor (TRAF)6 and IL-1 receptor associated kinase (IRAK)1 expression in inflammatory settings (Hou et al. 2009; Taganov et al. 2006). Moreover, miR-146a-mediated down-regulation of STAT1, a key transcription factor of Th1 cells, was necessary for Treg ability to suppress Th1 responses (Lu et al. 2010). In an experimental disease model, the treatment of mice with miR-146a in the course of collagen-induced arthritis (CIA) prevented joint destruction, whereas miR-155-deficient mice were completely resistant to CIA (Kurowska-Stolarska et al. 2011; Nakasa et al. 2011). Furthermore, expression of miR-146a was lowered in autoimmune diseases such as SLE (Tang et al. 2009).

It is still unclear if the number of Tregs is altered in RA, however there seems to be an increase of Tregs in the RA synovium (Cao et al. 2004; Sarkar et al. 2007). Additionally, the balance between Tregs and Th17 cells seems to be shifted towards an increased number of Th17 cells in

the presence of less functional Tregs (Nie et al. 2013). TGF- $\beta$  is crucial for extrathymic development of Tregs. Downstream of TGF- $\beta$  signaling, Foxp3 is induced after TCR stimulation. Small mothers against decapentaplegic-3 and NFAT, activated by TGF- $\beta$  and TCR signaling, respectively, cooperate in *Foxp3* gene remodeling and expression (Tone et al. 2008). However, TGF- $\beta$  might also play a role in the differentiation of Th17 cells (Bettelli et al. 2006). Furthermore, it is known that cell surface-bound TGF- $\beta$  plays an important role in immunosuppression by Tregs (Nakamura et al. 2004; Nakamura et al. 2001). Interestingly, anti-TNF therapy gives rise to a distinct Treg population in patients with RA that mediates suppression via TGF- $\beta$  and IL-10. This suggests that anti-TNF therapy generates a population that compensates for the defective RA-Treg function that relies on TGF- $\beta$ -mediated suppression of target cells (Nadkarni et al. 2007). Additionally, a generated soluble human GARP was able to repress proliferation and cytokine production in Th cells (Hahn et al. 2013). It could stimulate the differentiation of naïve Th cells into induced Tregs and, in the presence of the pro-inflammatory cytokines IL-6 and IL-23, soluble GARP promotes Th17 differentiation. TGF- $\beta$  receptor blockage abrogated the activity of soluble GARP indicating that TGF- $\beta$  is critical for these effects. Furthermore, Tregs expressing the latent TGF- $\beta$ /GARP complex on their surface are potent inducers of both Th17 differentiation in the presence of IL-6 and Treg differentiation in the presence of IL-2 (Edwards et al. 2013). A more recent study could show that blocking antibodies against human GARP can inhibit the immunosuppressive function of Tregs *in vitro* and *in vivo* similar to anti-TGF- $\beta$  antibodies (Cuende et al. 2015). However, anti-GARP antibodies inhibit only Treg-specific production of TGF- $\beta$  which could have implications in tumor therapy because it might reduce side effects. All of these observations indicate that GARP might be a suitable target for the treatment of autoimmune disorders or cancer in order to restore the balance of Tregs and effector cells.

The pathophysiology of RA is still not completely understood, however the existence of only one RA antigen is unlikely because several antigens are enriched in the joints of patients with RA (Snir et al. 2010). The antigens are loaded on MHC complexes on APCs and presented to T cells in the central lymphoid organs (Firestein 2005). Then, T cells can activate B cells. One of the earliest histopathological responses is the synovitis which is caused by the influx of mononuclear cells including T cells, B cells, plasma cells, DCs, macrophages, and mast cells into the synovial compartment and by angiogenesis. Production of pro-inflammatory cytokines such as IL-17, TNF, IL-1 $\beta$ , and IFN- $\gamma$  promotes the infiltration. The synovial intimal lining is the interface

between the synovium and the synovial fluid space (Firestein et al. 2012). Two major cell types are found in the lining, macrophage-like type A synoviocytes and fibroblast-like type B synoviocytes (FLS). There is an absolute increase in both cell types in RA. FLS have a powerful capacity to invade connective tissue mediating the stimulation of osteoclasts and destruction of cartilage. The destruction of cartilage and bone in RA is initiated largely by matrix metalloproteinases. In response to inflammation bone resorption outweighs bone formation in the RA joint. Bone destruction is promoted by several factors, such as TNF and receptor activator of NF- $\kappa$ B ligand, which support osteoclast formation. Furthermore, the precise role of B cells in RA is uncertain, but antibody complexes can initiate and enhance joint inflammation. Complement activation and its interaction with immune complexes, as well as additional inflammatory mediators contribute to RA pathogenesis. In this regard, cytokines play a pivotal role in initiation of RA. IL-1 $\beta$  is mainly produced by synovial macrophages and it can induce fibroblast proliferation and can activate NF- $\kappa$ B, thereby promoting the production of pro-inflammatory cytokines. Moreover, TNF increases cell migration and inflammation (Choy 2012). CD4 Th cell cytokines like IFN- $\gamma$  and IL-17 can drive T cell differentiation, recruit inflammatory cells, influence extracellular matrix synthesis, or enhance osteoclast formation (Firestein et al. 2012).

### **1.10 Objective of the thesis**

Tregs play a critical role in controlling autoimmune diseases. Their suppressive function and phenotype are compromised in autoimmune diseases, such as RA. The underlying mechanisms of impaired function are not yet completely elucidated. This thesis will address several levels of regulation of Treg function and phenotype:

- to analyze molecular mechanisms contributing to the characteristic phenotype of Tregs
  - a) Transcriptional regulation of *GARP* expression
  - b) Involvement of MafF in iTreg development
- to characterize molecular mechanisms regulating *GARP* expression and Treg function in RA

## 2 MATERIALS AND METHODS

### 2.1 Materials

#### 2.1.1 Reagents and cytokines

Reagent/Cytokine	Origin
Acetic acid (CH <sub>3</sub> COOH)	Merck, Darmstadt, Germany
Acetone (C <sub>3</sub> H <sub>6</sub> O)	Merck
Acrylamid/bis-acrylamid 30% (37.5:1)	Merck
Agarose	Merck
Ammonium chloride (NH <sub>4</sub> Cl)	Sigma-Aldrich, St. Louis, MO, USA
Ammonium persulfate (APS)	Sigma-Aldrich
Ampicillin, sodium salt	Life technologies, Carlsbad, CA, USA
β-mercaptoethanol	Sigma-Aldrich
Biotin	Sigma-Aldrich
Bovine serum albumin (BSA)	Merck
Bromophenol blue	Merck
Dimethylformamide	Sigma-Aldrich
Dimethylsulfoxid (DMSO)	Merck
Dipotassium hydrogen phosphate (K <sub>2</sub> HPO <sub>4</sub> )	Merck
Disodium hydrogen phosphate (Na <sub>2</sub> HPO <sub>4</sub> )	Merck
Dithiothreitol (DTT)	Sigma-Aldrich
DNA Gel Loading dye (6x)	Life technologies
Dulbecco's Modified Eagle Medium (DMEM)	Life technologies
dNTP set (100 mM solutions)	Life technologies
ECL Western Blotting Detection Reagent	GE Healthcare, Munich, Germany
Ethanol (C <sub>2</sub> H <sub>5</sub> OH)	Merck
Ethylendinitrotetraacetic acid (EDTA)	Sigma-Aldrich
Ficoll lymphoflot	Biotest, Dreieich, Germany
Formaldehyde 37%	AppliChem GmbH, Darmstadt, Germany
L-glutamine (C <sub>5</sub> H <sub>10</sub> N <sub>2</sub> O <sub>3</sub> )	Life technologies
Glycerol (C <sub>3</sub> H <sub>5</sub> (OH) <sub>3</sub> )	Merck
Glycine (NH <sub>2</sub> CH <sub>2</sub> COOH)	Merck

---

Heparin-sodium salt	Ratiopharm, Ulm, Germany
4-(2-hydroxyethyl)piperazin-1-ethanesulfonic acid (HEPES)	Merck
Hydrochloric acid 37% (HCl)	Merck
IL-2 (Proleukin, recombinant human)	Novartis, Basel, Switzerland
IL-4 (recombinant human)	Perbio Science, Bonn, Germany
Ionomycin	Merck
Isopropyl $\beta$ -D-1-thiogalactopyranoside (IPTG)	Life technologies
Isopropanol (C <sub>3</sub> H <sub>7</sub> OH)	Merck
Lysogeny Broth (LB) agar (Lennox L agar)	Life technologies
LB broth (1x)	Life technologies
Magnesium chloride (MgCl <sub>2</sub> )	Merck
Methanol (CH <sub>3</sub> OH)	Sigma-Aldrich
Monensin	Sigma-Aldrich
NP-40	Millipore, Billerica, MA, USA
Nonfat dry milk powder	Real
Oligonucleotide-dT <sub>12-18</sub> (Oligo(dT))	GE Healthcare
Paraformaldehyde (PFA)	Merck
Penicillin G/streptomycin	Life technologies
Phenylmethylsulfonylfluorid (PMSF)	Roche, Penzberg, Germany
Phorbol myristate acetate (PMA)	Sigma-Aldrich
Phosphate buffered saline (PBS)	Life technologies
Piperazine-N,N'-bis-2-ethanesulfonicacid (PIPES)	Millipore
Potassium chloride (KCl)	Merck
Potassium dihydrogen phosphate (KH <sub>2</sub> PO <sub>4</sub> )	Merck
Potassium bicarbonate (KHCO <sub>3</sub> )	Merck
Protease inhibitor cocktail (PIC)	Roche
RediLoad Loading buffer (10x)	Life technologies
Retinoic acid	Sigma-Aldrich
Roswell Park Memorial Institute (RPMI)1640	Life technologies
Saponin	Sigma-Aldrich
Sheep erythrocytes	Fiebig-Nährstofftechnik, Idstein, Germany
Sodium acetate (CH <sub>3</sub> COONa)	Merck

Sodium azide (NaN <sub>3</sub> )	Merck
Sodium chloride (NaCl)	Merck
Sodium deoxycholat (Na-Deoxycholat)	Merck
Sodium dihydrogen phosphate (NaH <sub>2</sub> PO <sub>4</sub> )	Merck
Sodium dodecyl sulfate (SDS)	Merck
Sodium hydrogen phosphate (Na <sub>2</sub> HPO <sub>4</sub> )	Merck
Sodium hydroxide (NaOH)	Merck
Streptavidin-peroxidase	Roche
Sulphuric acid (H <sub>2</sub> SO <sub>4</sub> )	Merck
SYBR safe DNA gel stain (10,000x)	Life technologies
TaqMan Universal PCR mastermix 2x	Life technologies
Tetramethylethylenediamine (TEMED)	Merck
TGF-β (recombinant human)	R&D Systems, Minneapolis, MN, USA
Triton X-100	Sigma-Aldrich
Tween 20	Sigma-Aldrich
X-Gal (5-Bromo-4-Chloro-3-Indolyl β-D-Galactopyranoside)	Life technologies
Zeocin powder	InvivoGen, San Diego, CA, USA

### 2.1.2 Antibodies

<i>Specificity</i>	<i>Conjugate</i>	<i>Clone</i>	<i>Provider</i>
<i>Antibodies for cell culture</i>			
Anti-human CD3	non	OKT3	LGC Standards Teddington, UK
Anti-human CD28	non	clone 28.2	BD Biosciences, San Diego, CA, USA
Dynabeads Human T-Activator CD3/CD28	non	not provided	Life technologies
<i>Antibodies for flow cytometry</i>			
Anti-human CD3	FITC	UCHT1	Sigma-Aldrich
Anti-human CD3/CD4 dual tag	FITC/PE	UCHT1/Q4120	BD Biosciences
Anti-human CD4	FITC	Q4120	Sigma-Aldrich
Anti-human CD14	FITC	UCHM-1	Sigma-Aldrich

Anti-human CD16	PE	3G8	Biolegend, San Diego, CA
Anti-human CD19	PE	J3-119	Immunotech, Beckman-Coulter, Brea, CA
Anti-human CD20	FITC	2H7	BD Biosciences
Anti-human CD25	PE	M-A251	BD Biosciences
Anti-human CD45RA	FITC	HI100	BD Biosciences
Anti-human CD45RO	PE	UCHL1	BD Biosciences
Anti-human CD127	AlexaFluor647	HL-7RM21	BD Biosciences
Anti-human Foxp3	PE	PCH101	ebioscience, San Diego, CA, USA
Anti-human GARP hybridoma supernatant	non	7H2	From our lab, Munich, Germany
Anti-human MafF (C-terminal)	non	polyclonal	Sigma-Aldrich
Anti-human STAT1 (N-terminus)	PE	1/Stat1	BD Biosciences
Anti-human STAT1 (pS727)	AlexaFluor647	K51-856	BD Biosciences
Anti-rat IgG2a, $\kappa$	PE	isotype control Foxp3	BD Biosciences
Anti-mouse IgG1	PE	isotype control STAT1	BD Biosciences
Anti-mouse IgG1, $\kappa$	APC	isotype control STAT1 (pS727)	BD Biosciences
Anti-rat IgG (H+L)	PE	polyclonal 2nd antibody GARP	Dianova, Hamburg, Germany
Rat IgG	non	isotype control GARP	Sigma-Aldrich
<i>Antibodies for Western Blot</i>			
Anti-human MafF (C-terminal)	non	polyclonal	Sigma-Aldrich
Anti-p38 MAP kinase	non	polyclonal	Cell Signaling, Cambridge, UK

<i>Specificity</i>	<i>Clone</i>	<i>Provider</i>
<i>Antibodies for Chromatin Immunoprecipitation (ChIP)</i>		
Anti-trimethyl-Histone H3 (Lysine4)	polyclonal	Merck
anti-acetyl-Histone H3	polyclonal	Merck
anti-trimethyl-Histone H3 (Lysine27)	polyclonal	Merck
anti-human c-Rel	D5G1A9	Cell Signaling
anti-human Foxp3	polyclonal	Thermo Scientific, Waltham, MA, USA
anti-human NFAT1	25A10.D6.D2	Abcam, Cambridge, UK
anti-human MLL/HRX	N4.4	Active Motif, Carlsbad, CA, USA
anti-human JARID1B (PLU-1)	polyclonal	Cell Signaling
anti-human p65	D14E12	Cell Signaling
anti-human p105/p50	D7H5M	Cell Signaling
anti-human RbBP5	polyclonal	Bethyl laboratories, Montgomery, TX, USA
Normal goat IgG	isotype control Foxp3	R&D Systems
Normal mouse IgG1	isotype control NFAT1	Sigma-Aldrich
Normal rabbit IgG	isotype control NF- $\kappa$ B, histone modifications	Cell Signaling
<i>Antibodies for DNA-protein binding assay</i>		
anti-human Foxp3	polyclonal	R&D Systems
anti-human NFAT1	D43B1	Cell Signaling
anti-human p105/p50	D7H5M	Cell Signaling
Normal goat IgG	isotype control Foxp3	R&D Systems
Normal rabbit IgG	isotype control p105/p50 and NFAT1	Cell Signaling

### 2.1.3 Ladders/Markers

<i>Name</i>	<i>Provider</i>
Biotinylated protein ladder	Cell Signaling
GeneRuler DNA ladder (100 bp)	Fermentas, St. Leon-Rot, Germany
GeneRuler DNA ladder (1 kb)	Fermentas
Prestained protein marker (broad range)	Cell Signaling

### 2.1.4 Serum

<i>Name</i>	<i>Provider</i>
Fetal calf serum (FCS)	Life technologies
Mouse serum	Sigma-Aldrich
Normal human serum (NHS)	From our lab, Munich, Germany
Rat serum	Sigma-Aldrich

### 2.1.5 Enzymes

<i>Enzyme</i>	<i>Supplied Reaction Buffer</i>	<i>Provider</i>
AmpliTaq DNA polymerase	10x PCR Buffer II	Life technologies
DpnI	none	Agilent Technologies, Santa Clara, CA, USA
EcoRI	10x NEBuffer EcoRI	New England Biolabs
EcoRV	10x NEBuffer 3	New England Biolabs
Epimark Hot Start Taq DNA Polymerase	5x Epimark Hot Start Taq reaction buffer	New England Biolabs
GeneAmp High Fidelity PCR Enzyme Mix	10x GeneAmp High Fidelity PCR buffer	Life technologies
Herculase II Fusion DNA Polymerase	5x Herculase II reaction buffer	Agilent Technologies
HindIII	10x NEBuffer 2	New England Biolabs
peqGOLD Proteinase K (20 mg/ml)		Peqlab
Quick T4 DNA Ligase	2x Quick ligation reaction buffer	New England Biolabs
RNase A, DNase and protease-free (10 mg/ml)		Life technologies
SalI	10x NEBuffer 3	New England Biolabs
XhoI	10x NEBuffer 2	New England Biolabs

### 2.1.6 Single nucleotide polymorphism (SNP) genotyping assays

<i>SNP location</i>	<i>SNP ID</i>	<i>Probe</i>	<i>Sequence</i>
GARP intergenic region	rs7122065	A=VIC, G=FAM	TCTGCACCCTACTCCAGCTCCATTC[A/G] CTGGGCCCTACCTTGCAGCTGGTGA
GARP intergenic region	rs11236851	A=VIC, G=FAM	CCTCCTTTAATGGCCTTCTTCCCGT[A/G]G CACCTTGGAAACACCCCTCCTGGC

GARP intergenic region	rs7342189	C=VIC, T=FAM	ACTCACGAAAGCAACAAGCATGCAT[C/T] GACCTCATAACACGAATTTACGTTAG
GARP 5'UTR	rs947998	G=VIC, T=FAM	TGAGTGCCCCACCTCCCCTCCCC[G/T] CCCCAGAGGCTGTGGTTGTGGTTA
GARP 5'UTR	rs3814710	A=VIC, G=FAM	GGCGGCGAAGCATCTTACCACCCT[A/G] GGACCTCGGCCGGGAAGGGGCGGGG
GARP Intron 1	rs6592657	A=VIC, G=FAM	CACTAAGGACATCAGCCAAGTGCTA[A/G] GGATGTACAAATCCACCCATGAATT
GARP Intron 1	rs4944115	G=VIC, T=FAM	AGACCCACCTGGCGGAAGACAGCC[G/T] JGGAGGGGATGCACAGAAGGCTGACA
GARP Intron 2	rs7944357	A=VIC, G=FAM	ATGCCATCCCCAACCAGATCCACAC[A/G] TGAACTCTTCACTGAGCTTCAGG
GARP Intron 2	rs7944463	C=VIC, T=FAM	CCAGCAGGGCCTTCGAGGCTGTTT[C/T] AGCCCCTGCCAACCTGTCCCCCACC

### 2.1.7 TaqMan Gene Expression assays

<i>Gene</i>	<i>Assay ID</i>	<i>Probe</i>	<i>Sequence (5' to 3')</i>
Cyclophilin A	4310x10783E	VIC-probe	not provided
b-actin	4310x10781E	VIC-probe	not provided
human GARP both transcript variants	Hs00194136_m1	FAM-probe	not provided
human GARP transcript variant 2	Hs00973758_m1	FAM-probe	not provided
human GARP transcript variant 1	customed	For primer Rev primer FAM-probe	CCTTGATTTGGTATAGTGGGAAC CAGGGTCACGATCAGAATCCA TTGCTTTGGAGACAGATGA

For - Forward; Rev - Reverse

### 2.1.8 Oligonucleotides

<i>Gene/Region</i>	<i>Oligonucleotide</i>	<i>Sequence (5' to 3')</i>
<i>Cloning primer</i>		
human GARP promoter full-length	For primer (EcoRV) Rev primer (HindIII)	GAGATATCCAGAGTGGACGGCTT GATAAGCTTAGCCCTGCCAACG
human GARP up-stream P2	For primer (EcoRV) Rev primer (HindIII)	GAGATATCCAGAGTGGACGGCTT GATAAGCTTATGGCGGGAGGGGAG
human GARP down-stream P1	For primer (EcoRV) Rev primer (HindIII)	GAGATATCGACGCCCCCAAACA GATAAGCTTAGCCCTGCCAACG
mouse GARP promoter	For primer Rev primer	TGGCTCAAGTCCACAGGGATTC CCACTAACCTTCAACCTGGACTGG

human GARP conserved non-coding sequence (CNS)	For primer Rev primer	AACTTTCTAACGGGCGGTGG CGAAGATGGCTGCTCTGAATCC
human MafF coding sequence (cgs)	For primer (Kozak) Rev primer	<u>CACCATGTCTGTGGATCCCCTATCC</u> CTAGGAGCAGGAGGCCGGGCC
<i>Bisulfite sequencing primer</i>		
human GARP up-stream P2	For primer Rev primer	TTGTAGGAAATTTGAATTTAAATTT CTACCAAACCCACCAAATAAAC
human GARP down-stream P1	For primer Rev primer	TTTTTGTATTATGAAGAAAAGGAGGTT CTTACCAAACACACAATAAAC
human GARP CNS	For primer Rev primer	GTGTTGGGAATTGGGAATTTAA AAAACAAAACAATAAAAACAAC
<i>ChIP assay realtime-polymerase chain reaction (PCR) primer</i>		
human GARP up-stream P2	For primer Rev primer	GACTTTGATGGTGCCGTTTC CAGGTCACTTTTCTCTCCG
human GARP down-stream P1	For primer Rev primer	AATGTGGCTGTGATGGCGG TCTCCAAGGGGCTCTGAACC
human GARP CNS	For primer Rev primer	TGCTAACTTTCTAACGGGCG GCATTACAGGTTGTGCTTTCAC
<i>Site-directed mutagenesis</i>		
human GARP down-stream P1 del311-317 retinoic X receptor (RXR)	For primer Rev primer	CCATTTCTCGTAGTGGGCAAGGGG CGTCCCACCGCTCTCCAAGG CCTTGGAGAGCGGTGGACGCCCT TGCCCACTACGAGAAATGG
human GARP up-stream P2 del101-102 (Foxp3)	For primer Rev primer	TCACCTCGCCTGTGCCCCCGCGTT AACGCGGGGGCACAGGCGAGGTGA
human GARP up-stream P2 del402-403 (Foxp3)	For primer Rev primer	CCGCCGGCTCCGGATACCGAGGC GCCTCGGTATCCGGAGCCGGCGG
human GARP up-stream P2 del751-752 (Foxp3)	For primer Rev primer	GGGACGCCCCCACACTCCCCTCC GGAGGGGAGTGTGGGGGGCGTCCC

Can – Canonical; Scr – Scrambled; For - Forward; Rev - Reverse; Com - Complementary

<i>Gene/Region</i>	<i>Oligonucleotide</i>	<i>Sequence (5' to 3')</i>
<i>DNA-protein binding assay</i>		
Foxp3 can	For oligo	CAAGGTAAACAAGAGTAAACAAAGTGCGGTAAACAAG AGTAAACAGTG
	Com oligo	GTTCCATTTGTTCTCATTGTTTCACGCCATTTGTTCTCA TTTGTCAC
Foxp3 scr	For oligo	GTGACAGATAGAAGAAAGACACAGACATACGAGAAGA CATAAGTAAGT
	Com oligo	CACTGTCTATCTTCTTTCTGTGTCTGTATGCTCTTCTGTA TTCATTCA
NFAT can	For oligo	CGCCCAAAGAGGAAAATTTGTTTCATACGCCCAGAGGA AAATTTGTTTCATA
	Com oligo	GCGGGTTTCTCCTTTTAAACAAAGTATGCGGGTCTCCTT TTAAACAAAGTAT
NFAT scr	For oligo	GATAGACACCTATTCTGAATGGGACTAAAGATGTGCTA CATAACATACACTGT
	Com oligo	CTATCTGTGGATAAGACTTACCCTGATTTCTACACGATG TATGTATGTGACA
NF-κB can	For oligo	GAGATCCGGGGACTTTCCATGGATGGGGACTTTCCATG GAG
	Com oligo	CTCTAGGCCCTGAAAGGTACCTACCCCTGAAAGGTAC CTC
NF-κB scr	For oligo	GGCCAGGCGTCAGTCTATGTGTAGATGGTGCGCAGAGT CAT
	Com oligo	CCGGTCCGCAGTCAGATACACATCTACCACGCGTCTCA GTA
GARP promoter	For oligo	GGCAAACCGGAATTTGAATTCAGGTTTCTGCAACGCT CCGA
	Com oligo	CCGTTTGGCCTTAAACTTAAGTCCAAAGGACGTTGCGA GGCT
GARP promoter scr	For oligo	ACATTCGTGCCTAAGAATCGCGTACATAAGCGTCGCTG TGCA
	Com oligo	TGTAAGCACGGATTCTTAGCGCATGTATTCGCAGCGAC ACG

Can – Canonical; Scr – Scrambled; For - Forward; Rev - Reverse; Com - Complementary

### 2.1.9 Kits, devices, and software

<i>Kit name</i>	<i>Origin</i>
ABI Prism 7000 Sequence Detection system	Life technologies
Affinity Script QPCR cDNA Synthesis kit	Agilent technologies
Amaxa Cell Line Nucleofector kit L	Lonza, Cologne, Germany
Amaxa Cell Line Nucleofector kit V	Lonza
Amaxa human T cell Nucleofector kit	Lonza
B Cell Isolation kit II, human	Miltenyi Biotec, Bergisch Gladbach, Germany
BioPhotometer	Eppendorf, Hamburg, Germany
Bioruptor® Plus (B01020001)	Diagenode, Denville, NJ, USA
CD4+ T Cell Isolation kit, human	Miltenyi Biotec
CD25 MicroBeads II, human	Miltenyi Biotec
CD127 MicroBead kit, human	Miltenyi Biotec
ChIP-IT High Sensitivity kit	Active Motif
EC-120 Mini Vertical Gel System	E-C Apparatus, Holbrook, NY, USA
EC-140 Mini Blot Module	E-C Apparatus
ELISA/ELISPOT Coating buffer powder	ebioscience
ELISA Wash buffer	ebioscience
EpiQuik General Protein-DNA Binding Assay Kit (Fluorometric)	Epigentek, Farmingdale, NY, USA
EpiQuik Nuclear Extraction Kit II	Epigentek
Dual-Glo Luciferase Assay System	Promega, Madison, WI, USA
FACS Cytomics FC500	Beckman Coulter
FUJIFILM LAS-3000	Fujifilm, Tokyo, Japan
Gel chamber Nautico 10x107	H. Hölzel Laborgeräte GmbH, Dorfen, Germany
Human Foxp3 Buffer set	BD Biosciences
Human IFN-gamma Quantikine ELISA kit	R&D Systems
Human IL-17 Quantikine ELISA kit	R&D Systems
Human TNF- $\alpha$ Quantikine ELISA kit	R&D Systems
MacVector Software	MacVector, Inc., Cary, NC, USA
MACSmix Tube rotator	Miltenyi Biotec
MethylDetector™ Bisulfite Modification kit	Active Motif
Microcentrifuge 5415R	Eppendorf

---

Monocyte Isolation kit II, human	Miltenyi Biotec
Naïve CD4+ T Cell Isolation kit II, human	Miltenyi Biotec
NucleoSpin Gel and PCR Clean-up	Macherey-Nagel, Düren, Germany
Power Pac 1000	Bio-Rad Laboratories, München, Germany
QIAamp DNA Blood Mini kit	Qiagen, Hilden, Germany
QIAGEN Plasmid Maxi kit	Qiagen
QIAprep Spin Miniprep kit	Qiagen
QIAquick Gel Extraction kit	Qiagen
QIAquick PCR Purification kit	Qiagen
QIAquick Nucleotide Removal kit	Qiagen
QuickChange Lightning Site-Directed Mutagenesis kit	Agilent technologies
Quick Ligation kit	New England Biolabs
5'RACE System for Rapid Amplification of cDNA Ends Version 2.0	Life technologies
RNeasy Plus Mini kit	Qiagen
Rotixa 50 RS centrifuge	Hettich AG, Bäch, Switzerland
Sigma GenElute PCR Clean-Up kit	Sigma-Aldrich
Tecan Spectra Microplate Reader	Tecan Group, Männedorf, Switzerland
TOPO TA Cloning kit	Life technologies
Tristar <sup>2</sup> LB942 Multimode Microplate Reader	Berthold technologies
Unimax 1010 Orbital Shaker	Heidolph GmbH, Schwabach, Germany
UVT-28 MP transilluminator	Herolab GmbH, Wiesloch, Germany

---

**2.1.10 Buffers and solutions**

<i>Buffers and solutions</i>	<i>Composition</i>
Annealing buffer	10 $\mu$ M oligonucleotide 10 mM Tris, pH 7.5 1 mM EDTA 50 mM NaCl
Cell Lysis buffer	5 mM PIPES, pH 8.0 85 mM KCl 0.5% NP-40 1x PIC
6x DNA Loading buffer	50 mM EDTA 26.1% glycerol 0.25% bromphenol blue
FACS buffer	PBS 2% FCS 0.01% NaN <sub>3</sub>
MACS buffer	PBS 0.5% BSA 2 mM EDTA
10x NH <sub>4</sub> Cl	41.45 g NH <sub>4</sub> Cl 5 g KHCO <sub>3</sub> 1 mM EDTA
Nuclear Lysis buffer	H <sub>2</sub> O ad 0.5 l 50 mM Tris-HCl, pH 8.0 10 mM EDTA 0.1% SDS 1x PIC
Resolving gel (15%)	380 mM Tris-HCl, pH 8.8 15% acrylamide/bis-acrylamide 0.2% SDS 0.2% APS 10 $\mu$ l TEMED H <sub>2</sub> O ad 10 ml
Stacking gel (4%)	126.6 mM Tris-HCl, pH 6.8 4% acrylamide/bis-acrylamide 0.1% SDS 0.1% APS 5 $\mu$ l TEMED H <sub>2</sub> O ad 5 ml
SDS Blot buffer	20 mM Tris-HCl, pH 7.6 140 mM NaCl

---

	0.1% Tween20
SDS Running buffer	12.5 mM Tris-HCl, pH 6.8 96 mM glycine 0.05% SDS
SDS Sample buffer	62.5 mM Tris-HCl, pH 6.8 2% SDS 10% glycerol 50 mM DTT
SDS Transfer buffer	0.01% bromophenol blue 12.5 mM Tris-HCl, pH 8.3 86 mM Glycine 0.05% SDS 20% Methanol
Sonication buffer	50 mM HEPES, pH 7.8 140 mM NaCl 1 mM EDTA 1% Triton X-100 0.1% Na-Deoxycholat 0.1% SDS 0.5 mM PMSF 1x PIC
Swelling buffer	25 mM HEPES, pH 7.8 1.5 mM MgCl <sub>2</sub> 10 mM KCl 0.1% NP-40 1 mM DTT 0.5 mM PMSF 1x PIC
50x Tris-Acetate-EDTA (TAE) buffer	242 g Tris-HCl 57.2 ml acetic acid 50 mM EDTA (pH7.6) H <sub>2</sub> O ad 1 l
TBST	20 mM Tris-HCl (pH7.6) 140 mM NaCl 0.1% Tween-20
TE buffer	10 mM Tris-HCl, pH 8.0 1 mM EDTA 0.5 mM PMSF 1x PIC
Wash buffer A	50 mM HEPES, pH 7.8 500 mM NaCl 1 mM EDTA 1% Triton X-100 0.1% SDS

---

	0.5 mM PMSF
	1x PIC
Wash buffer B	20 mM HEPES, pH 8.0
	250 mM LiCl
	1 mM EDTA
	0.5% NP-40
	0.5% Na-Deoxycholat
	0.5 mM PMSF
	1x PIC

---

## 2.2 Methods

### 2.2.1 Cell purification

#### 2.2.1.1 Isolation of human rosette-positive and -negative cells

Human peripheral CD4 Th cells from healthy donors and patients with RA were used in this work. Total populations of CD4 Th cells were isolated from heparinized peripheral blood. In the first step, PBMCs were isolated by centrifugation of the blood over a Ficoll (Biotest) layer. 10 ml Ficoll were loaded under 20 ml blood diluted with 20 ml PBS and centrifuged at 400 xg for 20 min at room temperature. PBMCs were harvested and washed once with PBS.

In the second step (rosetting), PBMCs were incubated with sheep erythrocytes to isolate the so-called rosette-positive cells. The CD58 homologue expressed on sheep erythrocytes binds to CD2 that is expressed on T cells and NK cells, but not on other PBMCs (e.g. monocytes and B cells) (Rosenberg et al. 1979). For rosetting, PBMCs were resuspended at  $10 \times 10^6$  cells/ml in RPMI1640 and incubated with 1/2 volume of FCS and 1/2 volume of sheep erythrocytes ( $2 \times 10^6$  cells/ml) at 37°C for 10 min. Afterwards, cells were centrifuged for 10 min at 255 xg and incubated at 4°C for 45 min to allow the rosette formation between sheep erythrocytes and CD2 positive cells. Later, cells were carefully resuspended and centrifuged over a 10 ml Ficoll layer for 20 min at 400 xg. The rosettes of T cells bound to the erythrocytes sedimented through the Ficoll and were collected in the pellet, while the rosette-negative cells formed a cell ring above the Ficoll layer. The pellet of rosette-positive cells was resuspended with 5 ml/pellet of 155 mM  $\text{NH}_4\text{Cl}$  to lyse the sheep erythrocytes and then washed twice with PBS. In the next step, CD4 T cells were isolated by negative selection from rosette-positive cells (see section 2.2.1.2).

In some cases, rosette-negative cells (T cell-depleted PBMCs) were collected and used to isolate B cells or monocytes. Rosette-negative cells were harvested, incubated with 10 ml 155 mM  $\text{NH}_4\text{Cl}$  for 2 min at room temperature to lyse contaminating sheep erythrocytes and washed with PBS. Afterwards, B cells or monocytes were isolated by negative selection from rosette-negative cells (see section 2.2.1.5 and 2.2.1.6).

#### 2.2.1.2 Isolation of CD4 T cells and naïve CD4 Th cells

For isolation of total CD4 Th cells the human CD4 T Cell Isolation kit (Miltenyi Biotec) was used. The magnetic activated cell sorting (MACS) isolation procedure is a magnetic separation

of cells. First, rosette-positive cells were resuspended in MACS buffer and non-CD4 Th cells were labeled with biotin-conjugated antibodies against CD8, CD14, CD16, CD19, CD36, CD56, CD123, TCR  $\gamma/\delta$  and Glycophorin A for 5 min at 4°C. Afterwards, antibodies were magnetically conjugated to anti-Biotin MicroBeads for 10 min at 4°C. Unbound beads were removed by washing the cells with PBS, and up to  $10 \times 10^7$  cells were resuspended in 1 ml MACS buffer. The cell suspension was applied onto an LS MACS column (large separation column) placed in the magnetic field. When the LS column is placed in the magnetic field, labeled non-CD4 Th cells stack in the column. The column was washed three times with 3 ml MACS buffer to let all unlabeled CD4 Th cells run through. CD4 Th cells were then used for further MACS separation. For isolation of naïve CD4 Th cells the human CD4 Th Cell Isolation kit II (Miltenyi Biotec) was used. First, rosette-positive cells were resuspended in MACS buffer and non-naïve CD4 Th cells were labeled with biotin-conjugated antibodies against CD8, CD14, CD15, CD16, CD19, CD25, CD34, CD36, CD45RO, CD56, CD123, TCR  $\gamma/\delta$ , HLA-DR, and Glycophorin A for 10 min at 4°C. Unbound antibodies were removed by washing the cells with PBS, and up to  $10 \times 10^7$  cells were resuspended in 1 ml MACS buffer. Afterwards, antibodies were magnetically conjugated to anti-Biotin MicroBeads for 10 min at 4°C. Unbound beads were removed by washing the cells with PBS, and up to  $10 \times 10^7$  cells were resuspended in 1 ml MACS buffer. The cell suspension was applied onto an LS MACS column placed in the magnetic field. When the LS column is placed in the magnetic field, labeled non-naïve CD4 Th cells stack in the column. The column was washed three times with 3 ml MACS buffer to let all unlabeled naïve CD4 Th cells run through. Naïve CD4 Th cells were then used for further MACS separation.

### ***2.2.1.3 Isolation of CD127- CD4 Th cells***

For isolation of CD127- CD4 Th cells the human CD127 MicroBead kit (Miltenyi Biotec) was used. First, CD4 Th cells were resuspended in MACS buffer and CD127+ cells were labeled with biotin-conjugated antibodies against CD127 for 10 min at 4°C. Afterwards, antibodies were magnetically conjugated to anti-Biotin MicroBeads for 15 min at 4°C. Unbound beads were removed by washing the cells with PBS, and up to  $10 \times 10^7$  cells were resuspended in 1 ml MACS buffer. The cell suspension was applied onto an LS MACS column placed in the magnetic field. When the LS column is placed in the magnetic field, labeled CD127+ cells stack in the column. The column was washed three times with 3 ml MACS buffer to let all unlabeled CD127- CD4 Th cells run through. CD127- CD4 Th cells were then used for further MACS separation.

#### **2.2.1.4 MACS separation of CD25+ and CD25- T cells**

For isolation of CD25+ (Tregs) and CD25- (Tconvs) CD4 Th cells the human CD25 MicroBeads II (Miltenyi Biotec) were used. First, the Tregs were magnetically labeled with biotin-conjugated antibodies against CD25 incubated at 4°C for 15 min. Unbound beads were removed by washing the cells with PBS, and up to  $10 \times 10^7$  cells were resuspended in 1 ml MACS buffer. The cell suspension was applied onto a MS MACS column (mini scale) placed in the magnetic field. When the MS column is placed in the magnetic field, labeled CD25+ cells stack in the column. The column was washed three times with 500  $\mu$ l MACS buffer to let all unlabeled cells run through. After removal of the MS column from the magnetic field, the Tregs were eluted with 1 ml MACS buffer. A part of the CD4 T cells were labeled with CD25 Microbeads as described above. Unlabeled Tconvs were applied onto an LD MACS column (large depletion column) to completely remove contaminating Tregs. The LD column was washed twice with 2 ml MACS buffer and Tconvs were collected as the flow through. Separated Tregs and Tconvs were washed once with PBS and used in further experiments.

#### **2.2.1.5 Isolation of B cells**

For isolation of B cells the human B cell Isolation kit II (Miltenyi Biotec) was used. First, rosette-negative cells were resuspended in MACS buffer and non-B cells were labeled with biotin-conjugated antibodies against CD2, CD14, CD16, CD36, CD43, Glycophorin A for 5 min at 4°C. Afterwards, antibodies were magnetically conjugated to anti-Biotin MicroBeads for 10 min at 4°C. Unbound beads were removed by washing the cells with PBS, and up to  $10 \times 10^7$  cells were resuspended in 1 ml MACS buffer. The cell suspension was applied onto an LS MACS column placed in the magnetic field. When the LS column is placed in the magnetic field, labeled non-B cells stack in the column. The column was washed three times with 3 ml MACS buffer to let all unlabeled B cells run through. B cells were then used for DNA methylation experiments.

#### **2.2.1.6 Isolation of monocytes**

For isolation of monocytes the human Monocyte Isolation kit II (Miltenyi Biotec) was used. First, rosette-negative cells were resuspended in MACS buffer, FcR Blocking reagent was added, and non-monocyte cells were labeled with biotin-conjugated antibodies against CD3, CD7, CD16, CD19, CD56, CD123 and Glycophorin A for 10 min at 4°C. Afterwards, antibodies were

magnetically conjugated to anti-Biotin MicroBeads for 15 min at 4°C. Unbound beads were removed by washing the cells with PBS, and up to  $10 \times 10^7$  cells were resuspended in 1 ml MACS buffer. The cell suspension was applied onto an LS MACS column placed in the magnetic field. When the LS column is placed in the magnetic field, labeled cells stack in the column. The column was washed three times with 3 ml MACS buffer to let all unlabeled monocytes run through. Monocytes were then used for DNA methylation experiments.

## **2.2.2 Cell culture**

Culturing of primary cells or cell lines was carried out in RPMI1640 medium or DMEM supplemented with penicillin G/streptomycin (50 units/ml), L-glutamine (2 mM) (all from Life technologies) and 10% NHS. Cell cultures were maintained at 37°C in a humidified atmosphere containing 5% CO<sub>2</sub>.

### **2.2.2.1 Maintenance of cell lines**

Human HeLa, human embryonic kidney (HEK)293, T cell leukemia (Jurkat), human megakaryoblastic leukemia (MEG-01) cell lines and murine T cell leukemia line (EL-4) were obtained from the American Type Culture Collection (ATCC). HeLa, HEK293, and EL-4 cells were split 2-3 times a week in DMEM complete medium. Jurkat and MEG-01 cells were maintained in RPMI complete medium and split every 2-3 days.

### **2.2.2.2 In vitro IL-4 stimulation**

The effect of IL-4 on MafF expression in effector T cells was assessed employing an *in vitro* culture. Freshly isolated naïve Tconvs ( $1.2 \times 10^6$ /well in a 12-well plate) were stimulated with anti-CD3/CD28-Dynabeads (bead to cell ratio 1:4) in the presence of human recombinant IL-2 (10 units/ml) and in the presence or absence of human recombinant IL-4 (31.25 ng/ml). After 5 days of stimulation, the cells were harvested, washed, counted, and either used for intracellular staining for MafF or lysed for SDS-polyacrylamide gel electrophoresis (PAGE) and Western blotting for MafF according to sections 2.2.3.4 or 2.2.14, respectively.

### **2.2.2.3 In vitro Treg induction**

Freshly isolated CD25- naïve Tconvs ( $1.2 \times 10^6$ /well in a 12-well plate) were cultivated for a total of 4 days in RPMI1640 supplemented with human recombinant IL-2 (50 units/ml), 10% NHS, anti-CD3/CD28-Dynabeads (bead to cell ratio 1:4), in the presence or absence of human

recombinant TGF- $\beta$  (5 ng/ml) and retinoic acid (100 nM). After 4 days of stimulation, the cells were harvested, counted, and stained for intracellular Foxp3-expression according to section 2.2.3.4.

#### **2.2.2.4 Activation of primary human T cells**

To analyze the effect of TCR engagement on the transcriptional regulation of *GARP*, Tregs and Tconvs were stimulated with anti-CD3/CD28-Dynabeads (Life technologies) at a ratio of 1:1 in the presence of 100 units/ml recombinant human IL-2. After 1-4 days of stimulation, the cells were harvested, washed, counted, and prepared for the respective experiment.

### **2.2.3 Flow cytometry**

Analysis of the expression of cell surface molecules or of intracellular cytokines and proteins on a single cell level was performed by fluorescence activated cell sorting (FACS) with a Cytomics FC500 flow cytometer (Beckman-Coulter). Fluorescence signals were determined using appropriate electronic compensation to exclude emission spectra overlap. All centrifugation steps were carried out at 3,000 xg for 2 min at room temperature.

#### **2.2.3.1 Flow cytometry of surface molecules**

For extracellular staining,  $0.05-0.1 \times 10^6$  cells/staining were washed with 1 ml FACS buffer, resuspended in 50  $\mu$ l FACS buffer and incubated with saturating amounts (2  $\mu$ l) of directly fluorochrome-conjugated antibodies for 15 min at 4°C in the dark. Afterwards, cells were washed twice with 1 ml FACS buffer, resuspended in 300  $\mu$ l FACS buffer and analyzed. The majority of the CD4 T cells ( $\geq 95$  %) were positive for CD3 and CD4. Tregs were CD127 negative and  $\sim 90$ % CD25 positive. Tconvs were  $\sim 80$ % positive for CD127 and  $\geq 98$ % negative for CD25. B cells were  $\geq 90$ % positive for CD19 and CD20. In addition, monocytes were  $\geq 90$ % positive for CD14 and negative for CD16.

#### **2.2.3.2 Flow cytometry for GARP**

For surface staining of GARP, equal amounts of cells were stained with 25  $\mu$ l of anti-GARP hybridoma supernatant (Clone 7H2) or 0.25  $\mu$ l of 0.5 mg/ml rat IgG as isotype control for 15 min at 4°C in the dark. Next, cells were washed with 1 ml FACS buffer, resuspended in 50  $\mu$ l, and incubated with 0.25  $\mu$ l of secondary antibody (PE-labeled anti-rat IgG) and 2  $\mu$ l of FITC-labeled anti-CD4 antibody for 15 min at 4°C in the dark. Finally, cells were washed, resuspended

in 300 µl FACS buffer and analyzed.

### **2.2.3.3 Intracellular flow cytometry for STAT1**

For intracellular staining of total STAT1 or phosphorylated STAT1 (pS727),  $1 \times 10^6$  cells/staining were fixed with 3% PFA for 10 min at 37°C, washed once with PBS and permeabilized with 0.1% (w/v) saponin in FACS buffer (FACS-Saponin). All incubation and washing steps were performed with FACS-Saponin. Unspecific binding sites were blocked with 4% rat and mouse serum for 10 min at 4°C. After blocking, cells were washed once and incubated with saturating amounts of PE-anti-total STAT1 and APC-anti-STAT1 (pS727) antibodies for 30 min at 4°C. Afterwards, cells were washed twice, resuspended in 300 µl FACS buffer and analyzed.

### **2.2.3.4 Intracellular flow cytometry for Foxp3 or MafF**

For intracellular staining of Foxp3 or MafF, the Human Foxp3 Buffer set (BD Biosciene) was used according to manufacturer's instructions. Briefly,  $1 \times 10^6$  cells/staining were fixed with 1x Human Foxp3 buffer A for 10 min at room temperature, washed once with FACS buffer and permeabilized in 1x Permeabilization solution for 30 min at room temperature. Then, cells were centrifuged and unspecific binding sites were blocked with 4% rat and mouse serum in FACS buffer for 10 min at 4°C. After blocking, cells were split into two tubes and either incubated with saturating amounts of PE/APC-anti-Foxp3, anti-MafF antibodies or respective isotype controls for 30 min at 4°C. Afterwards, cells stained for Foxp3 were washed twice, resuspended in 300 µl FACS buffer and analyzed. The cells stained for MafF were washed twice with FACS buffer and incubated with a PE-labelled secondary antibody for 30 min at 4°C. Afterwards, cells were washed twice, resuspended in 300 µl FACS buffer and analyzed.

## **2.2.4 Isolation of nucleic acids**

Total RNA isolation was performed using the RNeasy Mini Kit (Qiagen) according to the manufacturer's instructions. All centrifugation steps were performed at 16,000 xg at room temperature. In brief,  $1-5 \times 10^6$  cells were lysed with 700 µl RTL buffer containing 1% β-mercaptoethanol and centrifuged in a QIAShredder column for 2 min. One volume of 70% ethanol was added to the eluate and loaded onto an RNeasy column. After short centrifugation (30 sec), each column was washed with 700 µl RW1 buffer. After centrifugation, the columns were washed twice with 500 µl RW1 buffer. RNA was eluted with 32 µl of RNase-free water/column by centrifugation the columns for 1 min. The concentration of RNA was

determined by measuring the absorbance at 260 nm ( $A_{260}$ ).

Genomic DNA (gDNA) isolation was performed using the QIAamp DNA Blood Mini kit (Qiagen) according to the manufacturer's instructions. All centrifugations were performed at 300 xg at room temperature. In brief,  $0.5-5 \times 10^6$  cells were resuspended in 160  $\mu$ l PBS containing 40  $\mu$ g RNase A and 20  $\mu$ l QIAGEN Protease and 200  $\mu$ l of buffer AL were added. The reaction was incubated at 56°C for 10 min, 200  $\mu$ l 100% ethanol was added, and the mixture was applied to a QIAamp Mini spin column. After centrifugation, the column was washed with 500  $\mu$ l buffer AW1, followed by washing with 500  $\mu$ l buffer AW2. After drying the column, the DNA was eluted into a new 1.5 ml tube with 32  $\mu$ l of buffer AE. The concentration of DNA was determined by measuring the absorbance at 260 and 280 nm ( $A_{260}/A_{280}$ ).

### **2.2.5 Complementary DNA (cDNA) synthesis**

0.1-1  $\mu$ g of total RNA was transcribed to cDNA using the Affinity Script QPCR cDNA Synthesis kit (Agilent Technologies) according to manufacturer's protocol. Briefly, RNA was incubated for 5 min at 25°C, 5 min at 42°C, 30 min at 55°C and 5 min at 95°C in a total volume of 20  $\mu$ l containing 1x First strand mastermix, 12.75 nM Oligo(dT), 2.25 nM random primer, and 1  $\mu$ l Affinity Script RT/RNase Block Enzyme mixture.

### **2.2.6 Real-time PCR**

#### **2.2.6.1 TaqMan Gene Expression assays**

Real-time PCR was performed with TaqMan Gene Expression assays in an ABI Prism 7000 Sequence Detection System (Life technologies). The TaqMan assays contain two unlabeled primers (For and Rev) and one specific minor groove binder (MGB) probe. The 5' end of the probe is linked to a reporter dye (FAM or VIC) and the 3' end is linked to a non-fluorescent quencher (NFQ) and a MGB. During PCR, the probe anneals to the complementary sequence between For and Rev primers. However, the proximity of the NFQ and the reporter dye prevents the reporter fluorescence primarily by Förster-type energy transfer. During elongation of the PCR product the 5' nuclease activity of the polymerase cleaves the probe, thereby releasing the reporter dye. This results in increased fluorescence of the reporter. Each sample was amplified in duplicates. PCR amplification was performed using 1  $\mu$ l of cDNA in a final volume of 20  $\mu$ l. The TaqMan Gene Expression reaction contained 1x TaqMan Universal PCR mastermix and 1x TaqMan Gene Expression Assay mix. The thermal cycling conditions were as follows: hot

enzyme activation at 95°C for 10 min followed by 40 cycles of amplification – DNA denaturation at 95°C for 10 sec and annealing of primers/DNA extension at 60°C for 1 min. The list of genes analyzed by real-time PCR and the respective assays are listed in “Materials”. Relative quantification was performed by calculating the difference in cross-threshold values ( $\Delta C_t$ ) of the gene of interest and a housekeeping gene (*Cyclophilin*) according to the formula  $2^{-\Delta C_t}$ .

#### **2.2.6.2 SYBR Green detection**

Real-time PCR was performed with SYBR Green detection in an ABI Prism 7000 Sequence Detection System (Life technologies). Primers for ChIP analysis (For and Rev) for SYBR Green PCR were designed using the MacVector software to amplify fragments up to 120 base pair (bp) long. SYBR Green dye intercalates into ds DNA and emits fluorescence only when bound to DNA. During PCR, the polymerase amplifies the target sequence and the SYBR Green dye binds each new copy. The result is an increase in fluorescence intensity proportionate to the amount of PCR product produced. Each sample was amplified in duplicates or triplicates. PCR amplification was performed using 1  $\mu$ l of DNA in a final volume of 20  $\mu$ l. The SYBR Green PCR reaction included 1x Power SYBR Green PCR mastermix and 0.2  $\mu$ M primermix. The thermal cycling conditions were as follows: hot enzyme activation at 95°C for 10 min followed by 40 cycles of amplification – DNA denaturation at 95°C for 10 sec and annealing of primers/DNA extension at 60°C for 1 min. For SYBR Green-based detection, a dissociation curve was carried out by one cycle following the last amplification cycle to control for the specificity of PCR amplification: 95°C for 15 sec, 60°C for 30 sec, 95°C for 15 sec. The list of genes analyzed by real-time PCR and SYBR Green primers are listed in “Materials”. Relative quantification was performed by calculating the difference in cross-threshold values ( $\Delta C_t$ ) of the region of interest and the Input control (see section 2.2.11) according to the formula  $2^{-\Delta C_t}$ .

#### **2.2.6.3 Genotyping of SNPs**

Genotypes of the *GARP* gene locus were determined by TaqMan SNP Genotyping assays (Life technologies). SNP Genotyping assays contain two unlabeled PCR primers (For and Rev), one VIC dye-labeled probe that detects the allele 1 sequence and one FAM dye-labeled probe that detects the allele 2 sequence. The 5' end of the probe is linked to the reporter dye (FAM or VIC) and the 3' end is linked to a NFQ and a MGB. The principle of the PCR is the same as for

TaqMan Gene Expression assays. Each probe anneals specifically to a complementary sequence between the primers. The probes are designed so their off-target hybridization is highly reduced, thus, the fluorescence signal generated by the PCR amplification indicates which allele is in the sample. Signals of only one dye indicate homozygosity and signals of both dyes indicate heterozygosity.

PCR amplification was performed using 10 ng of DNA in a final volume of 10  $\mu$ l. The TaqMan SNP Genotyping reaction contained 1x TaqMan Universal PCR mastermix and 0.25  $\mu$ M SNP Genotyping Assay mix. The thermal cycling conditions were as follows: hot enzyme activation at 95°C for 10 min followed by 40 cycles of amplification – DNA denaturation at 95°C for 15 sec and annealing of primers/DNA extension at 60°C for 1 min. The list of SNPs analyzed by real-time PCR and the respective assays are listed in “Materials”.

### **2.2.7 5'Rapid Amplification of cDNA Ends (RACE)**

The 5'RACE was performed using the 5'RACE System for Rapid Amplification of cDNA Ends Version 2.0 (Life technologies) according to manufacturer's protocol. The method is used to amplify nucleic acid sequences from mRNA templates between a defined internal site and unknown sequences at the 5' end of the mRNA. 4  $\mu$ g total RNA from 4 different donors were used for each reaction. Reverse transcription with the gene-specific primer 1 (GSP1) was performed in a total volume of 25  $\mu$ l. Therefore, 2.5 pmol GSP1, 1x PCR Buffer, 2.5 mM MgCl<sub>2</sub>, 0.4 mM dNTPs, 10  $\mu$ M DTT, and 1  $\mu$ l of Superscript II RT were added to the RNA. The reaction was carried out at 42°C for 50 min, followed by 70°C for 15 min. Then, 1  $\mu$ l of the RNase Mix was added and incubated for 30 min at 37°C. The cDNA was purified with the S.N.A.P. column purification. The TdT-tailing of the cDNA was carried out in 25  $\mu$ l by adding 10  $\mu$ l of purified cDNA, 1x tailing buffer, 0.2 mM dCTP, and 1  $\mu$ l TdT. The reaction was incubated for 10 min at 37°C followed by 10 min at 65°C. The dT-tailed cDNA was then used in a PCR reaction with a total volume of 25  $\mu$ l adding the following contents: 1x Reaction buffer, 1.5 mM MgCl<sub>2</sub>, 0.2 mM dNTPs, 0.4  $\mu$ M GSP2, 0.4  $\mu$ M AAP, and 0.05 units Taq-DNA-Polymerase. The cycling parameters were as follows: 35 cycles at 94°C for 1 min, 55°C for 30 sec, 72°C for 2 min. The nested-PCR was carried out similar like above, except of the following changes: nested GSP and AUAP were used at the same concentrations. PCR products were then used in a real-time PCR with specific TaqMan Gene Expression assays for transcript variant 1 or 2 (see section 2.2.6.1).

## **2.2.8 DNA amplification and purification**

### ***2.2.8.1 AmpliTaq DNA Polymerase PCR (Life technologies)***

PCR amplification was performed using 1 µl of cDNA, gDNA or plasmid DNA in a final volume of 25 µl. The reaction contained 1x GeneAmp® PCR buffer I, 250 µM dNTPs, 0.5 µM Primermix, and 0.5 units AmpliTaq® DNA Polymerase. Cycling parameters were as follows: 95°C 5 min, 35 cycles at 95°C 30 sec, 60°C 30 sec, 72°C 1-2 min, and a final extension at 72°C for 7 min.

### ***2.2.8.2 Herculase II Fusion DNA Polymerase PCR (Agilent Technologies)***

PCR amplification was performed using 1 µl of cDNA or gDNA in a final volume of 25 µl. The reaction contained 1x Herculase II reaction buffer, 250 µM dNTPs, 0.5 µM Primermix, 3% DMSO, and 0.25 µl Herculase II fusion DNA polymerase. Cycling parameters were as follows: 98°C 4 min, 35 cycles at 98°C 20 sec, 60°C 20 sec, 68°C 1-2 min, and a final extension at 68°C for 3 min.

### ***2.2.8.3 GeneAmp High Fidelity PCR System (Life technologies)***

PCR amplification was performed using 1 µl of cDNA or gDNA in a final volume of 25 µl. The reaction contained 1x GeneAmp High Fidelity PCR buffer, 250 µM dNTPs, 0.5 µM Primermix, and 0.2 µl GeneAmp High Fidelity Enzyme mix. Cycling parameters were as follows: 95°C 5 min, 35 cycles at 95°C 30 sec, 60°C 30 sec, 72°C 1-2 min, and a final extension at 72°C for 7 min.

### ***2.2.8.4 EpiMark Hot Start Taq DNA Polymerase PCR (New England Biolabs)***

PCR amplification was performed using 1 µl of bisulfite treated DNA in a final volume of 25 µl. The reaction contained 1x EpiMark Hot Start Taq Reaction buffer, 200 µM dNTPs, 0.2 µM Primermix, and 1.25 units EpiMark Hot Start Taq DNA polymerase. Cycling parameters were as follows: 95°C 5 min, 35 cycles at 95°C 30 sec, 60°C 30 sec, 68°C 1-2 min, and a final extension at 68°C for 5 min.

### ***2.2.8.5 DNA fragment purification***

PCR products were purified with the QIAquick PCR Purification kit (Qiagen) according to manufacturer's protocol to remove primers, nucleotides, enzymes, mineral oil, salts, and other

impurities from DNA samples. Briefly, 5 volumes of PB buffer were added to one volume of PCR reaction and transferred on a QIAquick column, centrifuged for 30 sec to bind DNA. The column was washed once with 750  $\mu$ l PE buffer and eluted in 32  $\mu$ l Elution buffer.

PCR products were separated on a 1-2% agarose gel. Therefore, 1-2 g of agarose (1-2%) was boiled in 100 ml of 1x TAE buffer until the agarose was melted. The agarose solution was cooled to  $< 50^{\circ}\text{C}$ , mixed with 5  $\mu$ l of SYBR® Safe DNA Gel stain (Life technologies) and filled into the sealed gel tray. To perform DNA separation, the polymerized agarose gel was placed in the gel chamber Nautico 10x107 (H. Hölzel) filled with 1x TAE buffer to cover the gel. 5  $\mu$ l of each PCR sample were mixed with 1x DNA loading buffer and transferred into a gel pocket. To control the size of the PCR products, a suitable molecular weight standard (100 bp or 1 kb DNA ladder, Fermentas) was included in each electrophoresis run. Electrophoresis was performed at 100V for 30 min. The DNA bands were visualized and photographed on a UVT-28 MP transilluminator (Herolab). PCR fragments were excised from the gel with a scalpel and purified with the QIAquick Gel Extraction kit according to manufacturer's protocol to remove primers, nucleotides, enzymes, mineral oil, salts, and other impurities from DNA samples. Briefly, one volume of agarose gel was diluted in 5 volumes of QG buffer and incubated at  $50^{\circ}\text{C}$  for 10 min until the gel was dissolved completely. Then, one gel volume of 100 % isopropanol was added, the solution was loaded on a QIAquick column, and centrifuged for 30 sec to bind DNA. The column was washed once with 500  $\mu$ l QG buffer and once with 750  $\mu$ l PE buffer. Afterwards the DNA was eluted in 32  $\mu$ l Elution buffer.

### 2.2.9 Cloning

For and Rev primers (see section 2.1.8) were used for MafF cds amplification. The Kozak sequence was introduced in the For primer and is shown underlined, for consecutive cloning steps. The Herculase-PCR product for the MafF cds was cloned into pcDNA3.1D/V5-His-TOPO vector. Cloned sequences were confirmed by sequencing (Eurofins Genomics). The MafF cds was released from pcDNA3.1D/V5-His-TOPO by digestion with HindIII and XhoI restriction nucleases and inserted into pEGFP-N1 vector between HindIII and SalI sites.

For and Rev primers (see section 2.1.8) were used for GARP promoter and CNS region amplification. Restriction sites of EcoRV and HindIII shown underlined were introduced into For and Rev primers, for consecutive cloning steps. The PCR products for the promoter regions were cloned into pCR2.1-TOPO vector. Cloned sequences were confirmed by sequencing

(Eurofins Genomics). The promoter or CNS sequences were released from pCR2.1 by digestion with EcoRV and HindIII restriction nucleases and inserted into pGL4.10[luc2] vector or pCpGL-basic between EcoRV and HindIII sites.

NFAT-, Foxp3-, NF- $\kappa$ B-, RXR, and Sp1-binding sites were described using several *in silico*-prediction tools (Cartharius et al. 2005; Farre et al. 2003; Messeguer et al. 2002; Quandt et al. 1995). The down-stream P1 NFAT/Foxp3-mutant sequences were synthesized (Eurofins Genomics), digested with EcoRV and HindIII restriction nucleases (New England Biolabs) and inserted into pGL4.10[luc2] vector between EcoRV and HindIII sites. The up-stream promoter P2 Foxp3 sequences and the down-stream promoter P1 RXR mutant sequences were generated using site-directed mutagenesis. pDEST12.2 (Promega) expression vector including human Foxp3 cds was kindly provided by Prof. Dr. Heissmeyer (Ludwig-Maximilians-Universität, Munich).

#### **2.2.9.1 Restriction enzyme digestion**

1  $\mu$ g of DNA were digested in a total volume of 20  $\mu$ l containing 2.5 units/ $\mu$ l suitable restriction enzymes with respective 1x supplied Reaction buffer as listed in section 5.1.5. The reaction was carried out at 37°C for 1 hour followed by an inactivation step at 65°C for 20 min. If gel extraction was necessary, 8  $\mu$ g of DNA were digested in a total volume of 160  $\mu$ l.

#### **2.2.9.2 TOPO TA Cloning**

TOPO TA Cloning was performed using the TOPO TA Cloning kit (Life technologies) according to manufacturer's instructions. Briefly, 1-2  $\mu$ l freshly purified PCR product were mixed with 10 ng pCR2.1-TOPO or pcDNA3.1D/V5-His-TOPO and 1x Salt solution (0.2 M NaCl, 0.01 M MgCl<sub>2</sub>) in a total volume of 6  $\mu$ l. The ligation was carried out at room temperature for 30 min, transferred onto ice and 2  $\mu$ l were subsequently used in a transformation reaction.

#### **2.2.9.3 Quick Ligase Reaction**

Purified PCR products or cut out and purified fragments (e.g. after restriction enzyme digest) from pcDNA3.1D/V5-His-TOPO or pCR2.1-TOPO were ligated into pEGFP-N1, pGL4.10[luc2] or pCpGL-basic (Klug et al. 2006) using the Quick Ligation kit (New England Biolabs) in a final volume of 20  $\mu$ l. 50 ng of vector were combined with a 3-fold molar excess of insert, 1x Quick Ligation buffer and 1  $\mu$ l of Quick T4 DNA ligase. The ligation was carried out at room temperature for 30 min.

#### **2.2.9.4 Site-directed mutagenesis**

Up- or down-stream promoter plasmid inserts were mutated with the QuickChange® Lightning Site-Directed Mutagenesis kit (Agilent Technologies) according to manufacturer's protocol. Oligonucleotides listed in section 2.1.8 were used for mutation reactions. Oligonucleotide primers were designed that they include a restriction site to confirm mutagenesis with a restriction digest. The mutagenesis was performed in a total volume of 25 µl consisting of 1x Quick Change® Lightning buffer, 25 ng vector, 0.5 µl dNTP mix, 0.75 µl QuickSolution reagent, 62.5 ng oligonucleotide primers and 0.5 µl QuickChange® Lightning enzyme. The cycling parameters were as follows: 95°C 2 min, 18 cycles at 95°C 20 sec, 60°C 20 sec, 68°C 3 min, and a final extension at 68°C for 5 min. Afterwards, 2 µl of the provided *DpnI* restriction enzyme was added directly to each amplification reaction and incubated for 5 min at 37°C to digest parental methylated DNA. Subsequently, transformation with XL10-Gold® Ultracompetent cells was performed. Cells were pre-chilled in a 13 ml polypropylene round-bottom tube on ice and 2 µl of β-mercaptoethanol was added. After 2 min incubation, 2 µl of the *DpnI*-treated DNA from each reaction was transferred into the bacteria tube. The reaction was incubated for 30 min on ice and heated for 30 sec to 42°C. After 2 min incubation on ice, 100 µl of each transformation reaction was plated on an ampicillin-containing LB agar plate and incubated for 16 hours at 37°C. 5-10 colonies were picked and transferred into a 13 ml falcon with 3 ml of LB broth (liquid) containing ampicillin. After overnight culture at 37°C plasmid DNA was isolated and control restriction digest was performed to check that mutagenesis was working. Positive clones were then sent out for sequencing (Eurofins Genomics) to control for the right sequence.

#### **2.2.9.5 LB plates**

16 g LB agar (Life technologies) was diluted in 500 ml MilliQ. The solution was stirred for 10 min and autoclaved. After cooling to < 50°C, 50 mg ampicillin (Life technologies) or zeocin (InvivoGen) was added. 20 ml were transferred into each petri dish under the sterile bench. After polymerization, plates were stored at 4°C for a maximum of 2 weeks. Before use, plates were pre-warmed to 37°C and 30 µl of 20 mg/ml X-Gal (Life technologies) were spread onto one plate, if blue/white screening was performed (e.g. pCR2.1-TOPO).

### **2.2.9.6 Transformation**

2 µl of the ligation reaction were carefully added into one vial of One Shot TOP10 chemically competent *Escherichia coli* (*E.coli*) cells (Life technologies) and incubated for 30 min on ice. Then, cells were heat-shocked for 30 sec at 42°C, 250 µl S.O.C. medium was added and shaken horizontally at 200 rpm at 37°C for one hour. 100-200 µl from each transformation was spread on a pre-warmed selective plate. Plates were incubated at 37°C for 12 hours to ensure efficient blue/white selection and obtain visible colonies. 5-10 colonies were taken to be cultured overnight at 37°C and 225 rpm in 3 ml LB broth (liquid) containing ampicillin or kanamycin.

2 µl of the ligation reaction with pCpGL luciferase vectors were carefully added into one vial of One Shot PIR1 chemically competent *E.coli* cells (Life technologies) because the vector includes a R6K origin. Cells were incubated for 30 min on ice, heat-shocked for 30 sec at 42°C, 250 µl S.O.C. medium was added and shaken horizontally at 200 rpm at 37°C for one hour. 100-200 µl from each transformation was spread on a pre-warmed selective plate with zeocin. Plates were incubated at 37°C for 12 hours to obtain visible colonies. 5-10 colonies were taken to be cultured overnight at 37°C and 225 rpm in 3 ml LB broth (liquid) containing zeocin. Plasmid DNA was isolated, checked by PCR with appropriate primers and digested with suitable restriction enzymes to confirm the presence and the correct orientation of the insert. DNA sequencing was performed using either the “value read tube” or the “prepaid plate kit” service from Eurofins Genomics. 750 ng of plasmid DNA in a total volume of 15 µl were used per sequencing. 2 µl of 10 µM sequencing primer were enclosed if necessary. If “prepaid plate kits” were used (bisulfite sequencing), plasmid clones were send out as stab cultures in 96-well plates containing agar with ampicillin.

### **2.2.9.7 Plasmid DNA miniprep**

Miniprep was performed with the QIAprep Spin Miniprep kit (Qiagen) following manufacturer's instructions for a desired DNA yield lower than 20 µg. Briefly, 2 ml of overnight cultured bacteria were pelleted at 10,000 xg for 2 min and resuspended in 250 µl buffer P1. Next, 250 µl buffer P2 were added and tubes were inverted 4-6 times before the lysis was terminated with 350 µl of buffer N3. After centrifugation at 16,000 xg for 10 min, the supernatants were decanted onto a QIAprep spin column to bind plasmid DNA. The columns were washed once with 500 µl PB and 750 µl PE buffer. After centrifugation, DNA was eluted with 32 µl Elution buffer. The concentration and purity of the plasmid DNA was determined by measuring the absorbance at

230 nm, 260 nm, and 280 nm ( $A_{260}/A_{230}$ ,  $A_{260}/A_{280}$ ).

#### **2.2.9.8 Plasmid DNA maxiprep**

Maxiprep was performed with the QIAGEN Plasmid Maxi kit (Qiagen) following manufacturer's instructions for a desired DNA yield up to 500  $\mu$ g. Briefly, 300 ml of overnight cultured bacteria were pelleted at 10,000  $\times$ g for 2 min and resuspended in 10 ml buffer P1. Next, 10 ml buffer P2 was added and tubes were inverted 4-6 times and incubated for 5 min at room temperature. The lysis was terminated with 10 ml of buffer P3 on ice for 20 min. After centrifugation at 20,000  $\times$ g for 10 min, the supernatants were decanted onto an equilibrated column to bind plasmid DNA. The columns were washed twice with 30 ml buffer QC and DNA was eluted in pre-warmed 15 ml buffer QF. Then, DNA was precipitated with 10.5 ml isopropanol and centrifuged at 20,000  $\times$ g. After centrifugation, DNA was air-dried and redissolved in 500  $\mu$ l. The concentration and purity of the plasmid DNA was determined by measuring the absorbance at 230 nm, 260 nm, and 280 nm ( $A_{260}/A_{230}$ ,  $A_{260}/A_{280}$ ). Afterwards, DNA concentration was adjusted to 0.5  $\mu$ g/ $\mu$ l.

#### **2.2.9.9 Bacterial glycerol stock**

3 ml of overnight cultured bacteria in LB broth (liquid) were supplemented with 390  $\mu$ l 100 % glycerol and split into three 1.5 ml Cryotubes (Greiner, Kremsmünster, Austria). The bacteria stock were frozen and stored at  $-80^{\circ}\text{C}$ .

#### **2.2.10 Luciferase reporter assays**

Cell lines and primary T cells were transfected with reporter luciferase vectors using the appropriate Amaxa® Cell line or Human T Cell Nucleofector kit (Lonza). The Amaxa Nucleofector technology is based on the transient creation of small pores in cell membranes by electroporation in combination with cell-type specific reagents. The plasmid is directly transferred into the cytoplasm and nucleus. Luciferase reporter assays were carried out with the Dual-luciferase Reporter Assay system (Promega). The activities of firefly (*Photinus pyralis*) and renilla (*Renilla reniformis*) luciferases are measured sequentially from a single sample. Luciferases are enzymes that catalyze the oxidative carboxylation of a substrate in the presence of  $\text{O}_2$  to yield photo emission (bioluminescence). After detection of the firefly luminescence the reaction is quenched and the renilla reaction is initiated by adding the renilla-specific substrate.

### ***2.2.10.1 Transfection of the EL-4 cell line***

EL-4 cells were transfected with the Amaxa Cell Line Nucleofector kit L (Lonza) according to manufacturer's instructions. Briefly,  $9.6 \times 10^6$  cells were resuspended in 656  $\mu\text{l}$  Cell Line Nucleofector solution L + 144  $\mu\text{l}$  supplement and divided into 8 transfections. 5  $\mu\text{g}$  promoter-luciferase reporter vectors, 0.25  $\mu\text{g}$  renilla control vector and 2.5  $\mu\text{g}$  pDEST12.2-hFoxp3 expression vector or pcDNA3.1-CTGFP control vector were used per transfection. The appropriate program C-009 was selected and 550  $\mu\text{l}$  10% FCS/DMEM was added after transfection. Cells were transferred to a 48 well plate and incubated at 37°C for 2 hours. Then, 50  $\mu\text{l}$  of the cell suspension was divided into 12 wells of a 96 well plate (100,000 cells per well). Treatment of cells with different stimuli was performed in triplets in a total volume of 75  $\mu\text{l}$  per well. 10 ng/ml PMA, 1  $\mu\text{M}$  ionomycin, 5 ng/ $\mu\text{l}$  TGF- $\beta$ , 10  $\mu\text{M}$  retinoic acid, 1  $\mu\text{g}/\text{ml}$  CsA, and 160  $\mu\text{M}$  JSH-23 was used, respectively. Cells were incubated overnight at 37°C and 17 hours after transfection the dual-luciferase reporter assay was started.

### ***2.2.10.2 Methylation analysis with luciferase reporter assays***

Promoter sequences were cloned into the CpG-free vector, pCpGL-basic, as described above. Thus, upon methylation only the insert gets methylated. 1  $\mu\text{g}$  of the vector was methylated in a total volume of 20  $\mu\text{l}$  containing 1x NEBuffer 2, 3.2 mM S-Adenosylmethionine (SAM), and 4 units of SssI methylase (New England Biolabs). The reaction was carried out at 37°C for 1 hour, followed by heating at 65°C for 20 min to stop the reaction. The methylated vector was purified using the QIAquick PCR purification kit (Qiagen). EL-4 cells were transfected with the Amaxa Cell Line Nucleofector kit L (Lonza) according to manufacturer's instructions. Briefly,  $9.6 \times 10^6$  cells were resuspended in 656  $\mu\text{l}$  Cell Line Nucleofector solution L + 144  $\mu\text{l}$  supplement and divided into 8 transfections. 5  $\mu\text{g}$  methylated and non-methylated promoter-luciferase reporter vectors, 0.25  $\mu\text{g}$  renilla control vector and 2.5  $\mu\text{g}$  pDEST12.2-hFoxp3 expression vector or pcDNA3.1-CTGFP control vector were used per transfection. The appropriate program C-009 was selected and 550  $\mu\text{l}$  10% FCS/DMEM was added after transfection. Cells were transferred to a 48 well plate and incubated at 37°C for 2 hours. Then, 50  $\mu\text{l}$  of the cell suspension was divided into 12 wells of a 96 well plate (100,000 cells per well). Treatment of cells with different stimuli was performed in triplets in a total volume of 75  $\mu\text{l}$  per well. 10 ng/ml PMA and 1  $\mu\text{M}$  ionomycin were used, respectively. Cells were incubated overnight at 37°C and 17 hours after transfection the dual-luciferase reporter assay was started.

In some experiments inserts of the pGL4.10 vector were cut out and methylated separately. 1 µg of the insert was methylated in a total volume of 20 µl containing 1x NEBuffer 2, 3.2 mM SAM, 1, 0.1, or 0.01 units of SssI methylase (New England Biolabs), respectively. The reaction was carried out at 37°C for 1 hour, followed by heating at 65°C for 20 min to stop the reaction. The methylated insert was purified using the QIAquick PCR purification kit (Qiagen) and ligated via the Rapid Ligation system back into the cut pGL4.10 vector. EL-4 cells were transfected with the Amaxa Cell Line Nucleofector kit L (Lonza) according to manufacturer's instructions. Briefly,  $3.6 \times 10^6$  cells were resuspended in 492 µl Cell Line Nucleofector solution L +  $10 \times 10^7$  µl supplement and divided into 6 transfections. 1 µg methylated and non-methylated promoter-luciferase reporter vectors, 0.05 µg renilla control vector and 0.5 µg pDEST12.2-hFoxp3 expression vector or pcDNA3.1-CTGFP control vector were used per transfection. The appropriate program C-009 was selected and 250 µl 10% FCS/DMEM was added after transfection. Cells were transferred to a 48 well plate and incubated at 37°C for 2 hours. Then, 50 µl of the cell suspension was divided into 6 wells of a 96 well plate (100,000 cells per well). Treatment of cells with different stimuli was performed in triplets in a total volume of 75 µl per well. 10 ng/ml PMA and 1 µM ionomycin were used, respectively. Cells were incubated overnight at 37°C and 17 hours after transfection the dual-luciferase reporter assay was started.

### ***2.2.10.3 Transfection of primary human T cells***

After isolation of primary human Tregs or Tconvs, cells were transfected with the Amaxa Human T Cell Nucleofector kit (Lonza) according to manufacturer's instructions. Briefly, approximately  $5.4 \times 10^6$  cells were resuspended in 328 µl Human T Cell Nucleofector® Solution + 72 µl Supplement and divided into 4 transfections. 2.5 µg promoter-luciferase reporter vectors, 0.125 µg renilla control vector were used per transfection. The appropriate program U-014 was selected and 400 µl 10% NHS/RPMI was added after transfection. Cells were transferred to a 48 well plate and incubated at 37°C for 2 hours. Then, 50 µl of the cell suspension was divided into 9 wells of a 96 well plate (150,000 cells per well). Treatment of cells with different stimuli was performed in triplets in a total volume of 75 µl per well. Anti-CD3/CD28-Dynabeads (cell to bead ratio 1:1) in the presence of 100 units/ml human recombinant IL-2 or 10 ng/ml PMA and 1 µM ionomycin were used, respectively. Cells were incubated overnight at 37°C and 17 hours after transfection the dual-luciferase reporter assay was started.

#### **2.2.10.4 Dual-Luciferase Reporter assay**

After transfection and overnight-incubation of the cells 75  $\mu$ l of the Luciferase Assay reagent II was added to each well and the suspension was transferred into a 96-well plate appropriate for luciferase measurement. After 10 min incubation at room temperature in the dark, the firefly luminescence was measured at an emission wavelength of 560 nm. Next, 75  $\mu$ l of the Stop&Glo® reagent was added and after 10 min incubation at room temperature in the dark, the renilla luminescence was measured at an emission wavelength of 480 nm. The ratio of luciferase and renilla luminescence was calculated and those values were normalized to the empty control vector pGL4.10[luc2] and displayed as relative luciferase units.

#### **2.2.11 ChIP**

ChIP assay can be used to determine whether transcription factors or histone modifying complexes interact with a candidate gene sequence. Additionally, it is used to monitor the presence of histones with post-transcriptional modifications at specific genomic locations. Thus, targets of histone modifiers and transcription factors can be analyzed, the transcriptional state of the region can be detected, and regulatory regions (e.g. promoters, enhancers, or repressors) can be described.

##### **2.2.11.1 Histone modifications**

$2-3 \times 10^6$  cells were resuspended in 10 ml RPMI complete medium and 1% formaldehyde was added to crosslink the chromatin for 10 min at room temperature. The reaction was stopped with 125 mM glycine for 5 min at room temperature. All centrifugation steps were performed at 723 xg at 15°C for 5 min. After centrifugation, the cell pellet was washed twice with ice-cold PBS. Then, the cells were resuspended in 250  $\mu$ l Swelling buffer and incubated for 10 min at room temperature with iterated vortexing every 2 min. After centrifugation, cells were resuspended in 250  $\mu$ l Sonication buffer. The suspension was frozen at -80°C for at least 1 hour. Then, the sample was sonicated in a Bioruptor® Plus (Diagenode) for 25 cycles with 30 sec intervals. To sediment cell debris the sheared chromatin was centrifuged for 10 min at 16,000 xg at 4°C and supernatant was transferred to a new 1.5 ml tube. Afterwards, 34  $\mu$ l of the sheared chromatin was re-crosslinked by adding 250 mM NaCl, 40  $\mu$ g of Proteinase K and 20  $\mu$ g of RNase A and digest for 2 hours at 55°C followed by stopping the reaction for 30 min at 95°C. The DNA was isolated using the GenElute PCR Clean-Up kit (Sigma-Aldrich) according to manufacturer's protocol.

Briefly, 500  $\mu$ l Column Preparation solution was added to each column. Then, 170  $\mu$ l Binding solution (5 volumes) were added to the chromatin and transferred to the column. Centrifugation steps were performed at 13,000  $xg$  for 1 min. The DNA was bound to the column by centrifugation and washed once with 500  $\mu$ l Wash solution. The column was dried and DNA was eluted in 32  $\mu$ l Elution solution. 15  $\mu$ l were loaded with 2.2  $\mu$ l of 6x Loading dye on a 2% agarose gel to check the fragment size that should range from 200 bp to 1000 bp. The other 15  $\mu$ l were filled up to 30  $\mu$ l with MilliQ and used as Input control.

Next, Nunc Maxisorp 96 well plates (Thermo Scientific) were coated with antibodies. 100  $\mu$ l ELISA/ELISPOT Coating buffer (ebioscience) were prepared per well and 2  $\mu$ g of anti-H3K4me3, anti-H3ac, anti-H3K27me3 or rabbit IgG control were added per well. Plate was closed with an adhesive foil and incubated at 4°C overnight. The next morning, the plate was washed three times with 200  $\mu$ l of ELISA Wash buffer (ebioscience). To immunoprecipitate the fragmented DNA 100  $\mu$ l per IP was used. The sheared chromatin was filled up to 400  $\mu$ l with Sonication buffer and 100  $\mu$ l was transferred into each well. The plate was shaken on an Orbital Shaker (Heidolph) at 300 rpm at room temperature for 90 min. The plate was washed twice with Sonication buffer, Wash buffer A, Wash buffer B, and TE buffer. To re-crosslink the precipitated chromatin 75  $\mu$ l TE buffer, 250 mM NaCl, 40  $\mu$ g of Proteinase K, 20  $\mu$ g of RNase A and 0.5% SDS was added to each well in a total volume of 100  $\mu$ l. The plate was incubated for 2 hours at 65°C and 500 rpm. Then, 500  $\mu$ l Binding solution of the GeneElute PCR Clean-up kit (Sigma-Aldrich) was added to each sample and DNA purification was proceeded as stated above. The chromatin was stored at -20°C until real-time PCR analysis was performed with ChIP assay real-time PCR primers (see section 2.1.8).

#### ***2.2.11.2 Transcription factors and chromatin remodeling complexes***

For ChIP with antibodies against Foxp3, NFAT1, p50, c-Rel, p65, MLL1, RbBP5, and PLU-1 the ChIP-IT High Sensitivity kit (Active Motif) was used with the following changes. For 4 IPs  $12 \times 10^6$  Tregs and Tconvs were isolated from 8-10 donors and resuspended in 10 ml 10% NHS/RPMI and 1% formaldehyde was added to crosslink the chromatin for 10 min at room temperature. The reaction was stopped with 125 mM glycine for 5 min at room temperature. All centrifugation steps were performed at 723  $xg$  at room temperature for 5 min. After centrifugation, the cell pellet was washed three times with ice-cold PBS and 1 ml Cell Lysis buffer was added. After 10 min lysis on ice, cells were centrifuged and cell pellet was frozen for

at least 1 hour at  $-80^{\circ}\text{C}$ . The pellet was resuspended in 1 ml Nuclear Lysis buffer and sheared with a dounce homogenizer. The chromatin was sonicated in a Bioruptor® Plus (Diagenode) twice for 25 cycles with 30 sec intervals. To sediment cell debris the sheared chromatin was centrifuged for 10 min at  $16,000 \times g$  at  $4^{\circ}\text{C}$  and the supernatant was transferred to a new 1.5 ml tube. The sample was filled up with ChIP buffer (Active Motif) supplemented with 1x PIC and 1:100 PMSF to 930  $\mu\text{l}$ . 30  $\mu\text{l}$  were re-crosslinked by adding 144  $\mu\text{l}$  TE buffer, 250 mM NaCl, 80  $\mu\text{g}$  Proteinase K, and 20  $\mu\text{g}$  RNase A and incubate for 2 hours at  $55^{\circ}\text{C}$  followed by stopping the reaction at  $95^{\circ}\text{C}$  for 30 min. To purify the DNA, the MN PCR Purification kit (Macherey-Nagel) with the NTB buffer was used. Briefly, 60  $\mu\text{l}$  of NTB buffer were added to the sheared chromatin and transferred to a column to bind DNA. The centrifugation steps were performed at  $11,000 \times g$  for 1 min at room temperature. Membrane was washed with 700  $\mu\text{l}$  NT3 buffer and then dried by centrifugation. The DNA was eluted with 30  $\mu\text{l}$  NE buffer and 15  $\mu\text{l}$  were loaded with 2.2  $\mu\text{l}$  of 6x Loading dye on a 2% agarose gel to check the fragment size that should range from 200 bp to 1000 bp. The other 15  $\mu\text{l}$  were filled up to 30  $\mu\text{l}$  with MilliQ and used as Input control.

To immunoprecipitate, 220  $\mu\text{l}$  the chromatin was supplemented with 10  $\mu\text{g}$  of anti-human Foxp3, anti-human NFAT1, anti-human p50, anti-human c-Rel, anti-human p65, anti-human MLL1, anti-human RbBP5, anti-human PLU-1 antibodies, or 2  $\mu\text{g}$  IgG controls, 5  $\mu\text{l}$  Blocker solution, and 5  $\mu\text{l}$  PIC, respectively. The mixture was incubated at  $4^{\circ}\text{C}$  in a MACSmix Tube rotator (Miltenyi Biotec) overnight. Next morning, the Protein G agarose beads were washed twice with an equal volume of TE buffer. 30  $\mu\text{l}$  of beads were added to the antibody-chromatin mixture and incubated for 3 hours at  $4^{\circ}\text{C}$  in a MACSmix Tube rotator. To wash the beads with the bound antibodies and chromatin, an appropriate number of ChIP Filtration Columns was prepared by removing the tap from the bottom and put in a rack to allow gravity flow-through. After addition of 600  $\mu\text{l}$  ChIP buffer, the precipitation reaction with the beads was transferred to the columns. The columns were washed four times with 900  $\mu\text{l}$  Wash Buffer AM1. Next, columns were transferred into 1.5 ml tubes and 50  $\mu\text{l}$   $37^{\circ}\text{C}$  pre-warmed Elution Buffer AM4 was loaded on each column and incubated for 5 min at room temperature. After centrifugation at  $1250 \times g$  for 3 min, the elution was repeated with another 50  $\mu\text{l}$  Elution Buffer AM4. The flow-through (100  $\mu\text{l}$ ) was supplemented with 2  $\mu\text{l}$  Proteinase K and re-crosslinked for 30 min at  $55^{\circ}\text{C}$  followed by 2 hours at  $80^{\circ}\text{C}$ . To clean up the precipitated DNA, 5 volumes of DNA Purification Binding buffer were added, adjusted with 25 mM NaAcetate, and transferred onto a DNA Purification column. Centrifugations were performed at  $13,000 \times g$  for 2 min. The columns were washed with 750  $\mu\text{l}$

DNA Purification Wash Buffer, dried, and DNA was eluted in 36  $\mu$ l 37°C pre-warmed Elution buffer. The chromatin was stored at -20°C until real-time PCR analysis was performed with ChIP assay real-time PCR primers (see section 2.1.8).

### **2.2.12 Bisulfite DNA sequencing**

DNA methylation describes the addition of methyl groups to the carbon-5 position of cytosine residues of the dinucleotide CpG, and is often associated with the repression of transcriptional activity. Bisulfite sequencing is based on the use of bisulfite treatment of DNA to determine the pattern and level of methylation of specific gene loci. During bisulfite treatment unmethylated cytosine residues are deaminated to uracil, while methylated cytosine residues are unaffected. PCR amplification of regions of interest and subsequent cloning of amplicons into vectors allows analysis of the methylation status of these regions by sequencing. Bisulfite sequencing primers were designed using an online tool (Li et al. 2002a) and are listed in the section 2.1.8.

#### **2.2.12.1 Bisulfite conversion reaction**

After isolation of gDNA (see section 2.2.4), 0.5-1  $\mu$ g gDNA was converted using the MethylDetector<sup>TM</sup> Bisulfite Modification kit (Active Motif) according to manufacturer's protocol. Briefly, the conversion reaction was performed in a final volume of 140  $\mu$ l containing 7  $\mu$ l hydroquinone and 120  $\mu$ l Conversion buffer. The reaction was initiated at 94°C for 3 min, followed by incubation at 50°C for 5 hours, and by a hold at 4°C. The on-column desulfonation was performed by mixing the conversion reaction with 500  $\mu$ l DNA Binding buffer and loading it a DNA purification column. After spinning at 10,000 rpm for 30 sec, the column was washed with 200  $\mu$ l DNA Wash buffer. Then, 200  $\mu$ l Desulfonation buffer was added and incubated for 20 min at room temperature. After centrifugation, the column was washed again with 200  $\mu$ l DNA Wash buffer and dried by spinning for 2 min. The converted DNA was eluted with 52  $\mu$ l DNA Elution buffer. The DNA was stored at -20°C until the control PCR and the PCR with the bisulfite sequencing primers were performed.

#### **2.2.12.2 PCR with bisulfite-converted DNA**

1  $\mu$ l of the converted DNA was used in each PCR reaction. For positive control of the conversion reaction p16 outer and inner primers (Active Motif) were used. For the region-specific PCRs, bisulfite sequencing primers were used. The PCR amplification was performed according to EpiMark Hot Start Polymerase PCR in section 2.2.8.4. 5  $\mu$ l of the reaction were used for control

agarose gel electrophoresis, the remaining 20  $\mu$ l were used for agarose gel extraction of the right fragment size band. After isolation of the PCR product of interest, 2  $\mu$ l were used for ligation into pCR2.1-TOPO, followed by transformation into *E.coli* (see section 2.2.9). 12-24 clones were picked for each fragment and AmpliTaq PCR was performed to control for the right insert. 12-24 clones were sent out for sequencing (Eurofins Genomics). The sequencing results were analyzed with the MacVector Software and the percentage of methylation of each CpG was calculated and displayed in a heat map format.

### **2.2.13 DNA-protein binding assay**

To assess the binding ability of transcription factors to methylated and non-methylated ds oligonucleotides that span parts of the differentially methylated down-stream P1 promoter, DNA-protein binding assays were carried out. Oligonucleotides were designed by using the *in silico*-prediction tool (Farre et al. 2003; Messeguer et al. 2002). The ds oligonucleotides contained canonical binding sites for Foxp3, NFAT, or NF- $\kappa$ B. Scr oligonucleotides were generated using an online tool<sup>1</sup> and then tested for absence of respective binding sites using the above mentioned *in silico*-prediction tool. Additionally, oligonucleotides located within the differentially methylated region of the down-stream P1 promoter were tested for binding of Foxp3, NFAT1, or NF- $\kappa$ Bp50.

#### **2.2.13.1 Annealing and methylation of ds oligonucleotides**

Single-stranded oligonucleotides were annealed in Annealing buffer at 95°C for 10 min, followed by cooling down the reaction gradually to 25°C. The methylation of the ds oligonucleotide were performed at 37°C for 1 hour in a total volume of 50  $\mu$ l by adding 1.5  $\mu$ g ds oligonucleotide, 1x NEBuffer 2, 160  $\mu$ M SAM, and 10 units of SssI methylase. The reaction was stopped at 65°C for 20 min. The ds oligonucleotides were purified with the Qiaquick Nucleotide Removal kit (Qiagen) following manufacturer's protocol.

#### **2.2.13.2 Transfection and stimulation**

Jurkat cells were transfected with the Amaxa Cell Line Nucleofector kit V (Lonza) according to manufacturer's instructions. Briefly, 5x10<sup>6</sup> cells were resuspended in 328  $\mu$ l Cell Line Nucleofector® solution V + 72  $\mu$ l supplement and divided into 4 transfections.

<sup>1</sup> <https://www.genscript.com/ssl-bin/app/scramble>

2.5  $\mu\text{g}$  pDEST12.2-hFoxp3 expression vector was used per transfection. The appropriate program X-001 was selected and 1 ml 10% FCS/RPMI was added after transfection. Cells were transferred to a 6 well plate and incubated at 37°C overnight. For the assay with anti-NFAT1 or p50,  $20 \times 10^6$  Jurkat cells were stimulated overnight with 10 ng/ml PMA and 1  $\mu\text{M}$  ionomycin, respectively. The nuclear extracts were isolated from a total of  $20 \times 10^6$  Jurkat cells.

#### ***2.2.13.3 Nuclear extraction***

The nuclear extracts were isolated with the EpiQuik Nuclear Extraction Kit II (Epigentek) following the manufacturer's protocol. Briefly, cells were harvested and centrifuged for 5 min at 723 xg. The pellet was resuspended in 2 ml 1x NP1 supplemented with 1:1000 DTT and 1:1000 PIC and incubated on ice for 10 min. After vortexing for 10 sec, they were centrifuged for 1 min at 13,400 xg and the cytoplasmic extract was carefully removed from nuclear pellet. The pellet was resuspended in 200  $\mu\text{l}$  NP2 supplemented with 1:1000 DTT and 1:10 NP3. After incubation for 15 min on ice with iterative vortexing for 3 sec, the extract was centrifuged for 10 min at 16,100 xg and 4°C. The supernatant was transferred into a new tube and 1:100 NP4 was added and incubated at room temperature for 20 min. After centrifugation for 1 min at 16,100 xg and 4°C, the supernatant was transferred into a new tube and the protein concentration was measured.

#### ***2.2.13.4 Measurement of protein concentration***

Protein concentration in nuclear extracts was determined by Bio-Rad Protein Assay kit (Bio-Rad) based on the manufacturer's instructions. This measurement is based on the method of Bradford (Bradford 1976). The Coomassie brilliant blue G-250 dye binds primarily basic (especially arginine) and aromatic amino acid residues. By comparing the color change of a sample to a standard curve a relative measurement of protein concentration is provided. Briefly, 10  $\mu\text{l}$  of the nuclear lysates were incubated with 200  $\mu\text{l}$  of 1x protein assay dye reagent (freshly diluted 5x protein assay dye reagent concentrate) for 5 min at room temperature. The quality and quantity of protein were determined by analyzing the absorbance at 595 nm ( $A_{595}$ ) using a BioPhotometer (Eppendorf). Lysates were kept on ice or used immediately in the assay.

#### ***2.2.13.5 DNA-protein binding***

The DNA-protein binding assay was performed with the EpiQuik DNA-protein Binding assay (Fluorometric, Epigentek) according to the manufacturer's instructions with some modifications.

Briefly, nuclear extracts were washed with 1x PF1. Then, the antibodies were diluted in PF2 to a final concentration of 10 µg/ml. 50 µl antibody dilution were added per well and incubated for 1.5 hours at room temperature. Meanwhile, nuclear extracts were cleaned with a 1:10 dilution of NP3 and incubated on ice for 5 min. After centrifugation, the supernatant was collected. The antibody-solution was aspirated from the wells and the wells were washed three times with 1x PF1. Approximately 20 µg of cleaned nuclear extracts were then added to each well, except the negative control where only 1x PF1 was added. The strips were incubated for 1 hour at room temperature at 100 rpm. Afterwards, the extracts were aspirated and the wells were washed three times with 1x PF1. To test the binding ability of the methylated or non-methylated ds oligonucleotide, 400 ng were added in 50 µl Complete PF4 and incubated for 1 hour at 37°C. Next, the wells were washed five times with 1x PF1 and 100 µl PF5 Oligonucleotide Release solution was added. After 30 min of incubation at 55°C, the solution was transferred into a 96-well plate (Microplate 96 well, black, Berthold technologies) and 2 µl PF6 was added. After additional incubation of 30 min, the fluorescence was measured in a TriStar<sup>2</sup> LB 942 Multimode Plate Reader (Berthold technologies) with an extinction filter of 495 nm and an emission filter of 520 nm.

#### **2.2.14 SDS-PAGE and Western blotting**

To determine MafF protein expression in different CD4 T cell subsets under different treatment, Western blot analysis of cell lysates with anti-human MafF antibody was performed. Cells were lysed at  $1 \times 10^6$  cells/20 µl with SDS sample buffer and boiled at 95°C for 5 min or stored at -20°C until use. Gel electrophoresis was performed using the EC120 Mini Vertical Gel System (E-C Apparatus corporation). 3.5 ml of a 15% Resolving gel was first poured. After polymerization, 1.5 – 2 ml of a 4% Stacking gel was poured. The gel electrophoresis was carried out in SDS Running buffer. Boiled cell lysates were centrifuged at 16,000 xg for 5 min and loaded onto the gel. To identify the molecular weight of the bands protein molecular markers were included to each gel (see section 2.1.3). Cell lysates of human MafF-transfected cells were included to MafF detecting gels to control the specificity of the anti-MafF antibody (molecular weight: 18 kDa). The gel was run at a constant current for 30 min (100 V) and a constant 200 V for 1.5 hours. Following electrophoresis, proteins were transferred on a nitrocellulose membrane using the EC140 Mini Blot Module (E-C Apparatus corporation) in the SDS Transfer buffer. The transfer was performed at 150 mA for 1.5 hours. Afterwards, the membrane was blocked with

5% milk powder in SDS Blot buffer for 5 min at room temperature. Afterwards, the membrane was incubated with rabbit anti-human MafF antibodies (1:1000 diluted in SDS Blot buffer containing 5% BSA) for 1 hour at room temperature or overnight at 4°C. The membrane was then washed with SDS Blot buffer three times for 15 min each and incubated with peroxidase-conjugated anti-rabbit antibody diluted 1:1000 in SDS Blot buffer containing 5% milk powder for 1 hour at room temperature. After three washing steps for 15 min with SDS Blot buffer, the membrane was incubated for 1 min with 2 ml of the ECL Western Blotting Detection reagent (1:1 mixture of reagent 1 and reagent 2; all from GE Healthcare) and developed 1-5 min using a FUJIFILM LAS-3000 (Fujifilm, Tokyo, Japan).

#### **2.2.15 Enzyme-linked immunosorbent assay (ELISA)**

Human Quantikine ELISA kits (R&D Systems) were used to quantify cytokine levels in the serum and cell culture supernatants according to the manufacturer's protocol. First, 100 µl sample were applied to each well to allow the binding of cytokine molecules to plate-bound specific primary antibodies. After 3 hours incubation at room temperature, the plate was washed carefully with wash buffer to remove any remaining samples. The cytokine conjugate was applied to each well and incubated for 1 hour at room temperature to allow binding of the specific secondary antibody. The plate was washed again before adding the substrate solution. After 30 min in the dark, 50 µl stop solution was added and the absorption was determined at 450 nm with a wavelength correction at 620 nm with the Tecan Spectra Microplate Reader (Tecan Group).

### 3 RESULTS

#### 3.1 Characterization of molecular mechanisms contributing to the characteristic phenotype of Tregs

##### 3.1.1 Analysis of *GARP* transcription

###### 3.1.1.1 *Expression of two GARP transcript variants*

Two transcript variants transcribed from two alternative promoters are provided for the *GARP* gene by the NCBI Gene database<sup>2</sup>. Those variants differ in the 5'UTR however since the translation start site (ATG) is located in the second exon E2 both transcripts encode the same protein isoform (Figure 2A). Usage of alternative promoters with no variation in the resulting protein has been reported for many genes (Landry et al. 2003). Initially, I tested whether both transcripts account for *GARP* expression in human Tregs. Expression upon TCR/CD28 signaling was carried out by transcript-specific real-time PCR analysis on mRNA isolated from three healthy individuals. Both variants were expressed in freshly isolated CD25+ Tregs and none were detected in CD25- Tconvs (Figure 2B). Expression levels were significantly increased in Tregs after TCR/CD28 stimulation for 24 h and down-regulated after 48 h. Strikingly, the expression of the transcript variant from the P2 promoter located up-stream of P1 promoter was markedly higher compared to transcription from the intragenic P1 promoter. The real-time PCR data on the expression pattern of both transcript variants in Tregs were confirmed by 5' RACE analysis on mRNA pooled from Tregs of four individuals (Figure 2C). These data indicate that both promoters are active in human Tregs however this results in different expression levels.

###### 3.1.1.2 *Transcriptional activity of the alternative GARP promoters*

To analyze transcriptional activity of *GARP*, the non-overlapping 770 bp long up-stream P2 promoter and the 616 bp long down-stream P1 promoter sequences were inserted in front of the luciferase gene into pGL4.10 vector. Treg-specific stimuli, TCR/CD28 stimulation mimicked by PMA and ionomycin and ectopic Foxp3, were used to measure transcriptional activity in luciferase reporter assays. Both promoters were responsive to Treg-specific stimuli in a similar fashion (Figure 3A).

<sup>2</sup> <http://www.ncbi.nlm.nih.gov/gene>

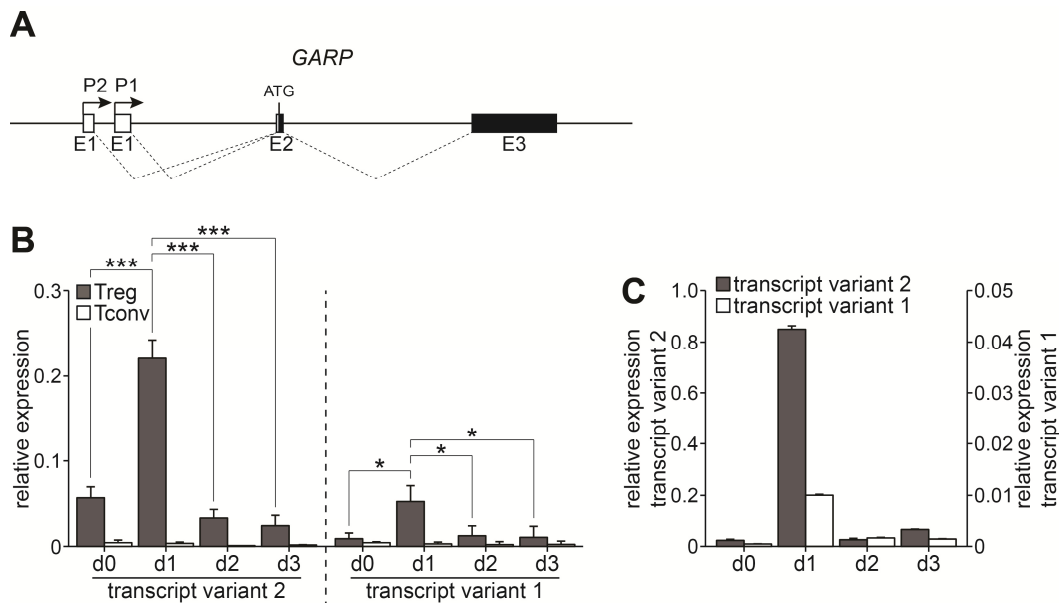


**Figure 2** *GARP* transcript variants are expressed at different levels in human Tregs. (A) Schematic overview of the *GARP* gene locus with indication of two promoters (arrows), non-coding (empty boxes) and coding (black boxes) exons. Two differentially spliced transcript variants are indicated by dashed lines. Transcript variant 2 is initiated from the up-stream promoter 2 (P2) and transcript variant 1 from the down-stream promoter 1 (P1). The translation start site (ATG) is located in the second exon. Both transcript variants encode the same protein isoform. (B, C) Tregs and Tconvs were isolated from healthy individuals and stimulated with anti-CD3/CD28-beads for a total of three days. The *GARP* transcript variant 2 and 1 expression was assessed in freshly isolated (d0) and in stimulated cells at day one (d1), two (d2), and three (d3). (B) Results of real-time PCR analysis using TaqMan gene expression assays specific for each transcript variant are shown as mean  $\pm$  SD of three independent donors. Relative mRNA expression was normalized to the expression levels of *Cyclophilin A* mRNA. (C) Data of 5'RACE assay on RNA pooled from four different donors and subsequent transcript-specific realtime-PCR are depicted as mean  $\pm$  SD of triplet measurements. Statistical analysis was performed using Student's T-test \*  $p < 0.05$ , \*\*\*  $p < 0.001$ .

In both cases, treatment with PMA/ionomycin only slightly increased the luciferase activity whereas ectopic Foxp3-expression was able to increase promoter activity significantly. Of note, the combination of Treg-specific stimuli was able to up-regulate the luciferase activity synergistically. In accordance with a higher abundance of transcript 2, the up-stream P2 promoter activity was prominently stronger than the P1 promoter activity. Next, I investigated the transcriptional activity of the *GARP* promoters in primary human T cells. It was induced from both promoters in response to TCR/CD28 or PMA/ionomycin stimulation only in Foxp3-expressing Tregs and not in Tconvs confirming the Treg-specificity of both promoters (Figure 3B). Also in primary Tregs, luciferase activity induced from up-stream P2 promoter was more pronounced than that from the down-stream P1 promoter. Thus, both promoters were responsive to the Treg-specific stimulation. The up-stream P2 promoter possessed much stronger transcriptional activity compared to the down-stream P1 promoter. Both promoters are

responsible for *GARP* expression in human Tregs upon activation however the stronger responsiveness of the up-stream P2 promoter suggests that this is the main promoter of *GARP*.

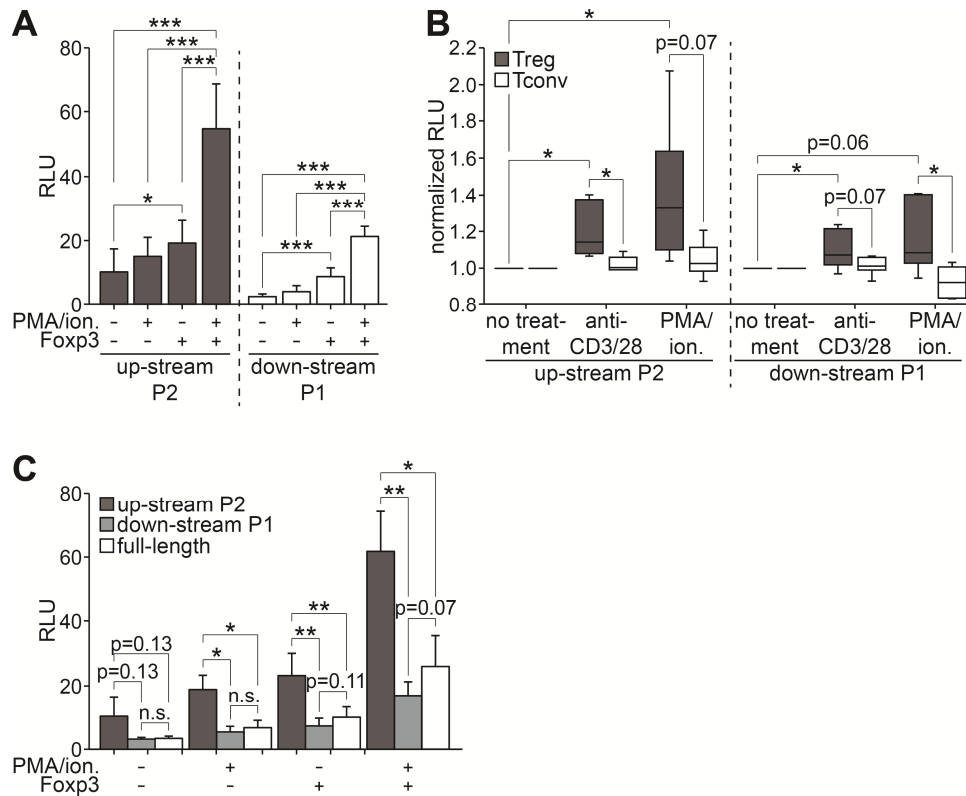


**Figure 3 Two interfering alternative promoters initiate *GARP* transcription in a Treg-specific manner. (A, B)** Up-stream P2 or down-stream P1 promoter sequences were amplified and cloned into pGL4.10 vector. Transcriptional activity was analyzed in a luciferase assay (A) after cotransfection of EL-4 cells with a Foxp3-encoding vector and/or treatment with PMA and ionomycin (ion.) or (B) in primary Tregs and Tconvs in response to stimulation with PMA/ionomycin or with anti-CD3/CD28 for one day. Means  $\pm$  SD of three to six independent experiments are shown. (C) The full-length promoter spanning over both alternative promoters was cloned into pGL4.10 vector. EL-4 cells were treated with PMA and ionomycin or left untreated as a control. Comparison of the transcriptional activity by the three promoter sequences was carried out with luciferase reporter assays after cotransfection of EL-4 cells with a Foxp3-encoding vector and/or treatment with PMA and ionomycin. Means  $\pm$  SD of six independent experiments are shown. Statistical analysis was performed using Student's T-test \*  $p < 0.05$ , \*\*  $p < 0.01$ , \*\*\*  $p < 0.001$ , n.s. not significant.

### 3.1.1.3 Transcriptional activity of the full-length *GARP* promoter region

The transcriptional activity of the full-length promoter region was analyzed by inserting the 1432 bp long region encompassing P2 and P1 promoters in front of the luciferase gene into pGL4.10 vector. Transcriptional activity was investigated in a luciferase reporter assay in response to Treg-specific stimuli (Figure 3C). Again, stimulation of the full-length region with Treg-specific stimuli resulted in a significant increase of the promoter activity. Interestingly, the luciferase activity of the full-length promoter region was decidedly lower than the transcriptional activity of the up-stream P2 promoter and only slightly higher than that by the down-stream P1 promoter.

This observation indicates that the interaction of the alternative promoters leads to inhibition of the up-stream P1 promoter by the down-stream P2 promoter.

#### **3.1.1.4 DNA methylation of the *GARP* gene locus**

Since DNA methylation has been proposed to be involved in the regulation of alternative promoter usage (Cheong et al. 2006), I next analyzed the methylation status of the *GARP* promoter regions and a highly conserved CNS. The up-stream P2 promoter represents a CpG island with 93 CpGs, whereas the down-stream P1 promoter contains 15 individual CpGs. The CNS located in the first intron consists of 16 individual CpGs and was recently reported to be specifically hypomethylated in Tregs (Schmidl et al. 2009) (Figure 4A). Bisulfite sequencing revealed that the up-stream P2 promoter was completely demethylated (< 10% methylation) in all analyzed cell subsets of the hematopoietic system, namely T cells, B cells, monocytes, and the megakaryoblastic cell line MEG-01 (Figure 4B, 4C, 4D, 4E). TCR/CD28 stimulation of Tregs or Tconvs for 24 h did not change the P2 promoter methylation pattern (Figure 4B and 4C). In the epithelial cell lines, HeLa and HEK293, the CpG island of P2 promoter was found to be fully methylated (> 90% methylation) (Figure 4E).

CpGs of the down-stream P1 promoter showed around 50% methylation in either freshly isolated or activated Tconvs (Figure 4B and 4C). In contrast, in freshly isolated or activated Tregs the average methylation of the P1 promoter was around 30%. Again, TCR/CD28 stimulation did not alter the DNA methylation of the *GARP* P1 promoter in the analyzed T cell subsets. The CpGs of the down-stream P1 promoter were methylated in monocytes up to 55% and in B cells up to 38% (Figure 4D). In all cell lines this region was highly methylated (> 70%) (Figure 4E).

Additionally, the CNS region was almost completely methylated in all cells (>80 %), with the exception of Tregs in which the methylation level averaged 55%. In MEG-01 cells, the P1 promoter and the CNS were highly methylated similar to the other analyzed cell lines (Figure 4E). It appears that the downstream P1 promoter and the intronic CNS get specifically hypomethylated in Tregs, but not in all the other cells analyzed. In contrast, the strong up-stream P2 promoter undergoes demethylation and gets prepared for transcriptional initiation early in hematopoietic development. Given the Foxp3-dependency of both promoters (Figure 3A and 3B), the data suggests that Treg-specificity is rather ensured by Foxp3 and not through Treg-specific demethylation. It seems that Treg-specific demethylation of the P1 promoter is apparently necessary to generate a Treg-specific attenuation of the *GARP* expression level. In this

regard, Treg-specific demethylation of the intronic CNS might also play an important regulatory function.

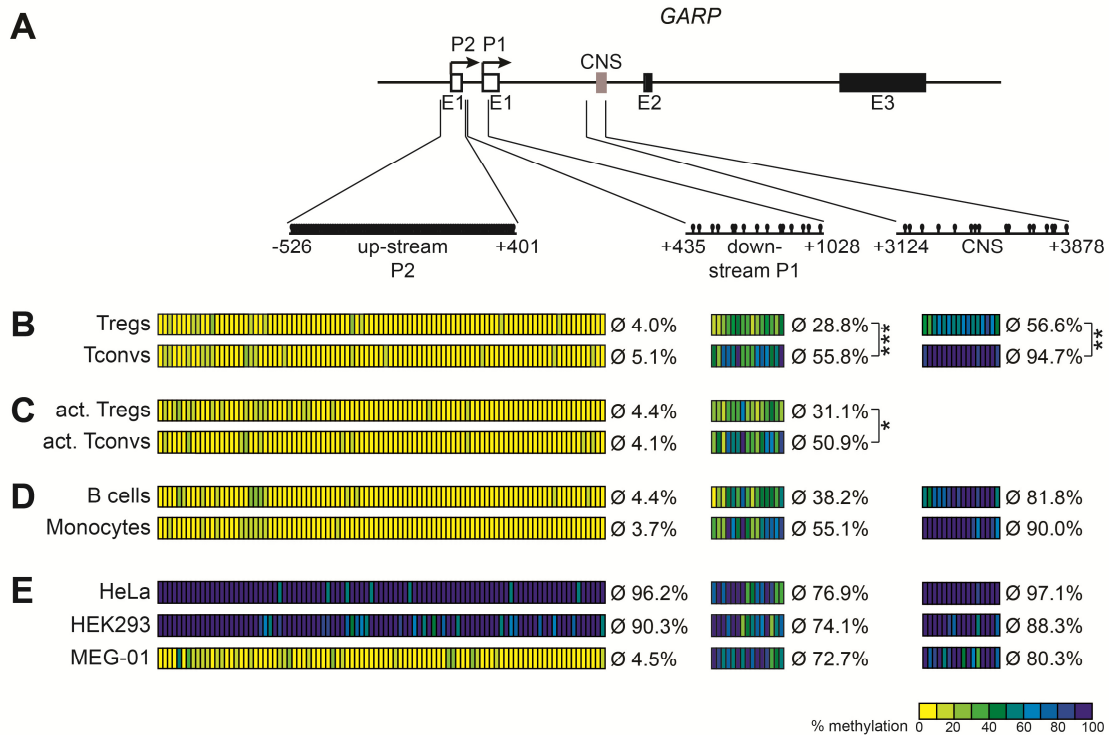


**Figure 4 Down-stream P1 promoter and the intronic CNS undergo a Treg-specific DNA demethylation.** (A) Schematic overview of the *GARP* gene locus with indication of the up-stream P2, the down-stream P1 promoter (arrows), and an intronic CNS (grey box) analyzed by bisulfite sequencing. Pins indicate individual CpGs. Open boxes represent non-coding, black boxes coding exons. (B to E) Genomic DNA from (B) freshly isolated or (C) activated human Tregs and Tconvs, (D) B cells and monocytes, (E) HeLa, HEK293, and MEG-01 cell lines was extracted and subjected to bisulfite conversion. The up- and down-stream promoter regions, as well as the CNS were amplified, cloned, and sequenced. Heat maps depict the aggregate methylation levels (yellow, 0% to blue, 100%) at each CpG from at least 12 clones from nine (B), three (C), two (D), or one (E) independent experiment(s). Statistical analysis was performed using Student's T-test \*  $p < 0.05$ , \*\*  $p < 0.01$ , \*\*\*  $p < 0.001$ .

### 3.1.1.5 Regulation of the down-stream P1 promoter by DNA methylation

Differential intragenic DNA methylation is a common mechanism regulating the usage of alternative promoters embedded in gene bodies (Kulis et al. 2013). The weak *GARP* P1 promoter is located intragenically down-stream of the strong distal promoter. Binding of transcription factors and the transcription initiation complex to the demethylated P1 promoter might inhibit the elongation from the up-stream P2 promoter influencing the overall transcriptional activity of the full-length promoter region. To test whether DNA methylation modifies the binding of transcription factors to the P1 promoter, I conducted several DNA-protein binding assays. A number of putative binding sites for Foxp3, NFAT, or NF- $\kappa$ B were predicted *in silico* in the down-stream P1 promoter (Figure 5A). Several CpGs are located within transcription factor

binding sites. Two oligonucleotides were designed: One spanning over binding sites for NFAT and/or Foxp3 and a second one spanning over a binding site for NF- $\kappa$ B. Both oligonucleotides are located within the differentially methylated region of the proximal P1 promoter. The selected transcription factor binding sites include CpGs. The oligonucleotides were used in methylated and non-methylated form and their binding capacity to NFAT1, Foxp3 and the NF- $\kappa$ B subunit, p50, were compared in fluorometric DNA-protein binding assay. As controls, oligonucleotides with respective canonical binding sequences or the scrambled versions were used. All three transcription factors were found to bind to the non-methylated oligonucleotides in an extent comparable to the binding to the respective canonical oligonucleotides (Figure 5B).

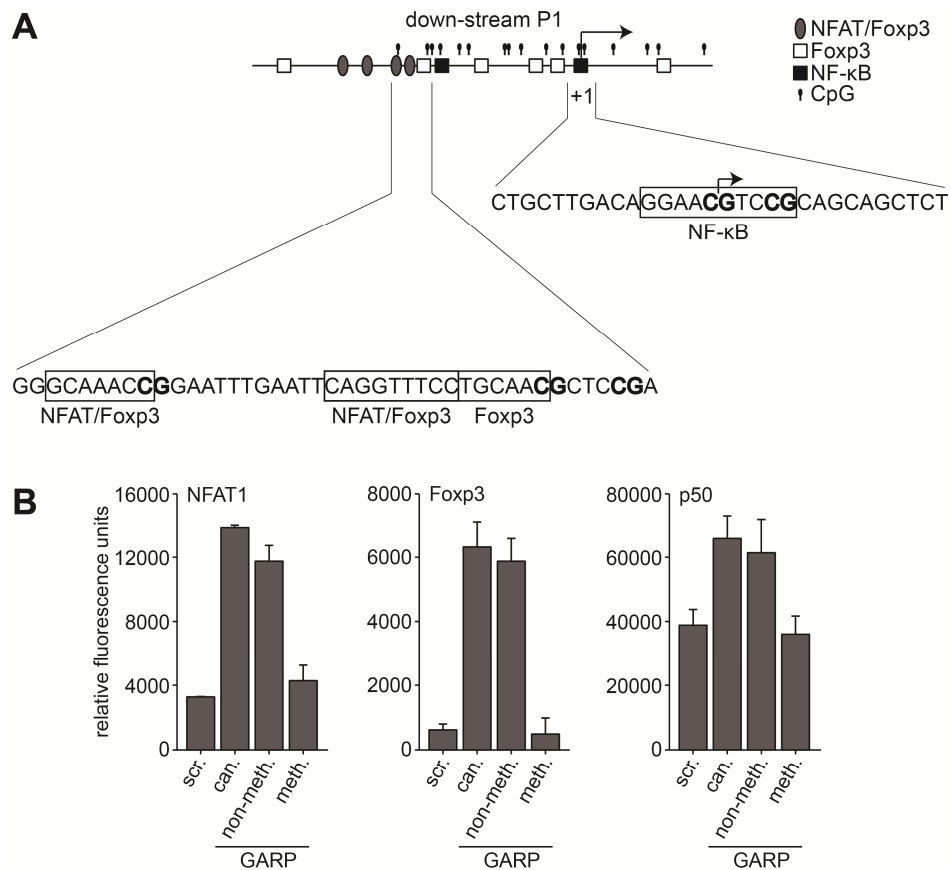


**Figure 5 Methylation of CpGs in the down-stream P1 promoter prevents transcription factor binding.** (A) Schematic presentation of the downstream P1 promoter with indication of putative transcription factor binding sites (boxes), CpGs (black pins) and oligonucleotide sequences used for DNA-protein binding analysis. NFAT/Foxp3 stands for overlapping NFAT/Foxp3 binding sites capable to bind both; Foxp3 binding sites only bind Foxp3; NF- $\kappa$ B binding sites bind to various NF- $\kappa$ B subunits. Arrows mark the TSS. (B) The oligonucleotides were synthesized and methylated by SssI methylase. NFAT1, Foxp3, or p50 binding to the methylated (meth.) or non-methylated (non-meth.) oligonucleotides was analyzed by DNA-protein binding assay in nuclear extracts of Jurkat cells. As negative controls, scrambled oligonucleotides (scr.) were used. For positive control, oligonucleotides encoding the respective canonical sequence (can.) were used. Means  $\pm$  SD of one representative of two independent experiments measured in triplicates are shown.

In contrast, methylation of the oligonucleotides led to pronounced diminution of binding of all three transcription factors in the range of binding to the scrambled oligonucleotides. Therefore, DNA methylation within binding sites is able to inhibit binding of the respective transcription factor.

### 3.1.1.6 Transcription initiated by the up- and down-stream promoter is regulated by *Foxp3*, *NFAT*, and *NF- $\kappa$ B*

Since methylation was able to regulate the binding of transcription factors to the *GARP* promoter region, I investigated the molecular mechanisms underlying *GARP* expression.

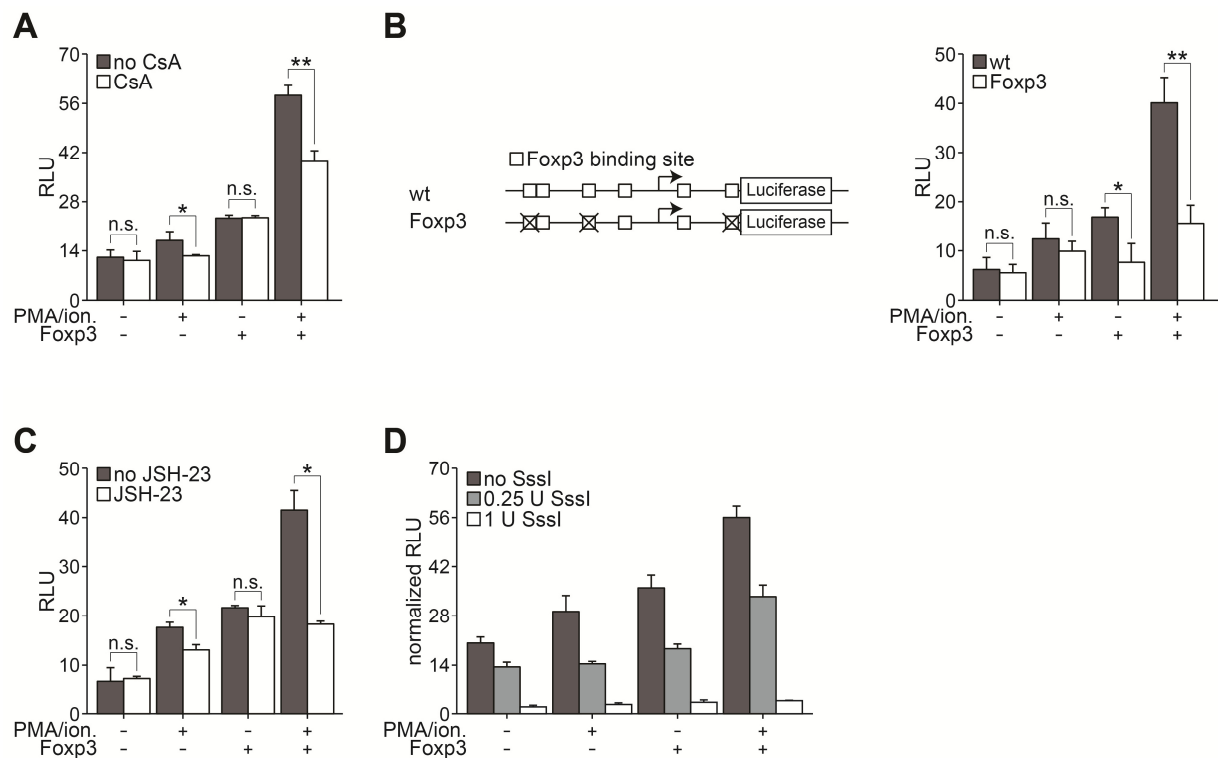


**Figure 6** *Foxp3*, *NFAT*, and *NF- $\kappa$ B* binding to the demethylated up-stream P2 promoter initiates transcription. (A-C) Transcriptional activity of the up-stream P2 promoter cloned into the pGL4.10 vector was analyzed after transfection with the *Foxp3*-encoding vector and/or treatment with PMA and ionomycin by luciferase reporter assays. (A) Transcriptional activity was investigated in the presence or absence of CsA. Means  $\pm$  SD of three independent experiments are shown. (B) Vector containing a mutated promoter variant was generated by site mutations of three *Foxp3* binding sites (*Foxp3*). Transcriptional activity of the mutated promoter in comparison to wild-type (wt) promoter was analyzed. Means  $\pm$  SD of three independent experiments are shown. (C) Transcriptional activity was analyzed in the presence or absence of JSH-23. Means  $\pm$  SD of three independent experiments are shown. (D) Transcriptional activity in response to methylation was determined. The up-stream promoter sequence was inserted into a CpG-free luciferase vector, pCpGL. The construct was treated with different concentrations of *SssI* methylase and measured in a luciferase reporter assay. Means  $\pm$  SD of three independent experiments are shown. Statistical analysis was performed using Student's T-test \*  $p < 0.05$ , \*\*  $p < 0.01$ , n.s. not significant.

Signaling pathways and transcription factors down-stream of TCR/CD28 activation were analyzed by transfection of EL-4 cells with the pGL4.10 vector containing the up- or down-stream promoter sequences and treatment with the NFAT signaling inhibitor, CsA, in the presence of Treg-specific stimuli (PMA/ionomycin and ectopic Foxp3 expression). Additional treatment with CsA repressed the up-stream P2 promoter activity after PMA/ionomycin stimulation and ectopic Foxp3-expression (Figure 6A). Furthermore, P2 promoter activity in the presence of ectopic Foxp3 was almost reduced to background levels upon deletion of putative Foxp3 binding sites, indicating the strong Foxp3 dependency of this promoter (Figure 6B). The p65 activation inhibitor, JSH-23, also reduced the transcriptional activity of the up-stream P2 promoter when the cells were stimulated with PMA/ionomycin with or without addition of ectopic Foxp3, respectively (Figure 6C).

Moreover, treatment with CsA resulted in significant decrease of P1 promoter activity in the presence of PMA/ionomycin and ectopic Foxp3 (Figure 7A). However, CsA had no effect on P1 promoter activity in the presence of only PMA/ionomycin or only Foxp3. These results indicate that NFAT signaling is involved in the regulation of P1 promoter activity. To verify that NFAT is necessary, four overlapping NFAT/Foxp3 binding sites were deleted in the down-stream P1 promoter (NFAT/Foxp3, Figure 7B). The deletion led to a significant decrease of the promoter activity in the presence of PMA/ionomycin and Foxp3, confirming the results with CsA. Additional deletion of all putative Foxp3 and NFAT binding sites in the P1 promoter led to further, but not complete loss of activity (complete, Figure 7B). The remaining transcriptional activity of the completely mutated P1 promoter was inhibited by JSH-23 (Figure 7C).

In complementary experiments, the transcriptional activity of the alternative promoters upon methylation was tested. Remarkably, methylation of both promoter regions abrogated transcriptional activity in a concentration-dependent manner (Figure 6D and 7D). Taken together, it seems that demethylation of both promoters enables binding of Foxp3, NFAT, and NF- $\kappa$ B. The results indicate that both promoters are regulated in a similar fashion by transcription factor binding which in turn initiates the transcription.

### ***3.1.1.7 Chromatin configuration of the GARP gene locus in Tregs***

Gene transcription is associated with the presence of permissive histone modifications, such as H3ac and H3K4me3, or the absence of repressive chromatin marks, such as H3K27me3, in promoter or enhancer regions. Since TCR signaling is frequently reported to induce changes in

histone modifications, I examined the chromatin configuration of the *GARP* gene locus in response to TCR/CD28 stimulation.

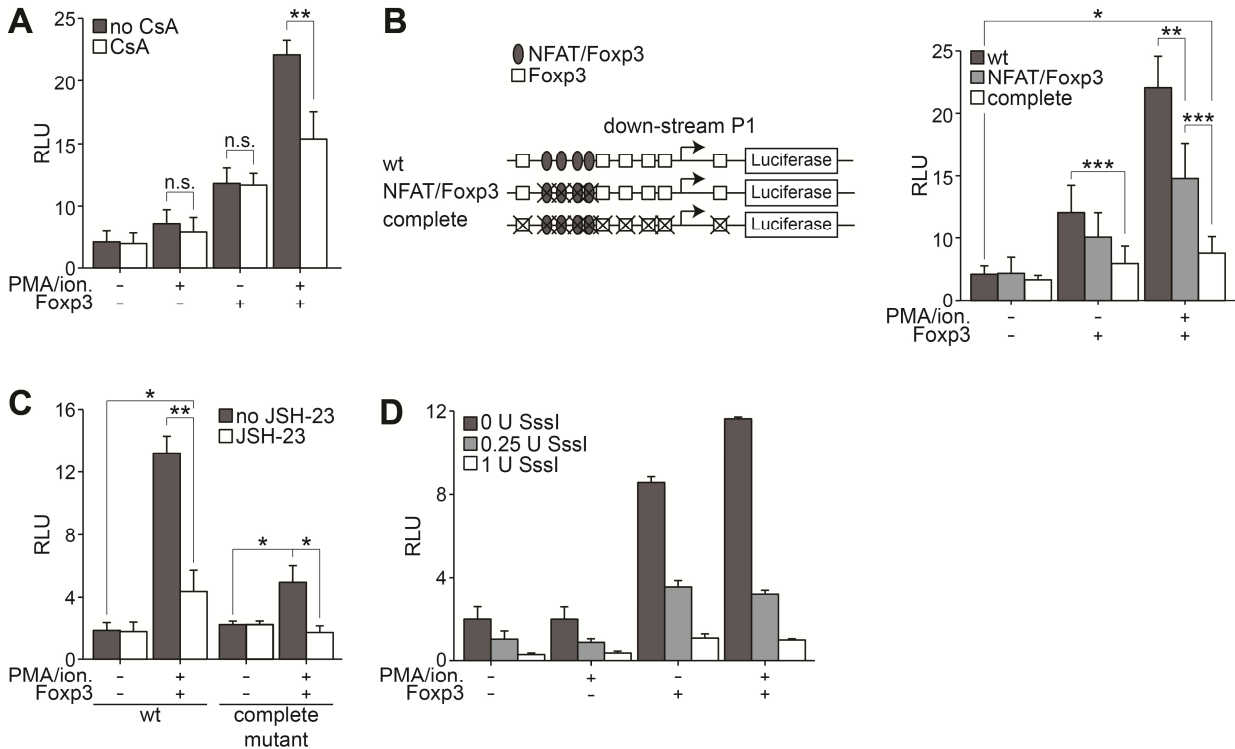


**Figure 7 Foxp3, NFAT, and NF- $\kappa$ B binding to the demethylated down-stream P1 promoter initiates transcription. (A-C)** Transcriptional activity of the down-stream P1 promoter cloned into the pGL4.10 vector was analyzed after transfection with the Foxp3-encoding vector and/or treatment with PMA and ionomycin by luciferase reporter assays. (A) Transcriptional activity was investigated in the presence or absence of CsA. Means  $\pm$  SD of four independent experiments are shown. (B) Vectors containing mutated promoter variants were generated by site mutations of either four overlapping NFAT/Foxp3 binding sites (NFAT/Foxp3) or of NFAT/Foxp3 binding sites along with only Foxp3 binding sites (complete). Activity of the mutated promoters in comparison to wild-type (wt) promoter was analyzed. Means  $\pm$  SD of three independent experiments are shown. (C) Transcriptional activity was analyzed in the presence or absence of JSH-23. Means  $\pm$  SD of three independent experiments are shown. (D) Transcriptional activity in response to methylation was determined. The down-stream promoter sequence was inserted into a CpG-free luciferase vector, pCpGL. The construct was treated with different concentrations of Sssl methylase and measured in a luciferase reporter assay. Means  $\pm$  SD of three independent experiments are shown. Statistical analysis was performed using Student's T-test \*  $p < 0.05$ , \*\*  $p < 0.01$ , \*\*\*  $p < 0.001$ , n.s. not significant.

Therefore, freshly isolated or activated Tregs and Tconvs were used in ChIP assays. Permissive histone modifications were enriched in the *GARP* promoter regions, as well as the intragenic CNS in Tregs upon TCR/CD28 stimulation (Figure 8). No enrichment of these modifications was detected in unstimulated Tregs or Tconvs. The suppressive H3K27me3 showed no enrichment at all gene locations in the analyzed cells, suggesting a regulation of *GARP* gene expression rather by the presence of permissive marks than by the absence of repressive marks.

The MLL complex is involved in Foxp3-dependent changes of histone modifications and gene transcription by displacing the H3K4-specific demethylase PLU-1 (Kato et al. 2011). This

complex catalyzes H3K4 methylation and is often associated with H3ac (Ruthenburg et al. 2007). Thus, enrichment of components of the MLL core complex at the *GARP* gene locus was analyzed by ChIP assay.

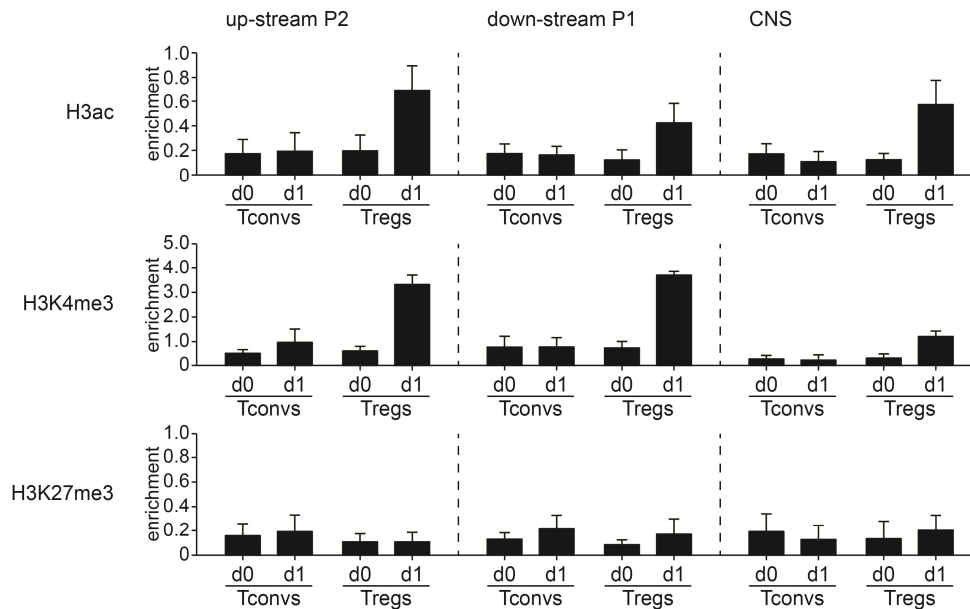


**Figure 8** *GARP* gene locus changes towards an open, transcriptionally active chromatin upon TCR stimulation in Tregs. Tregs and Tconvs were isolated and stimulated with anti-CD3/CD28 for one day. Chromatin was immunoprecipitated with antibodies against H3K4me3, H3ac, or H3K27me3. Presence of *GARP* sequences in immunoprecipitates was detected by real-time PCR. Results were normalized to DNA input and are depicted as means  $\pm$  SD of five independent experiments.

Interestingly, the H3K4-specific methyltransferase MLL1, as well as RbBP5, another member of the complex, showed a constant level of enrichment at all three *GARP* locations (Figure 9). In accordance with higher amounts of permissive H3K4me3 in Tregs upon activation, H3K4-specific demethylase PLU-1 was reduced in the *GARP* promoter regions and the CNS after TCR/CD28 activation.

The MLL1 core complex has been reported to interact with various transcription factors, such as Foxp3 and the NF- $\kappa$ B subunit, p65 (Kato et al. 2011; Wang et al. 2012b). Since Foxp3, NFAT, and NF- $\kappa$ B are involved in *GARP* regulation, I decided to analyze the enrichment of these transcription factors in the *GARP* gene locus. NFAT1 and Foxp3 were increased at the *GARP* promoters and the CNS only in Tregs upon TCR/CD28 stimulation for 24 h (Figure 10). The NF- $\kappa$ B subunits, p50, p65, and c-Rel were only bound to the *GARP* promoter regions, but not to the CNS in activated Tregs. In unstimulated Tregs and Tconvs the transcription factors were not enriched in the analyzed regions.

In summary, the *GARP* gene locus is accessible for the transcriptional regulatory complex only in activated Tregs, but not in unstimulated Tregs, unstimulated Tconvs, or activated Tconvs. The

open chromatin configuration at the *GARP* gene locus in activated Tregs might be mediated by binding of Foxp3, NFAT, and NF- $\kappa$ B, as well as the dissociation of H3K4-specific demethylase PLU-1.

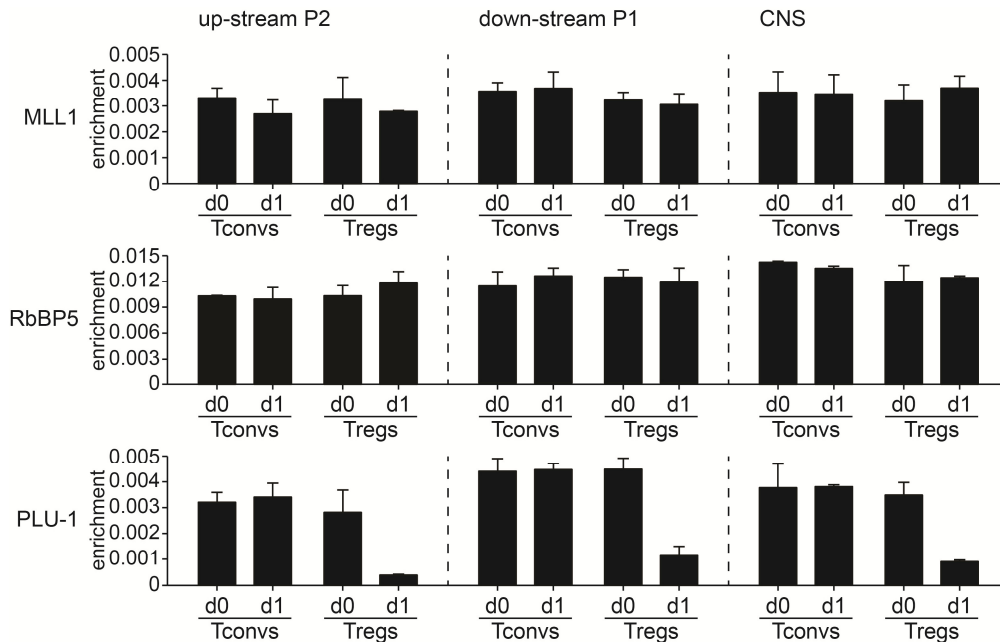


**Figure 9 H3K4-specific demethylase PLU-1 is reduced at the *GARP* gene locus upon TCR stimulation in Tregs.** Tregs and Tconvs were isolated and stimulated with anti-CD3/CD28 for one day. Chromatin was immunoprecipitated with antibodies against the H3K4-specific methyltransferase (MLL1), a core component of the MLL-complex (RbBP5), and the H3K4-specific demethylase (PLU-1). Presence of *GARP* sequences in immunoprecipitates was detected by realtime-PCR. Results were normalized to DNA input and are depicted as means  $\pm$  SD of triplet measurements of one of two independent experiments performed on cells pooled from five to ten individuals.

### 3.1.1.8 Analysis of Treg-specific inducing factors on human and murine *GARP* promoter activity

To determine the *GARP* promoter activity in iTregs, I tested several stimulatory factors that are reported to generate Tregs. Tregs can be induced from CD25- naïve T cells *in vitro*. For human cells, TCR/CD28 stimulation in the presence of TGF- $\beta$  and retinoic acid is used. I determined the influence of the inducing conditions on *GARP* transcription by measuring the P2 and P1 promoter activity in the presence of Treg-specific stimuli and in the presence or absence of TGF- $\beta$  or retinoic acid, respectively. Up-stream P2 promoter activity was not influenced by TGF- $\beta$  or retinoic acid when stimulated only with PMA/ionomycin (Figure 11). However, under Treg-specific stimulating conditions (PMA/ionomycin and ectopic Foxp3), TGF- $\beta$  or retinoic acid reduced promoter activity significantly.

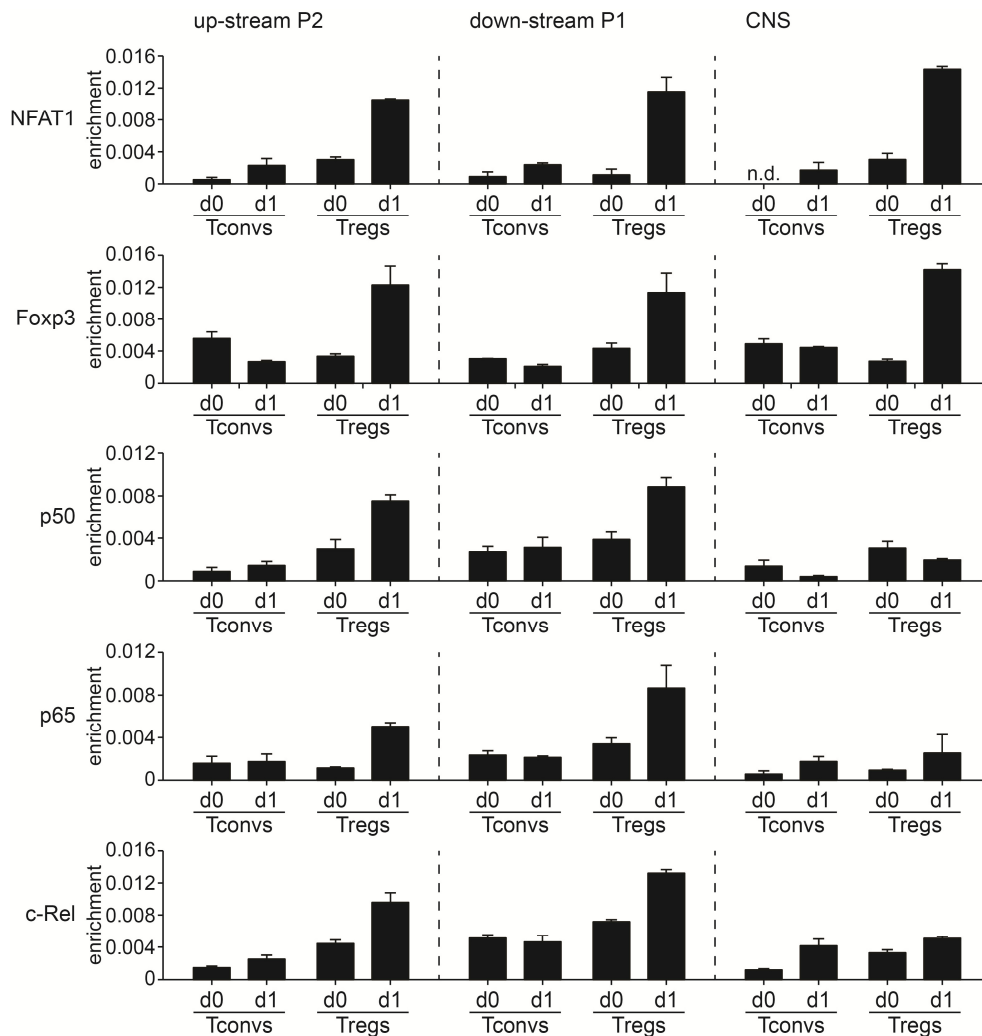


**Figure 10** Foxp3, NFAT1, and NF- $\kappa$ B are enriched at the *GARP* gene locus upon activation in Tregs. Tregs and Tconvs were isolated and stimulated with anti-CD3/CD28 for one day. Chromatin was immunoprecipitated with antibodies against the transcription factors NFAT1, Foxp3, and the NF- $\kappa$ B subunits, p50, p65, and c-Rel. Presence of *GARP* sequences in immunoprecipitates was detected by real-time PCR. Results were normalized to DNA input and are depicted as means  $\pm$  SD of triplet measurements of one of two independent experiments performed on cells pooled from five to ten individuals.

Down-stream promoter P1 activity was not influenced by TGF- $\beta$  (Figure 12A). Interestingly, retinoic acid decreased the promoter activity in the presence of ectopic Foxp3 expression independently of the presence or absence of PMA/ionomycin (Figure 12B). To test whether *GARP* promoter activity is negatively regulated by RXR signaling, a putative RXR binding site in the P1 promoter was deleted (Figure 12C). This deletion resulted in a reduction of promoter activity below background levels irrespective of the stimulation. Another *in silico* prediction of this region revealed a putative Sp1 binding site, possibly explaining the marked decrease.

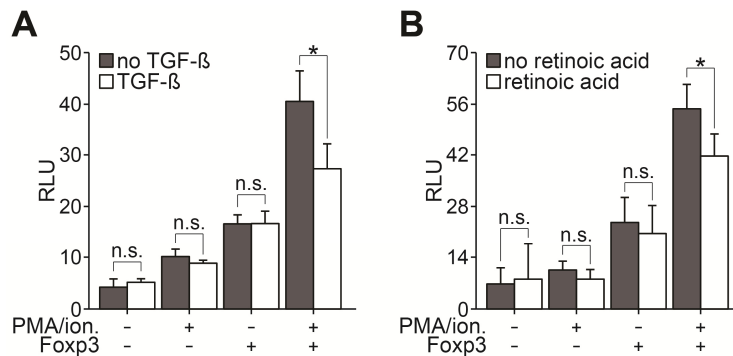


**Figure 11 Up-stream P2 promoter is negatively regulated by TGF- $\beta$  and retinoic acid.** Up-stream P2 promoter sequence was amplified and cloned into pGL4.10 vector. Transcriptional activity was analyzed in a luciferase reporter assay. **(A)** Transcriptional activity was measured in the presence or absence of TGF- $\beta$ . Means  $\pm$  SD of three independent experiments are shown. **(B)** Transcriptional activity was measured in the presence or absence of retinoic acid. Means  $\pm$  SD of three independent experiments are shown. Statistical analysis was performed using Student's T-test \*  $p < 0.05$ , n.s. not significant.

Taken together, transcriptional activity of *GARP* is negatively influenced by TGF- $\beta$  and retinoic acid in the presence of Treg-specific stimuli. However, these Treg-inducing factors had no influence on *GARP* transcriptional activity in the presence of PMA and ionomycin indicating that the widely used *in vitro* inducing conditions for Tregs are not sufficient to upregulate *GARP* expression.

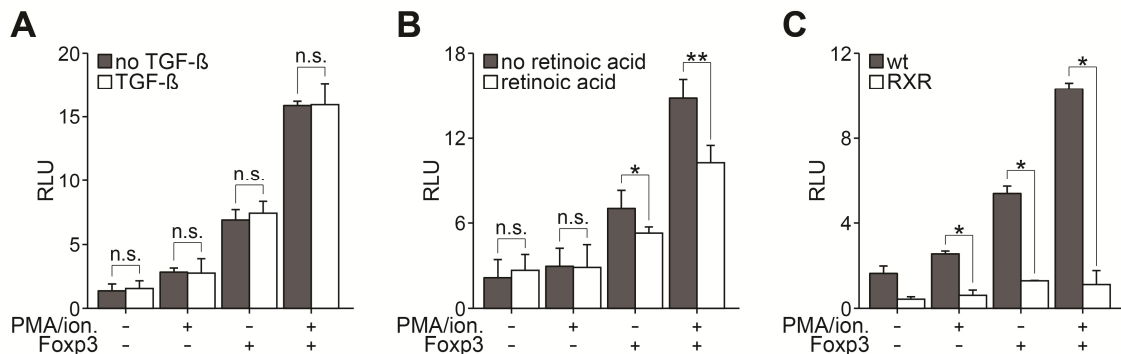


**Figure 12 Down-stream P1 promoter is negatively regulated by retinoic acid.** Down-stream P1 promoter sequence was amplified and cloned into pGL4.10 vector. Transcriptional activity was analyzed in a luciferase reporter assay. **(A)** Transcriptional activity was measured in the presence or absence of TGF- $\beta$ . Means  $\pm$  SD of three independent experiments are shown. **(B)** Transcriptional activity was measured in the presence or absence of retinoic acid. Means  $\pm$  SD of three independent experiments are shown. **(C)** Vector containing a mutated promoter variant was generated by site mutation of a putative RXR binding site (RXR). Transcriptional activity of the mutated promoter in comparison to wild-type (wt) promoter was analyzed. Means  $\pm$  SD of three independent experiments are shown. Statistical analysis was performed using Student's T-test \*  $p < 0.05$ , \*\*  $p < 0.01$ , n.s. not significant.

In order to determine whether transcription of the murine *Garp* promoter differs from the human system, the murine promoter sequence was cloned into pGL4.10 vector.

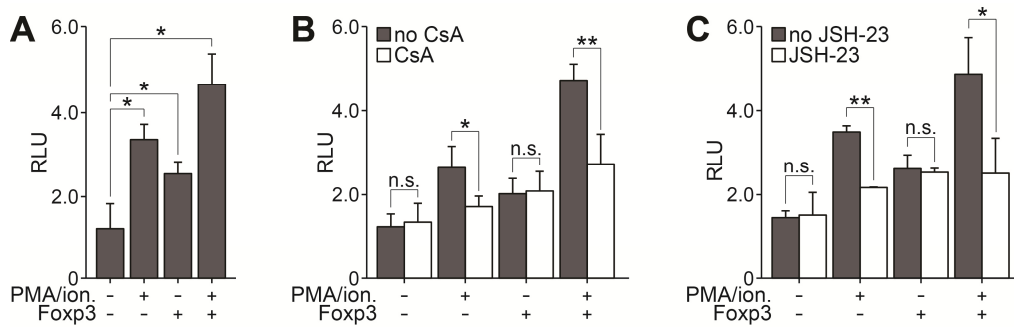


**Figure 13 Transcriptional regulation of murine *Garp*.** Murine *Garp* promoter sequence was amplified and cloned into pGL4.10 vector. (A) Transcriptional activity was analyzed in a luciferase assay after cotransfection of EL-4 cells with a Foxp3-encoding vector and/or treatment with PMA and ionomycin. Means  $\pm$  SD of five independent experiments are shown. (B) Transcriptional activity in the presence or absence of CsA was assessed. Means  $\pm$  SD of four independent experiments are shown. (C) Transcriptional activity in the presence or absence of JSH-23 was assessed. Means  $\pm$  SD of three independent experiments are shown. Statistical analysis was performed using Student's T-test \*  $p < 0.05$ , \*\*  $p < 0.01$ , n.s. not significant.

I analyzed the transcriptional activity in luciferase reporter assays in response to Treg-specific stimulation. Murine *Garp* promoter activity was markedly upregulated by treatment with PMA/ionomycin (Figure 13A). Ectopic Foxp3 expression also increased promoter activity, although to a lower extent than PMA/ionomycin treatment. Combination of PMA/ionomycin and Foxp3 led to the most pronounced transcriptional activity. Similar to the human promoters, murine *Garp* promoter activity is negatively influenced by the NFAT signaling inhibitor, CsA (Figure 13B) and the NF- $\kappa$ B subunit, p65, activation inhibitor, JSH-23 (Figure 13C).

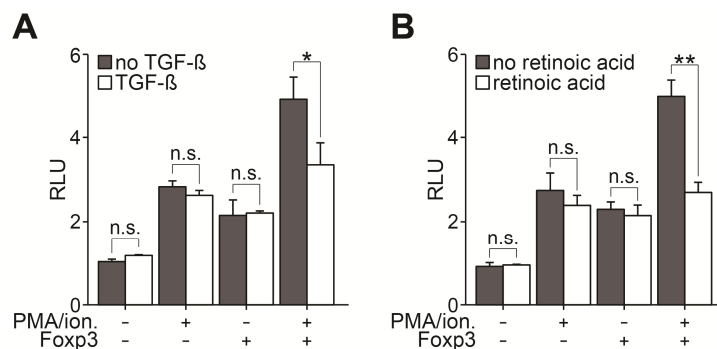


**Figure 14 Murine *Garp* promoter is negatively regulated by TGF- $\beta$  and retinoic acid.** Murine *Garp* promoter sequence was amplified and cloned into pGL4.10 vector. Transcriptional activity was analyzed in a luciferase reporter assay. (A) Transcriptional activity was measured in the presence or absence of TGF- $\beta$ . Means  $\pm$  SD of three independent experiments are shown. (B) Transcriptional activity was measured in the presence or absence of retinoic acid. Means  $\pm$  SD of four independent experiments are shown. Statistical analysis was performed using Student's T-test \*  $p < 0.05$ , \*\*  $p < 0.01$ , n.s. not significant.

Murine *Garp* promoter regulation by Treg-inducing factors resembles that of the human promoters. These observations indicate certain parallels between transcriptional regulation of human *GARP* and murine *Garp* gene. Both inhibitors reduced the luciferase activity in the

presence of PMA/ionomycin alone or in combination with ectopic Foxp3 expression. When murine promoter activity was tested in the presence of TGF- $\beta$  or retinoic acid, PMA/ionomycin/ectopic Foxp3-induced transcriptional activity was significantly decreased (Figure 14A and 14B).

### 3.1.2 Analysis of MafF expression in Tconvs and MafF-mediated regulation of Foxp3

#### 3.1.2.1 *MafF protein expression in Tconvs can be inhibited by IL-4*

Recently, down-regulation of the expression of the transcription factor MafF was associated with the generation of iTregs (Prots et al. 2011). In this study, microarray and real-time PCR analyses were performed with functionally competent iTregs generated *in vitro* from CD25- naïve T cells in the presence of autologous feeder cells and IL-4 and in effector T cells generated in the same system without IL-4. *MafF* mRNA was specifically upregulated at early developmental stages (day 3 to 5) in T cells activated in the absence of IL-4, whereas *MafF* expression seemed to be downregulated in Tregs induced in the presence of IL-4. To confirm these results on protein level, I analyzed the MafF protein expression in naïve CD25- T cells activated with anti-CD3/CD28 in the presence and absence of exogenous IL-4. TCR/CD28 stimulated T cells in the presence of exogenous IL-4 showed no upregulation of MafF protein during the five days of culture (Figure 15A and 15B). However, T cells stimulated without exogenous IL-4 expressed constant levels of MafF protein during the first two days and then showed an increase on day three and four followed by a decrease on day five. Intracellular staining of MafF and subsequent flow cytometry analysis confirmed the upregulation of MafF in Tconvs stimulated without exogenous IL-4 on day four (Figure 15C). This data indicates that MafF might be a regulator of effector T cell function and can be downregulated by addition of exogenous IL-4.

#### 3.1.2.2 *Overexpression of MafF attenuates induction of Foxp3+ Tregs*

*MafF* is expressed in Tconvs upon TCR/CD28 expression, whereas this transcription factor is rather downregulated during the induction of Tregs (Prots et al. 2011). Thus, I next analyzed the influence of enforced *MafF* expression during the *in vitro* generation of Tregs. *MafF* was overexpressed in iTregs generated by TCR/CD28 stimulation in the presence of TGF- $\beta$  or in the presence of TGF- $\beta$  in combination with retinoic acid (Figure 15D).

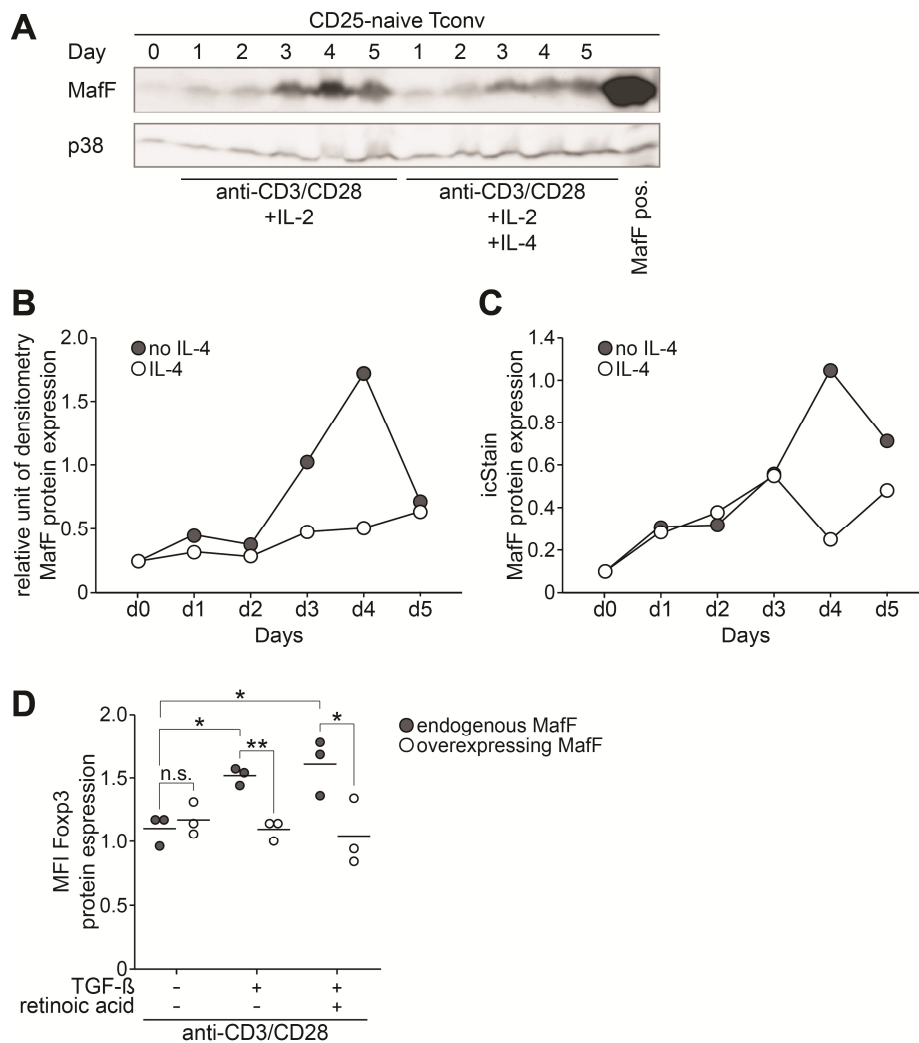


**Figure 15 MafF expression in Tconvs is constrained by IL-4 and overexpression of MafF attenuates induction of Foxp3<sup>+</sup> Tregs.** (A,B,C) Naïve CD25<sup>-</sup> Tconvs were stimulated with anti-CD3/CD28 and IL-2, in the presence or absence of IL-4 for a total of five days. (A) Western blot of MafF and p38 expression was performed. (B) Relative units of densitometry from one representative experiment are displayed. (C) Intracellular staining and FACS analysis of MafF was performed and one representative of three independent experiments is shown. (D) Tregs were generated by treatment of naïve CD25<sup>-</sup> Tconvs with anti-CD3/CD28 in the presence of IL-2 and TGF-β, and in the presence or absence of retinoic acid for a total of 4 days. Intracellular staining of Foxp3 was performed and cells were analyzed by flow cytometry. Mean fluorescence intensity (MFI) from three independent experiments is depicted.

Interestingly, *MafF* overexpression in Tregs resulted in significant lower Foxp3 expression levels during the four days of culture when compared to iTregs induced only with endogenous *MafF* levels. Foxp3 expression in iTregs overexpressing *MafF* was similar to T cells that were activated without addition of TGF-β. Taken together, these data suggest that *MafF* is only upregulated in effector T cells and negatively regulates Foxp3 induction and therefore *in vitro* generation of Tregs. However, further analyses are necessary to understand underlying molecular mechanisms.

## 3.2 Characterization of molecular mechanisms regulating *GARP* expression and Treg function in RA

### 3.2.1 Influence of DNA methylation on *GARP* expression in RA

Recently, profound alterations in the Treg phenotype in RA were reported (Zhou and Haupt et al. 2015). The surface marker and TGF- $\beta$  transporter, *GARP*, might be implicated in these alterations. In this regard, I analyzed in a cooperative work with Dr. Qihui Zhou and the medical students, Viktoria Söntgerath and Johannes Kreuzer, *GARP* expression and DNA methylation in 34 patients with RA and 37 age- and gender-matched healthy controls (HCs). All patients fulfilled the 2010 ACR/EULAR or the ACR 1987 classification criteria for RA (Aletaha et al. 2010; Arnett et al. 1988). Demographic and clinical parameters were collected and recorded at the Division of Rheumatology and Clinical Immunology, Medizinische Klinik und Poliklinik IV, Ludwig-Maximilians-Universität München and summarized in Table 1.

**Table 1 Clinical and demographic characteristics of the study population\***

	RA patients (n=34)	HC (n=37)
Age, years	60.0 $\pm$ 12.7	51.7 $\pm$ 8.1
Female/male (n)	26/8	29/8
Disease duration, years	3.4 $\pm$ 6.5	n.a. <sup>§</sup>
RF positive, %	80.0	n.d. <sup>a</sup>
Anti-CCP positive, %	68.6	n.d.
DAS28	4.0 $\pm$ 1.8	n.a.
TJC28 (n)	5.3 $\pm$ 6.4	n.a.
SJC28 (n)	4.4 $\pm$ 5.6	n.a.
CRP, mg/dL	1.4 $\pm$ 2.4	n.d.
ESR, mm/hour	21.6 $\pm$ 14.3	n.d.
Erosions, %	51.5	n.a.

\*Data are shown as means  $\pm$  SD or absolute numbers.

<sup>§</sup>n.a., not applicable.

<sup>a</sup>n.d., not determined.

Abbreviations: RA, rheumatoid arthritis; RF, rheumatoid factor; Anti-CCP, anti-cyclic citrullinated peptide; DAS28, disease activity score in 28 joints; TJC28, tender joint count on 28 joints; SJC28, swollen joint count on 28 joints; CRP, C-reactive protein; ESR, erythrocyte sedimentation rate.

*GARP* mRNA was significantly lowered in Tregs isolated from patients with RA and activated for 24 or 48 h compared to activated Tregs from HCs (Figure 16A). The decreased *GARP* expression upon TCR stimulation correlated inversely with the disease activity (Figure 16B) and was reflected by the diminished *GARP* protein expression at the cell surface (Figure 16C).

Furthermore, DNA methylation levels of the down-stream P1 promoter and the intragenic CNS were analyzed in 10 patients with RA and HCs, respectively. Both regions were demethylated to

a greater extent in RA-Tregs than in Tregs from HCs (Figure 17A). There was no difference in DNA methylation observed in Tconvs from RA patients and HCs. The higher degree of demethylation at the *GARP* gene locus coincided with lower *GARP* mRNA expression upon Treg activation and with higher disease activity. This observation strongly supports the hypothesis that transcription initiation from the down-stream P1 promoter hinders the transcription from the up-stream P2 promoter and attenuates the overall transcriptional activity.

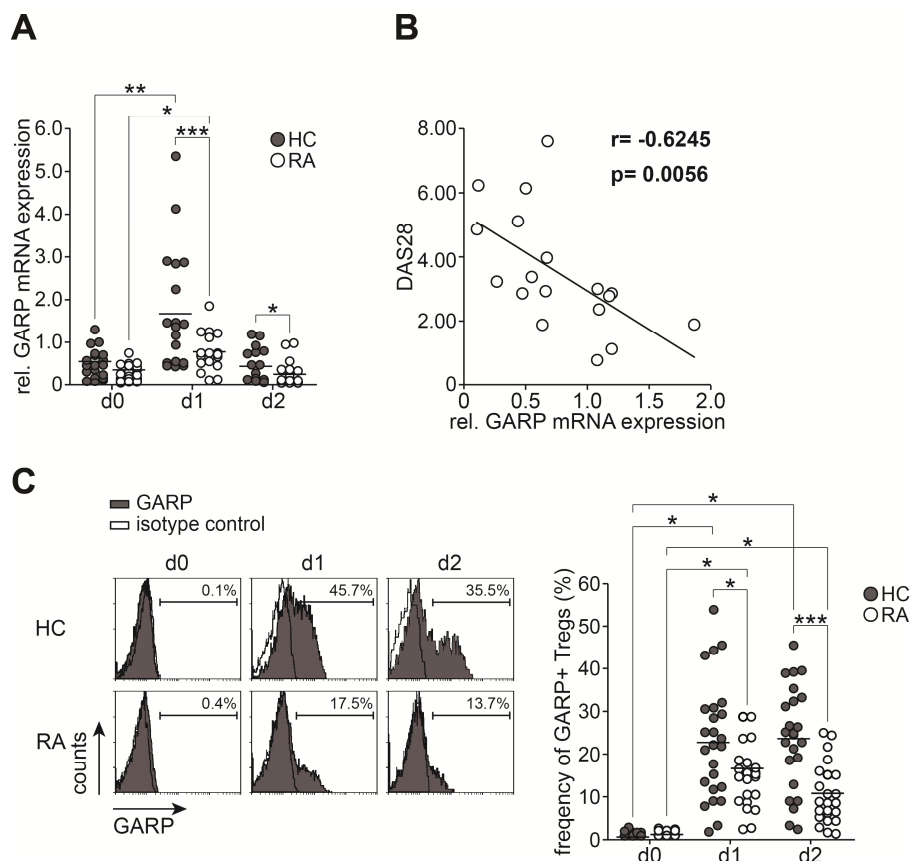


**Figure 16** *GARP* expression is reduced in Tregs from patients with RA and contributes to disease activity. (adapted from Haupt et al., 2015) Tregs were isolated from peripheral blood of patients with RA and of age- and gender-matched healthy controls (HCs). *GARP* expression was assessed at mRNA (A, B) and protein (C) levels in freshly isolated (d0) and in anti-CD3/CD28-stimulated Tregs at day one (d1) and day two (d2). (A) *GARP* mRNA expression was assessed by real-time PCR in Tregs from 19 RA patients and 21 HCs. Relative mRNA expression normalized to the expression levels of *Cyclophilin A* mRNA is shown. (B) Correlation between *GARP* mRNA expression on day one in Tregs and disease activity reflected by DAS28 was assessed by Spearman's rank correlation coefficient. (C) Surface *GARP* expression was evaluated by flow cytometry. Representative staining histograms with indications of frequencies of *GARP* positive Tregs are shown in the left panel. The right panel summarizes results from 23 RA patients and 26 controls. Statistical analysis was performed using Student's T-test. \*  $p < 0.05$ , \*\*  $p < 0.01$ , \*\*\*  $p < 0.001$ , n.s. not significant.

It is possible that binding of transcription factors to the intragenic promoter further impedes transcriptional elongation. To prove this hypothesis, a region spanning the P1 promoter was methylated separately with increasing amounts of SssI methylase (Figure 17B). I analyzed the

activity of the full-length promoter with the partially methylated P1 region in a luciferase reporter assay. Indeed, the lower the methylation of the down-stream P1 promoter was, the lower was the transcriptional activity of the full-length *GARP* promoter region.

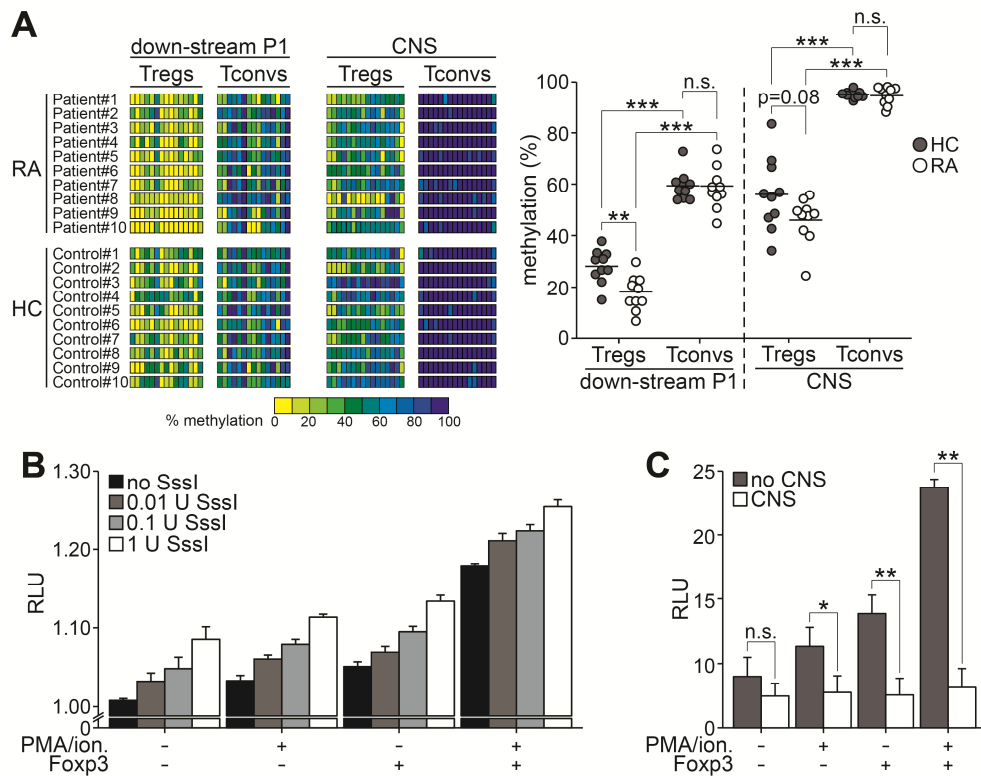


**Figure 17** *GARP* expression in Tregs is regulated by DNA methylation at the down-stream P1 promoter and the intragenic CNS. (A) DNA methylation of the down-stream P1 promoter and the intragenic CNS was assessed in 10 patients with RA and 10 age- and gender-matched HCs. gDNA from Tregs and Tconvs was purified and subjected to bisulfite conversion. The down-stream promoter region and the CNS were amplified, cloned, and sequenced. Heat maps depict the aggregate methylation levels at each CpG from at least 12 clones for each individual patient or control. Summarized results are depicted in the graph on the right. (B) A sequence spanning the differentially methylated region of the down-stream P1 was released by enzymatic digestion from the pGL4.10 vector containing the full-length *GARP* promoter, subjected to DNA methylation with increasing amounts of SssI methylase and ligated back into the origin vector. Purified ligations were used to transfect EL-4 cells. Transcriptional activity of the full-length promoter, containing the down-stream promoter methylated to different degrees, was analyzed in a luciferase reporter assay. Means  $\pm$  SD of one representative of two independent experiments performed in triplicates are shown. (C) The demethylated CNS sequence was inserted down-stream of the full-length promoter sequence and in front of the luciferase gene into pGL4.10 vector. Transcriptional activity of the full-length promoter together with the CNS was analyzed in a luciferase reporter assay. Means  $\pm$  SD of three independent experiments are shown. Statistical analysis was performed using Student's T-test \*  $p < 0.05$ , \*\*  $p < 0.01$ , \*\*\*  $p < 0.001$ , n.s. not significant.

Additionally, the CNS was inserted behind the demethylated full-length promoter construct and assessed in a luciferase assay. The promoter activity was markedly decreased by inserting the CNS behind the full-length construct (Figure 17C). These observations suggest that the recruitment of transcription factors and accessory proteins to the demethylated down-stream

promoter and the CNS attenuates the transcription from the up-stream P2 promoter specifically in Tregs. The methylation of the proximal P1 promoter prevents binding of the transcriptional machinery and therefore favors transcription from the strong up-stream P2 promoter. Hence, it seems as if the demethylation-induced transcriptional attenuation of *GARP* expression in RA Tregs facilitate disease activity.

### 3.2.2 SNP frequencies in the *GARP* gene locus in patients with RA and HCs

Several polymorphisms are associated with altered gene expression and susceptibility to RA. SNPs located in the *GARP* gene locus might influence the gene expression in Tregs of RA patients. Therefore, I chose nine SNP sites distributed over the *GARP* gene locus (Figure 18 and table 2).

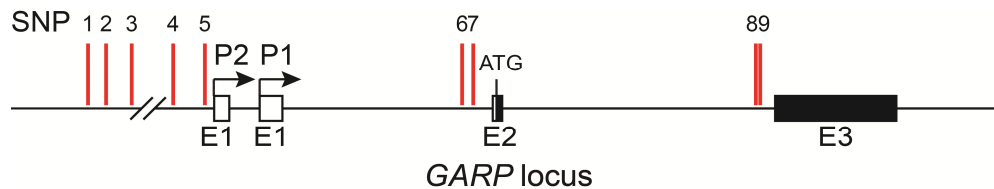


**Figure 18 SNP locations in the *GARP* gene locus.** Schematic overview of the *GARP* gene locus with indication of two promoters (arrows), non-coding (empty boxes) and coding (black boxes) exons. The translation start site (ATG) is located in the second exon. The analyzed SNPs one to nine are indicated by red lines.

**Table 2 Location, minor and major alleles of the analyzed *GARP* SNPs**

Name	SNP ID	Location (genome)	Allele (major/minor)
SNP1	rs7122065	intergenic	G/A
SNP2	rs11236851	intergenic	G/A
SNP3	rs7342189	intergenic	C/T
SNP4	rs947998	5'UTR	G/T
SNP5	rs3814710	5'UTR	G/A
SNP6	rs6592657	intron 1	G/A
SNP7	rs4944115	intron 1	T/G
SNP8	rs7944357	intron 2	G/A
SNP9	rs7944463	intron 2	T/C

Demographic and clinical parameters of the RA patients were collected and recorded at the Division of Rheumatology and Clinical Immunology, Medizinische Klinik und Poliklinik IV, Ludwig-Maximilians-Universität München and summarized in Table 3. 623 RA patients and 430 HCs were included in the study and analyzed for the selected SNPs by using Taqman SNP genotyping assays. Allele and genotype frequencies were calculated (Table 4 and 5). Significantly lower frequencies of the minor allele of SNP 2 (A) and 8 (A) were found in RA

(Table 4). Additionally, for SNP 7 significantly higher frequencies of the minor allele (G) in RA were observed. These polymorphisms were located in the intergenic region and the intron 1 and 2 of the *GARP* gene locus. None of the SNPs located in the 5'UTR showed significant differences in the allele frequencies in HCs compared to patients with RA.

**Table 3 Clinical and demographic characteristics of the study population \***

	RA patients (n=623)	HC (n=430)
Age, years	57.4±15.0	52.1±16.4
Female/male (%)	73/27	68/32
Disease duration, years	7.8±12.7	n.a. <sup>§</sup>
RF positive, %	81.0	n.d. <sup>a</sup>
Anti-CCP positive, %	55.0	n.d.
DAS28	n.d.	n.a.
TJC28 (n)	n.d.	n.a.
SJC28 (n)	n.d.	n.a.
CRP, mg/dL	2.4±3.4	n.d.
ESR, mm/hour	27.2±25.4	n.d.
Erosions, %	35.2	n.a.

\*Data are shown as means ± SD or absolute numbers.

<sup>§</sup>n.a., not applicable.

<sup>a</sup>n.d., not determined.

Abbreviations: RA, rheumatoid arthritis; RF, rheumatoid factor; Anti-CCP, anti-cyclic citrullinated peptide; DAS28, disease activity score in 28 joints; TJC28, tender joint count on 28 joints; SJC28, swollen joint count on 28 joints; CRP, C-reactive protein; ESR, erythrocyte sedimentation rate.

In line with the observed differences of allele frequencies, significantly higher frequencies of the major (GG) and the heterozygote (GA) genotypes were found for SNP 2 in RA (Table 5). For SNP8 the major (GG) genotype was increased and the minor (AA) genotype was decreased. Additionally, for SNP 7 significantly higher frequencies of the minor (GG) and significantly lower frequencies of the major (TT) genotype were observed.

**Table 4 Allele counts in analyzed *GARP* SNPs in RA patients and HCs**

Name	Allele (major/minor)	Allele count (major/minor) and frequencies (%)		P*
		HC (n=430)	RA (n=623)	
SNP1	G/A	542/318 (63/37)	763/485 (61/39)	0.4063
SNP2	G/A	746/114 (87/13)	1160/98 (93/7)	<b>&lt;0.0001</b>
SNP3	C/T	745/115 (87/13)	1108/150 (89/11)	0.3562
SNP4	G/T	744/116 (87/13)	1104/152 (89/11)	0.3814
SNP5	G/A	561/299 (66/34)	784/474 (63/37)	0.1866
SNP6	G/A	481/379 (56/44)	715/531 (57/43)	0.5372
SNP7	T/G	671/189 (78/22)	878/368 (70/30)	<b>0.0001</b>
SNP8	G/A	595/265 (69/31)	930/316 (75/25)	<b>0.0069</b>
SNP9	T/C	466/394 (54/46)	673/573 (54/46)	0.9729

\*P-values were calculated based on the individual numbers, using Fisher's exact test.

**Table 5 Individual numbers and frequencies of genotypes in analyzed *GARP* SNPs in RA patients and HCs**

Name	Genotypes AA/AB/BB <sup>§</sup>	Genotypes AA/AB/BB <sup>§</sup> , frequencies (%)		$\chi^2$ *	P*
		HC (n=430)	RA (n=623)		
SNP1	GG/GA/AA	171/200/59 (39/47/14)	236/291/97 (38/47/15)	0.8229	0.6627
SNP2	GG/GA/AA	320/106/4 (74/25/1)	537/86/6 (85/14/1)	20.768	<b>&lt;0.0001</b>
SNP3	CC/CT/TT	320/105/5 (74/25/1)	484/140/5 (77/22/1)	1.097	0.5779
SNP4	GG/GT/TT	319/106/5 (74/25/1)	482/140/6 (77/22/1)	0.9379	0.6257
SNP5	GG/GA/AA	191/179/60 (44/42/14)	242/300/87 (38/48/14)	4.289	0.1172
SNP6	GG/GA/AA	132/217/81 (31/50/19)	202/311/110 (32/50/18)	0.4496	0.7987
SNP7	TT/TG/GG	263/145/22 (61/34/5)	332/214/77 (54/34/12)	17.017	<b>0.0002</b>
SNP8	GG/GA/AA	222/151/57 (52/35/13)	357/216/50 (57/35/8)	8.353	<b>0.0153</b>
SNP9	TT/TC/CC	121/224/85 (28/52/20)	180/313/130 (29/50/21)	0.3722	0.5536

\* $\chi^2$  and P-values were calculated based on the individual numbers, using Chi-square test.

<sup>§</sup> AA: major allele homozygote; AB: heterozygote; BB: minor allele homozygote.

### 3.2.3 Haplotype distribution in patients with RA and HCs

Analysis of the haplotype using Haploview defined three different blocks of haplotypes that were distributed along the *GARP* gene locus and termed as block 1, 2, and 3 (Figure 19) (Barrett et al. 2005). Linkage disequilibrium (LD) was calculated from the estimates of haplotypic frequencies and very high LDs are displayed in red. Block 1 comprises SNP 1 to 5 and is mainly located in the intergenic region and the 5'UTR.

Block 2 consist of SNP 6 and 7, block 3 consists of SNP 8 and 9. These blocks are located in the intragenic regions 1 and 2, respectively. The haplotype distributions are summarized in Table 6. The haplotypes AGCGA and GGTTG of block 1, GG of block 2, and GT of block 3 were significantly increased in RA. The haplotypes GATTG and AGCGG of block 1, GT of block 2, and AT of block 3 showed lower frequencies in RA. In summary, these results suggest that the haplotype distribution of SNPs located in the *GARP* gene is altered in patients with RA.

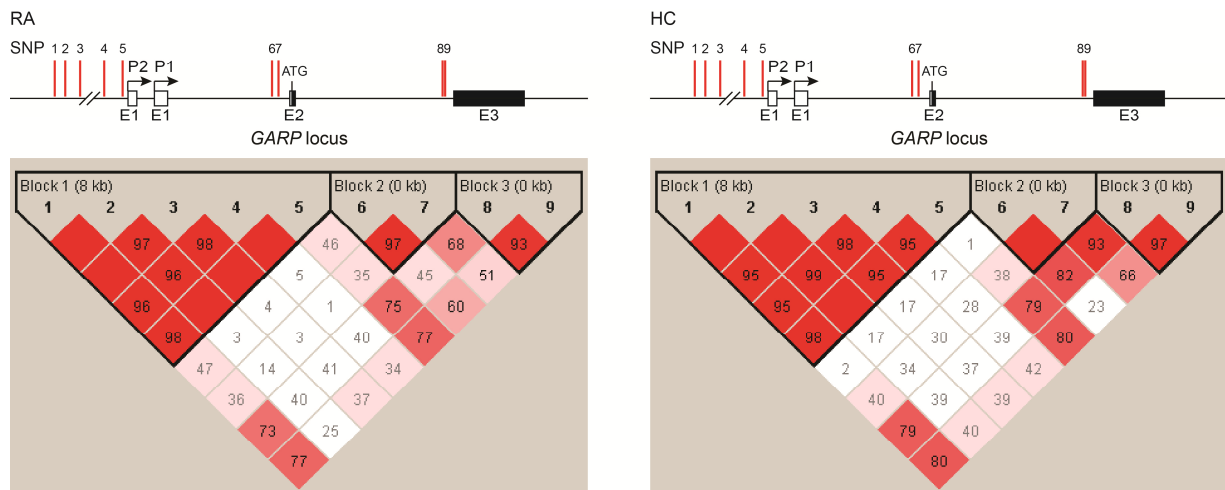


**Figure 19 Haplotype of SNPs in the *GARP* gene locus.** The schematic overview of the *GARP* gene locus with indication of SNP1 to 9 is shown in the upper panel. Haplotype block structure on the basis of the strength of pairwise LD, which is presented as a 2x2 matrix is depicted in the lower panel. Red represents very high LD, white indicates absence of correlation between SNPs. The numbers in the boxes also indicate the degree of LD with 100 being the highest and 0 being the lowest.

**Table 6 Haplotype distribution in the *GARP* gene locus**

Haplotype	Count (RA/HC)	Frequency (RA/HC)	Global P*	P§
<i>Haplotype block 1</i>				
GGCGG	602:634/427:433	0.487/0.496	<b>&lt;0.0001</b>	0.6701
AGCGA	461:775/292:568	0.373/0.339		0.1165
GATTG	94:1142/113:747	0.076/0.131		<b>&lt;0.0001</b>
AGCGG	18:1218/20:840	0.014/0.023		0.1423
GGTTG	52:1184/0:860	0.042/0.000		<b>&lt;0.0001</b>
<i>Haplotype block 2</i>				
AT	524:718/368:492	0.422/0.428	<b>0.0001</b>	0.7841
GT	352:890/303:557	0.283/0.352		<b>0.0008</b>
GG	362:880/189:671	0.291/0.220		<b>0.0002</b>
<i>Haplotype block 3</i>				
GC	559:683/391:469	0.450/0.455	<b>0.0020</b>	0.8360
AT	305:937/262:598	0.246/0.305		<b>0.0027</b>
GT	368:874/204:656	0.296/0.237		<b>0.0028</b>

\*Global p-values were calculated based on the individual numbers, using Chi-square test.

§P-values were calculated based on the individual numbers, using Fisher's exact test.



I, in cooperation with Dr. Qihui Zhou, analyzed the expression and function of the Treg-specific miRNA-146a. The expression of miR-146a was decreased in RA patients with active disease (Zhou and Haupt et al. 2015). MiR-146a is involved in the regulation of the NF- $\kappa$ B pathway by a negative feedback loop (Ma et al. 2011). Therefore, the NF- $\kappa$ B activity was tested in eight RA patients with active disease (DAS28>3.2) and nine age- and gender-matched HCs (Figure 20A). The NF- $\kappa$ B reporter luciferase vector was transfected into Tregs. After TCR/CD28 or PMA/ionomycin stimulation, no differences in the NF- $\kappa$ B activity were observed. Thus, no correlation between the expression levels of miR-146a and NF- $\kappa$ B activity was observed. Since STAT1 is another target of miR-146a, we measured the expression and phosphorylation of STAT1 in Tregs from patients with RA and HCs. Interestingly, higher levels of STAT1 were detected in Tregs from patients with RA and HCs. Interestingly, higher levels of STAT1 were detected in Tregs from patients with active disease, when compared to HCs or patients with low disease activity (Figure 20B). Given the fact that miR-146a levels in Tregs from patients with active disease are lowered, the STAT1 expression correlated with the levels of miR-146a.

### 3.2.5 Increased expression of pro-inflammatory cytokines in Tregs from patients with RA

In order to analyze the meaning of lower miR-146a expression in Tregs from RA patients, levels of the pro-inflammatory cytokines IFN- $\gamma$ , TNF, and IL-17 were measured in the cell culture supernatants of activated Tregs from 24 patients with RA and 14 HCs (Figure 21). The Tregs from RA patients with active disease produced significantly higher levels of all measured cytokines when compared to RA patients with low disease activity or HCs. Thus, the expression of pro-inflammatory cytokines by Tregs correlated with higher STAT1 protein expression and phosphorylation and lower abundance of miR-146a.

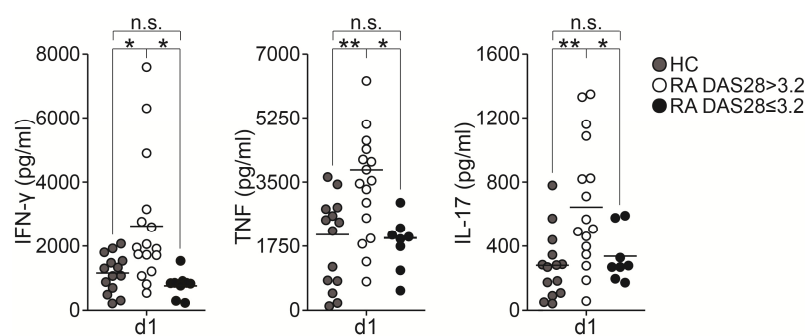


**Figure 21 IFN- $\gamma$ , TNF, and IL-17 expression in Tregs from patients with RA.** Protein levels of IFN- $\gamma$ , TNF, and IL-17 were measured in the cell culture supernatants of Tregs after anti-CD3/CD28 stimulation for one day (d1) by ELISA. Results from 16 RA patients with active disease, eight RA patients with low disease activity, and 14 age- and gender-matched HCs are displayed. DAS28>3.2 – active disease; DAS28 $\leq$ 3.2 – low disease activity. Statistical analysis was performed using Student's T-test \*p<0.05, \*\*p<0.01.

These data indicate that changes in the expression of miR-146a might lead to alterations in the STAT1 expression and phosphorylation, thereby influencing the production of pro-inflammatory cytokines. To test this hypothesis, the STAT1 expression, phosphorylation and the cytokine production of Tregs were measured after transfection of the cells with either mimics or antagonists of miR-146a, respectively (Figure 22). Indeed, treatment of the cells with mimics led to a significant decrease of STAT1 expression and phosphorylation in comparison to the control (scr). However, the treatment of the cells with antagonists resulted in a significant increase of STAT1 expression and phosphorylation (Figure 22A). Consistently, Tregs treated with mimics showed lower expression of pro-inflammatory cytokines, whereas treatment with antagonists resulted in significant increase (Figure 22B). Taken together, these data provide evidence for miR-146a-mediated changes in Tregs from patients with RA that might explain some alterations of the Treg phenotype.

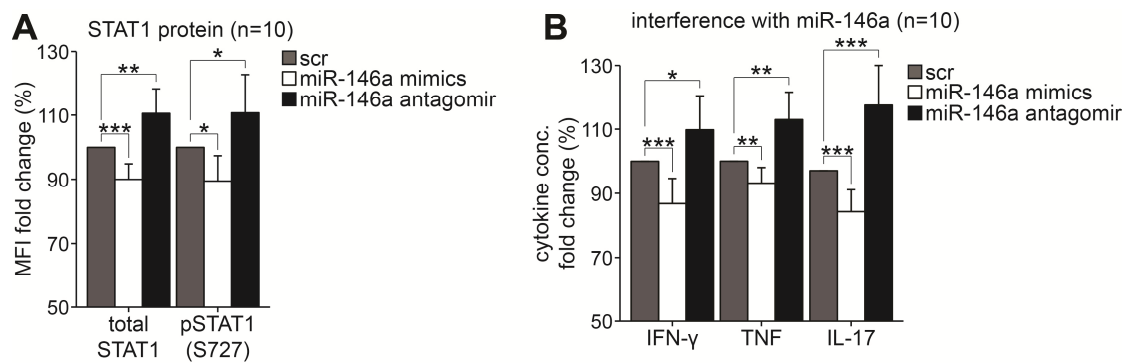


**Figure 22** Effect of miR-146a on STAT1 expression and cytokine production in Tregs (adapted from Zhou and Haupt et al. 2015). Tregs were isolated and transfected with mimics or antagonists of miR-146a. After anti-CD3/28 stimulation for one day, (A) STAT1 protein expression and phosphorylation, as well as (B) cytokine production in the cell culture supernatants were assessed. Means  $\pm$  SD of ten independent experiments are shown. Statistical analysis was performed using Student's T-test \*  $p < 0.05$ , \*\*  $p < 0.01$ , \*\*\*  $p < 0.001$ .

## 4 DISCUSSION

### 4.1 DNA methylation of alternative promoters and Foxp3 regulate *GARP* expression

#### 4.1.1 Molecular mechanisms underlying *GARP* transcriptional regulation

Phenotypic complexity of higher eukaryotes is achieved by complex gene regulation in order to get larger protein diversity. This protein variety is ensured by regulatory mechanisms, such as alternative splicing and existence of alternative promoters and TSS (Kelemen et al. 2013; Kornblihtt 2005). Alternative promoters have different tissue specificities, developmental activities, transcriptional or translational efficiencies (Landry et al. 2003). In the first part of the study, I analyzed transcriptional interference between two alternative *GARP* promoters. These promoters control *GARP* transcription in combination with the Treg-specific transcription factor, Foxp3, and the TCR-mediated transcription factors, NFAT and NF- $\kappa$ B.

DNA methylation often regulates usage of alternative promoters. Up to 70 % of genes that are regulated by alternative promoter usage possess one promoter containing a CpG-island (Kimura et al. 2006). Surprisingly, CpG-island containing promoters are in most cases completely demethylated regardless of whether the gene is expressed or not. In addition, those promoters often possess stronger transcriptional activity acting as the major promoter of the gene (Cheong et al. 2006). This is in line with the result that the up-stream *GARP* promoter contains a CpG-island which is completely demethylated in all analyzed cells, independently of *GARP* expression and acts as the strong major promoter. In contrast, alternative promoters with lower CpG content often demonstrate a correlation between tissue-specific demethylation and gene expression. Consistent with this, the weaker down-stream promoter of *GARP* contains only several CpGs that once methylated inhibit accessibility and transcriptional activity (Figure 5). Tissue- and cell type-specific demethylation occurs across gene bodies, often coinciding with highly conserved sequences (Maunakea et al. 2010). In line with this, demethylation of the intragenic *GARP* promoter and the intragenic CNS only occurs in Tregs. Intragenic methylation is paradoxically often associated with enhanced elongation efficiency from the up-stream TSS. One example is the *angiomin like 2 (AMOTL2)* gene which is involved in angiogenesis. Hypomethylation within the gene body of *AMOTL2* is associated with reduced transcription (Movassagh et al. 2010). In addition, the human *retinoblastoma (Rb1)* gene contains a weak imprinted promoter in

the second intron. The methylation of this promoter is associated with high levels of the main transcript, whereas demethylation of this promoter correlates with high expression of the alternative transcript and low expression of the main *Rb1* transcript (Kanber et al. 2009). It has been proposed that the transcription initiation complex bound to the un-methylated alternative promoter acts like a roadblock and reduces the elongation speed from the up-stream promoter (Kulis et al. 2013). Here, I observed that the usage of the down-stream *GARP* promoter attenuated the transcriptional activity of the up-stream P2 promoter. Moreover, transcriptional activity regulated by DNA methylation of the down-stream P1 promoter region influenced the overall activity of the *GARP* promoter region.

In addition, the Treg-specific transcription factor, Foxp3, and the TCR/CD28-mediated factors, NFAT and NF- $\kappa$ B, bind to the *GARP* gene locus (Figure 10). Putative binding sites were predicted and their close vicinity might indicate a cooperation of the transcription factors in *GARP* regulation. In this regard, inhibition of NFAT or NF- $\kappa$ B signaling and impaired binding of Foxp3 decreased *GARP* promoter activity (Figure 6 and 7). Genome-wide analyses of Foxp3 targets have revealed that Foxp3 induces both activation and repression of its target genes (Gavin et al. 2007; Marson et al. 2007; Zheng et al. 2007). Thus, it is conceivable that the final outcome of the Foxp3-mediated gene regulation is strongly influenced by cofactors and multimerization. NFAT cooperates with Foxp3 via the C-terminal forkhead domain, whereas NF- $\kappa$ B was reported to bind to the N-terminal part (Bandukwala et al. 2011; Bettelli et al. 2005; Loizou et al. 2011; Wu et al. 2006). Thus, it is possible that the interaction of Foxp3 with NFAT and NF- $\kappa$ B is necessary for Treg-specific and TCR-dependent *GARP* expression.

Furthermore, Foxp3, NFAT1, and NF- $\kappa$ B binding to *GARP* were accompanied by permissive histone modifications indicating chromatin remodeling of *GARP* upon TCR/CD28 stimulation (Figure 8). In addition, Foxp3 binding and chromatin remodeling towards an open chromatin configuration was accompanied by displacement of the H3K4-specific demethylase, PLU-1 (Katoh et al. 2011). PLU-1 is a histone demethylase whose presence in chromatin leads to continuous demethylation of H3K4me3 (Yamane et al. 2007). Steady-state methylation of H3K4 might be maintained on the other hand by the H3K4-specific methyltransferase, MLL1 (Katoh et al. 2011; Milne et al. 2002). Furthermore, the MLL1 complex was found to bind to Foxp3 and the NF- $\kappa$ B subunit, p65 (Katoh et al. 2011; Wang et al. 2012b). Binding sites for PLU-1 could be predicted adjacent to Foxp3 binding sites in the *GARP* promoter regions and the intronic CNS. Thus, it is possible that binding of Foxp3 to the *GARP* locus replaces PLU-1 from the MLL-1

complex which in turn leads to permissive H3K4me3. In addition, the MLL-1 complex associates with histone acetyltransferases which might explain the presence of H3ac marks (Zhao et al. 2013). Indeed, upon TCR/CD28 stimulation PLU-1 binding to the *GARP* gene locus was decreased while MLL-1 and other members of the complex remained unchanged (Figure 9). Foxp3 expression alone is not sufficient for the regulatory activity of Tregs, since they also need TCR activation for their suppressive functions. Foxp3 binding to DNA and stability is promoted post-translationally by phosphorylation in response TCR stimulation (Chen et al. 2006; Nie et al. 2013). Additionally, the subcellular localization of Foxp3 from a cytoplasmic to a nuclear pattern is regulated by TCR stimulation (Chen et al. 2006). This might provide the basis for the TCR-mediated upregulation of *GARP* expression. Upon TCR stimulation of Tregs, Foxp3 gets phosphorylated and shuttles to the nucleus (Figure 23). Furthermore, TCR/CD28 stimulation promotes phosphorylation and nuclear localization of NFAT and degradation of I $\kappa$ B and translocation of NF- $\kappa$ B to the nucleus (Hogan et al. 2003; Schmitz et al. 2003). In Tregs, Foxp3 replaces PLU-1 and enables the permissive H3K4me3 at both regions by the MLL1 complex. Then, other transcription factors activated by TCR stimulation can bind to the demethylated P2 and P1 promoters in order to up-regulate *GARP* expression. The strong transcription from the upstream P2 promoter is attenuated by the binding of the transcriptional machinery to the downstream P1 promoter and the CNS region. This mechanism might be necessary for fine-tuning *GARP* expression.

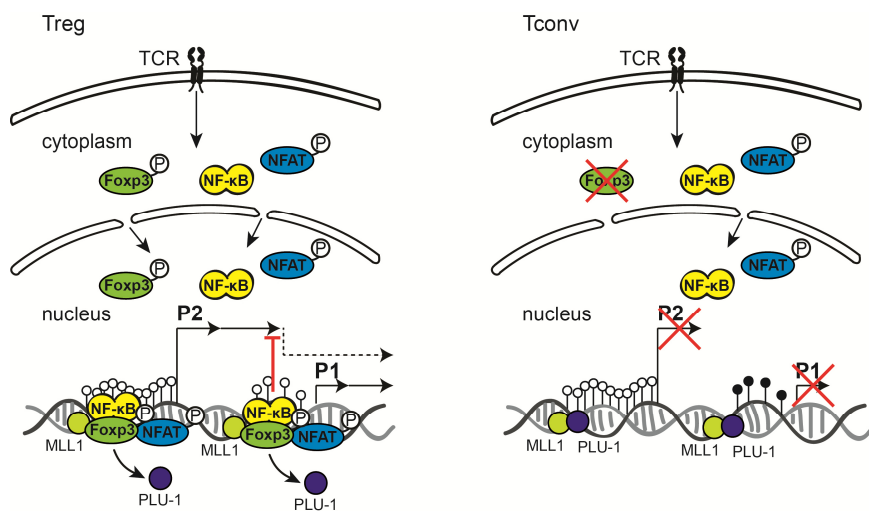


**Figure 23** *GARP* expression is regulated by DNA methylation, Foxp3, NFAT and NF- $\kappa$ B. A proposed model by which DNA methylation of *GARP* and binding of Foxp3 regulate expression of *GARP* in Tregs by displacement of H3K4 demethylase, PLU-1, and recruitment of TCR-induced transcription factors.

In Tconvs, the P1 promoter is methylated and the *GARP* gene locus is closed, since they lack stable Foxp3 expression. This mechanism does not exclude other transcription factors that might be involved in regulating *GARP* expression in humans.

*GARP* is implicated in anchoring TGF- $\beta$  to the surface of Tregs (Stockis et al. 2009a; Tran et al. 2009). TGF- $\beta$  is a pleiotropic cytokine involved in many biological processes, such as proliferation, apoptosis, cell differentiation, and regulation of the immune system. It can act as a potent immune suppressor, however depending on the context it also displays pro-inflammatory properties (Mantel et al. 2011). Additionally, TGF- $\beta$  is known to inhibit the cell cycle in benign cells, but promotes progression and metastasis in cancer cells (Inman 2011; Principe et al. 2014). LTBPs are secreted multidomain glycoproteins central to TGF- $\beta$  regulation. *GARP* was recently described as a new LTBP that regulates TGF- $\beta$  bioavailability (Wang et al. 2012a). Interestingly, other latent LTBPs were reported to be regulated by differential promoter usage facilitating tissue specificity and abundance of transcripts (Bultmann et al. 2013; Davis et al. 2014; Koski et al. 1999). Since TGF- $\beta$  has potential harmful implications and contributes to tumor progression or tissue fibrosis, it is conceivable that bioavailability is tightly regulated. In this regard, *GARP* expression has been linked to various cancers, such as squamous cell carcinoma, colorectal cancer, breast cancer, ovarian carcinoma, and prostate cancer (Bekri et al. 1997; Edwards et al. 2003; Goode et al. 2013; Lassmann et al. 2007; Liu et al. 2006; Ollendorff et al. 1992). TGF- $\beta$  producing Tregs could be isolated from hepatocellular carcinoma patients (Han et al. 2014). These cells suppressed Th cell response via membrane bound TGF- $\beta$  *in vitro*. High surface expression of *GARP* and subsequently high membrane bound or local TGF- $\beta$  concentrations might suppress tumor immunity through TGF- $\beta$  signals, which at least partly contribute to iTreg generation (Chen et al. 2005; Li et al. 2007; Liu et al. 2007). In addition, presence and accumulation of TGF- $\beta$  and/or *GARP* positive Tregs at tumor sites and in the circulation of cancer patients have been reported (Kalathil et al. 2013; Schuler et al. 2013; Schuler et al. 2012). In contrast, mouse Tregs that express latent TGF- $\beta$ /*GARP* complexes on their surface are able to induce Th17 cells in the presence of IL-6 (Edwards et al. 2013). Thus, it is possible that uncontrolled TGF- $\beta$  production at sites of inflammation might lead to production of pro-inflammatory Th17 responses known as major contributors to autoimmune conditions, such as RA (Leipe et al. 2010; Leipe et al. 2014). Therefore, considering the versatile potential pathologic effects of immoderate *GARP* expression, tight regulation of the surface molecule

through the observed transcriptional attenuation by the down-stream P1 promoter on Tregs is essential.

#### 4.1.2 Effect of TGF- $\beta$ on *GARP* expression

No alternative promoter could be predicted for *Garp* in the mouse. Although murine *Garp* promoter activity was more dependent on TCR stimulation, the presence of Foxp3 was still necessary for induction (Figure 16). This is consistent with previous findings which show the necessity of Foxp3 for stable GARP expression in the mouse (Edwards et al. 2013). However, in this study cytokines like IL-2 and IL-4 were sufficient to induce murine GARP expression on Foxp3+ Tregs. This can be explained by the fact that IL-2, IL-4 and TCR/CD28 signaling share some pathways, such as those that activate NFAT and NF- $\kappa$ B. Therefore, IL-2 or IL-4 could also induce NFAT/NF- $\kappa$ B signaling in Foxp3+ Tregs, thereby mediating GARP expression. However, influence of these cytokines on *GARP* promoter activity remains to be elucidated. In contrast to human iTregs, *in vitro* and *in vivo* induced mouse Tregs express GARP on their surface (Edwards et al. 2013; Tran et al. 2009). This is in line with the finding that PMA/ionomycin stimulation in the presence of TGF- $\beta$  is not able to increase human *GARP* promoter activity. However, the mouse *Garp* promoter activity was not influenced by TGF- $\beta$  stimulation. Interestingly, for both mouse and human promoters, TGF- $\beta$  rather seemed to negatively regulate transcriptional activity in the presence of Treg-specific stimuli. This is consistent with the observed decrease of GARP expression on activated human Tregs after treatment with TGF- $\beta$  (Zhou et al. 2013a). In addition, treatment of murine or human Tregs with a TGF- $\beta$  inhibitor resulted in significant higher expression of GARP. Furthermore, Tregs isolated from T cell conditional TGF- $\beta$  knock-out mice expressed GARP equivalent to Tregs from wildtype mice. This confirms studies where human Tregs continued to express GARP after siRNA-mediated knock-down of TGF- $\beta$  (Tran et al. 2009). Inhibiting TGF- $\beta$  signaling in Tregs seems to upregulate GARP expression in both human and mouse. This is consistent with my observations that promoter activity of both human and murine genes is decreased after addition of TGF- $\beta$ . One possible explanation is the existence of a negative feedback loop, where GARP-bound TGF- $\beta$  gets activated and via autocrine signaling down-regulates GARP expression and thereby TGF- $\beta$  activation on Tregs. This tight regulation of GARP and TGF- $\beta$  signaling might be again a mechanism to control Treg-mediated effects in malignant or autoimmune processes.

## 4.2 MafF expression in Tconv and iTregs

The small Maf family of proteins consists of three members, MafF, MafG, and MafK. They can form homo- and heterodimers thereby regulating activation or repression of gene transcription (Blank et al. 1997). One member of the family, *MafF*, was found to be downregulated during the differentiation of iTregs, whereas this transcription factor was upregulated during the differentiation of effector T cells (Prots et al. 2011). In this thesis, I analyzed MafF protein expression in effector T cells. TCR/CD28 stimulation in the presence of IL-2 was able to temporarily increase MafF, whereas IL-4 impedes this effect (Figure 15). Interestingly, the pro-inflammatory cytokines IL-1 $\beta$  and TNF are able to induce *MafF* transcript and protein levels in myometrial cells, but the expression of the highly homologous *MafG* and *MafK* genes is not modulated (Massrieh et al. 2006). IL-1 $\beta$  and TNF have been described as pro-inflammatory cytokines, whereas IL-4 rather exerts anti-inflammatory effects, suggesting a specific function of MafF in the inflammatory response (Yoshimura et al. 2003). Pro-inflammatory Th1 or Th17 cells secrete IFN- $\gamma$  or IL-17 thereby enhancing macrophage functions by inducing the secretion of IL-1 $\beta$  and TNF (Winer et al. 2009). In contrast, IL-4 producing Th2 cells or Foxp3+ Tregs influence macrophage differentiation in a way that they become IL-10-secreting macrophages (Odegaard et al. 2007; Tiemessen et al. 2007). However, IL-6 was not able to induce *MafF* expression (Massrieh et al. 2006). One possibility is that IL-1 $\beta$  and TNF can upregulate MafF by using similar signaling pathways. MafF was shown to function as a transcriptional activator or repressor depending on the dimerization partner (Marini et al. 2002; Ye et al. 2006). Furthermore, MafF is downregulated in diverse carcinoma cell lines (Amit et al. 2007). TGF- $\beta$  produced by the tumor seems to mediate conversion of Foxp3+ Tregs (Moo-Young et al. 2009). In line with this, MafF overexpression is able to negatively influence Foxp3 during induction of Tregs (Figure 15). Foxp3 expression is not completely inhibited by MafF overexpression, but further upregulation by TGF- $\beta$  and retinoic acid is attenuated suggesting that MafF negatively influences generation of iTregs. Concerning the inhibitory effect of MafF on Foxp3 expression, there might be a connection between MafF downregulation and increased abundance of Tregs in tumors. Further experiments are necessary to show the molecular mechanisms underlying MafF-mediated inhibition of Foxp3.

Overexpression of MafF was not able to inhibit Foxp3 expression in activated Tregs completely. Mouse studies could only show a mild if any phenotype after the knock-out of a single member of the small Maf family (Motohashi et al. 2000; Onodera et al. 1999; Shavit et al. 1998).

However, knock-out of all three small Mafs led to embryonic lethality (Katsuoka et al. 2005). Therefore, it was suggested that small Mafs have partial redundant functions, but lack complete functional redundancy. Supporting this, the three small Mafs exhibit distinct spatial and temporal expression profiles (Onodera et al. 1999; Onodera et al. 2000; Shavit et al. 1998). It is conceivable that also in T cells small Maf proteins might share some functions. More detailed studies of MafF in T cells might provide further insights into regulation and function of small Maf proteins in the adaptive immune response.

### 4.3 GARP in RA

#### 4.3.1 Diminished GARP expression in RA-Tregs correlates with DNA demethylation

Increased demethylation of the down-stream P1 promoter correlated with lower *GARP* expression in Tregs from patients with RA (Figure 16 and 17). In addition, we could observe that the methylation status of the Treg-specific demethylated intronic CNS at least partially correlated with *GARP* expression. The binding of transcription factors to the CNS and the P1 promoter could be demonstrated. Therefore, the binding of transcription factors to these regions might hinder the elongation from the up-stream promoter region. The usage of alternative promoters, regulation of alternative transcripts by DNA methylation, and as a result changes in transcription levels or tissue-specific expression of genes have been suggested to be involved in inflammatory processes and autoimmune diseases (Doig et al. 2014; Guthridge et al. 2014; Le Dantec et al. 2015; Yan et al. 2004). Therefore, aberrant use of the alternative down-stream *GARP* promoter over the main up-stream promoter may contribute to altered GARP expression on Tregs in autoimmune diseases. GARP is implicated in Treg expansion in response to TCR activation and suppressive function (Wang et al. 2009; Zhou et al. 2013b). In addition soluble GARP is able to exert potent immunoregulatory activity by inhibiting effector functions of naïve T cells (Hahn et al. 2013). In this study, the addition of soluble GARP in differentiation cultures of naïve Th cells resulted in upregulation of Foxp3 and decreased cytokine production. Furthermore, it facilitated the generation of iTregs probably through TGF- $\beta$  activation. In line with this, lowered *GARP* expression on Tregs from patients with RA might contribute to decreased function of Tregs and diminished peripheral tolerance. In this regard, we could demonstrate that Tregs from RA patients are prone to a pro-inflammatory phenotype (Zhou and Haupt et al. 2015). Thus, administration of soluble GARP or modulation of GARP expression on RA-Tregs might be useful for the treatment of RA. Interestingly, in the presence of the cytokines IL-6 and IL-23,

GARP was also able to promote Th17 cells (Edwards et al. 2013; Hahn et al. 2013). In the presence of IL-2, the induction of Tregs was favored. However, in a humanized mouse model it could be shown that soluble GARP is able to enhance the suppressive function of Tregs thereby preventing graft-versus-host disease. Recently, monoclonal antibodies against GARP were generated that could inhibit the immunosuppressive activity of human Tregs *in vivo* (Cuende et al. 2015). In this study, inhibition of TGF- $\beta$  activation by anti-GARP antibodies was able to abrogate the Treg-mediated suppression of graft-versus-host disease. Thus, it can be assumed that GARP has some therapeutic potential. The application has to be tested in autoimmune disorders, but the observed decrease of GARP on RA-Tregs might indicate a positive outcome. In contrast, inhibition of GARP function on Tregs might be beneficial in other human diseases, such as cancer or chronic infections.

In addition, it has been demonstrated that T cells from RA patients display global hypomethylation when compared to HCs (Richardson et al. 1990). In line with this, RA-Tregs were hypomethylated in the down-stream P1 promoter and the CNS. Compromised Treg function in patients with RA has been recently associated with diminished expression of the Treg signature gene, *CTLA-4* (Cribbs et al. 2014). DNA methylation in an NFAT binding site inhibited binding of NFAT2 resulting in reduced *CTLA-4* transcription. These results indicate that epigenetic changes in Treg signature genes in RA influence their expression thereby contributing to diminished Treg function.

#### **4.3.2 SNP alleles in the *GARP* gene locus are associated with RA**

*GARP* gene polymorphisms were analyzed regarding their potential to confer susceptibility to RA. Several risk genes are associated with the disease. For instance, one substitution in the *CTLA-4* gene can result in diminished *CTLA-4* export to the membrane (Lee et al. 2012). Furthermore, a genome-wide association study identified RA risk loci, such as *REL*, *CTLA-4*, and *BLK* (Gregersen et al. 2009). The *REL* locus encodes the NF- $\kappa$ B subunit c-Rel which has some distinct roles in the production of IL-12 and IL-23 subunits by macrophages and DCs and Th1 immune responses (Grumont et al. 2001; Mason et al. 2004; Mise-Omata et al. 2007). In addition, alternative promoter variants in the *BLK* gene locus were recently associated with SLE (Guthridge et al. 2014). A risk allele (T) of rs922483 reduced the activity of the ubiquitous, proximal promoter and most likely removed attenuation from the up-stream, B-cell specific

promoter. However, analysis of SNP variants in the 5'UTR of the *GARP* gene locus revealed that none of the two SNPs in the *GARP* promoter region is associated with RA (Table 4 and 5).

Interestingly, I found that an associated allele (G) of rs11236851 (SNP2) is located around 7.5 kb up-stream of the distal P2 promoter. It is conceivable that this region might have enhancer or repressor functions. *In silico* prediction revealed a  $\kappa$ B binding site that is deleted upon the G substitution. Further analysis has to be done determining the function of this region in *GARP* regulation. However, it can be speculated that binding of NF- $\kappa$ B to this region might have enhancer function. This would be in line with the observed NF- $\kappa$ B-mediated regulation of *GARP* (Figure 6 and 7).

Furthermore, two intronic SNPs were associated with RA. Studies have demonstrated that intronic polymorphisms can affect mRNA splicing, stability, and structure, as well as protein folding (Hunt et al. 2009). In addition, intronic regions can enhance or repress transcription (Han et al. 2012; Zhang et al. 2014). Higher frequency of the minor allele G of rs4944115 (SNP7) deletes a binding site for the basic helix-loop-helix (bHLH) E2A immunoglobulin enhancer-binding factor E47. E47 has been shown to bind to the Foxp3 promoter and is implicated in Foxp3 transcription in Tregs (Maruyama et al. 2011). In addition, increased abundance of the minor allele (G) of rs7944357 (SNP8) resulted in the formation of a binding site for the bHLH transcription factor Dec1. Dec1 is involved in the upregulation of CD25 expression and has been shown to bind to E47 (Miyazaki et al. 2010). Both intronic alleles result in the formation and higher prevalence of CpGs in the *GARP* gene locus in patients with RA. Interestingly, the methylation of a single intronic CpG can already mediate silencing of gene expression (Zhang et al. 2010). Thus, it is possible that other factors involved in the regulation of *GARP* expression or higher methylation within the *GARP* gene locus in Tregs promote the observed decrease of *GARP* expression in RA. The abundance of a combination of several risk alleles might additionally promote the diminished *GARP* expression in Tregs of patients with RA thereby influencing Treg function and phenotype. In line with this, haplotype analysis revealed several haplotype distributions that are associated with a higher susceptibility to RA (Figure 19 and table 7).

#### **4.4 Decreased expression of miR-146a in Tregs from patients with RA**

In the last part of my thesis, contribution of miR-146a expression to alterations in the Treg function and phenotype was assessed in the context of RA. Several studies demonstrated that

disturbed expression of miRNAs could lead to complex alterations in Treg function and phenotype, resulting in the development of autoimmune-like conditions (Cobb et al. 2006; Liston et al. 2008; Zhou et al. 2008). More specific, alterations in miR-146a expression were often found to be associated with autoimmune diseases (Tang et al. 2009; Yang et al. 2015). Using a miRNA microarray, it has been shown that miR-146a levels were not altered in naïve or memory Tregs from patients with RA (Smigielska-Czepiel et al. 2014). We demonstrated that miR-146a is decreased in Tregs from RA patients with active disease (Zhou and Haupt et al. 2015). MiR-146a expression levels negatively correlated with the DAS28. These opposing observations might result from different patient cohorts used in the studies. In the microarray analysis six patients were included, whereas we compared miR-146a expression levels in 61 patients. In addition, different Treg populations were used. In line with our results, it was consistently shown that miR-146a expression is increased in Tregs compared to Tconvs (Lu et al. 2010; Smigielska-Czepiel et al. 2014). Induction of this miRNA is NF- $\kappa$ B dependent. Interestingly, miR-146a down-regulates TRAF6 and IRAK1, two of the signal transducers in the NF- $\kappa$ B pathway, leading to a negative feedback loop (Taganov et al. 2006). In line with this, TRAF6 and IRAK1 expression was elevated in RA patients with active disease (Zhou and Haupt et al. 2015). However, analysis of the NF- $\kappa$ B activity in Tregs revealed no differences between Tregs from RA patients and HCs suggesting that the NF- $\kappa$ B pathway is irrelevant for the observed defect of Tregs in RA (Figure 20A).

It is reported that miR-146a deficient Tregs fail to control Th1 responses which is most likely mediated by unrestrained expression and activation of STAT1 (Lu et al. 2010). In line with that, expression and phosphorylation of STAT1 protein was increased in Tregs from patients with active disease (Figure 20B). Tregs from patients with low disease activity showed comparable levels to HCs. Tregs from miR-146a deficient mice show impaired function and produced more IFN- $\gamma$  which in turn might facilitate pathogenic Th1 responses (Lu et al. 2010). Here, we could show that increased STAT1 expression and phosphorylation correlated with higher production of pro-inflammatory cytokines, such as IFN $\gamma$ , TNF, and IL-17 (Figure 21). Mir-146a was previously shown to negatively regulate TLR/IL-1R signaling in macrophages by targeting TRAF6 and IRAK1 (Hou et al. 2009; Taganov et al. 2006). In addition, Th17 differentiation and IL-17 production seems to be facilitated by IL-1R signaling (Chung et al. 2009; Maitra et al. 2009). Therefore, it is conceivable that a decrease in miR-146a in Tregs from patients with RA results in higher expression of IL-17 in these cells. It seems that lower miR-146a levels mediate STAT1

---

expression and phosphorylation, as well as TRAF6/IRAK1 expression in Tregs. Thus, the pro-inflammatory phenotype of Tregs in RA patients with active disease might be promoted by decreased miR-146a expression. Indeed, inhibition of miR-146a in Tregs from HCs using antagomirs led to increased STAT1 expression and phosphorylation (Figure 22). This was accompanied by augmented levels of pro-inflammatory cytokines. This study confirms the results obtained by Tregs isolated from miR-146a-deficient mice. MiR-146a seems to positively regulate the suppressive capacity of Tregs by targeting STAT1, TRAF6 and IRAK1. In summary, diminished miR-146a expression in Tregs from patients with RA seems to contribute to their altered phenotype observed in the disease by promoting the production of pro-inflammatory cytokines.

**BIBLIOGRAPHY**

Abbas AK, Benoist C, Bluestone JA, Campbell DJ, Ghosh S, Hori S, Jiang S, Kuchroo VK, Mathis D, Roncarolo MG et al. 2013. Regulatory T cells: recommendations to simplify the nomenclature. *Nat Immunol* **14**: 307-8.

Abbas AK, Murphy KM, Sher A. 1996. Functional diversity of helper T lymphocytes. *Nature* **383**: 787-93.

Acosta-Rodriguez EV, Napolitani G, Lanzavecchia A, Sallusto F. 2007. Interleukins 1beta and 6 but not transforming growth factor-beta are essential for the differentiation of interleukin 17-producing human T helper cells. *Nat Immunol* **8**: 942-9.

Acuto O, Michel F. 2003. CD28-mediated co-stimulation: a quantitative support for TCR signalling. *Nat Rev Immunol* **3**: 939-51.

Afkarian M, Sedy JR, Yang J, Jacobson NG, Cereb N, Yang SY, Murphy TL, Murphy KM. 2002. T-bet is a STAT1-induced regulator of IL-12R expression in naive CD4+ T cells. *Nat Immunol* **3**: 549-57.

Alamanos Y, Drosos AA. 2005. Epidemiology of adult rheumatoid arthritis. *Autoimmun Rev* **4**: 130-6.

Alberts B, Johnson A, Lewis J, Raff M, Roberts K, Walter P. 2002. Molecular Biology of the Cell. Lymphocytes and the Cellular Basis of Adaptive Immunity. **4th**, Garland Science, New York.

Aletaha D, Neogi T, Silman AJ, Funovits J, Felson DT, Bingham CO, 3rd, Birnbaum NS, Burmester GR, Bykerk VP, Cohen MD et al. 2010. 2010 Rheumatoid arthritis classification criteria: an American College of Rheumatology/European League Against Rheumatism collaborative initiative. *Arthritis Rheum* **62**: 2569-81.

Amit I, Citri A, Shay T, Lu Y, Katz M, Zhang F, Tarcic G, Siwak D, Lahad J, Jacob-Hirsch J et al. 2007. A module of negative feedback regulators defines growth factor signaling. *Nat Genet* **39**: 503-12.

Annunziato F, Romagnani S. 2009. Heterogeneity of human effector CD4+ T cells. *Arthritis Res Ther* **11**: 257.

Aran D, Toperoff G, Rosenberg M, Hellman A. 2011. Replication timing-related and gene body-specific methylation of active human genes. *Hum Mol Genet* **20**: 670-80.

Arnett FC, Edworthy SM, Bloch DA, McShane DJ, Fries JF, Cooper NS, Healey LA, Kaplan SR, Liang MH, Luthra HS. 1988. The American Rheumatism Association 1987 revised criteria for the classification of rheumatoid arthritis. *Arthritis Rheum* **31**: 315-24.

- Asseman C, Mauze S, Leach MW, Coffman RL, Powrie F. 1999. An essential role for interleukin 10 in the function of regulatory T cells that inhibit intestinal inflammation. *J Exp Med* **190**: 995-1004.
- Asseman C, Read S, Powrie F. 2003. Colitogenic Th1 cells are present in the antigen-experienced T cell pool in normal mice: control by CD4+ regulatory T cells and IL-10. *J Immunol* **171**: 971-8.
- Ayoubi TA, Van De Ven WJ. 1996. Regulation of gene expression by alternative promoters. *FASEB J* **10**: 453-60.
- Ball MP, Li JB, Gao Y, Lee JH, LeProust EM, Park IH, Xie B, Daley GQ, Church GM. 2009. Targeted and genome-scale strategies reveal gene-body methylation signatures in human cells. *Nat Biotechnol* **27**: 361-8.
- Bandukwala HS, Wu Y, Feuerer M, Chen Y, Barboza B, Ghosh S, Stroud JC, Benoist C, Mathis D, Rao A et al. 2011. Structure of a domain-swapped FOXP3 dimer on DNA and its function in regulatory T cells. *Immunity* **34**: 479-91.
- Barrett JC, Fry B, Maller J, Daly MJ. 2005. Haploview: analysis and visualization of LD and haplotype maps. *Bioinformatics* **21**: 263-5.
- Bartel DP. 2004. MicroRNAs: genomics, biogenesis, mechanism, and function. *Cell* **116**: 281-97.
- Bekri S, Adelaide J, Merscher S, Grosgeorge J, Caroli-Bosc F, Perucca-Lostanlen D, Kelley PM, Pebusque MJ, Theillet C, Birnbaum D et al. 1997. Detailed map of a region commonly amplified at 11q13-->q14 in human breast carcinoma. *Cytogenet Cell Genet* **79**: 125-31.
- Belkaid Y. 2008. Role of Foxp3-positive regulatory T cells during infection. *Eur J Immunol* **38**: 918-21.
- Bettelli E, Carrier Y, Gao W, Korn T, Strom TB, Oukka M, Weiner HL, Kuchroo VK. 2006. Reciprocal developmental pathways for the generation of pathogenic effector TH17 and regulatory T cells. *Nature* **441**: 235-8.
- Bettelli E, Dastrange M, Oukka M. 2005. Foxp3 interacts with nuclear factor of activated T cells and NF-kappa B to repress cytokine gene expression and effector functions of T helper cells. *Proc Natl Acad Sci U S A* **102**: 5138-43.
- Bettelli E, Korn T, Kuchroo VK. 2007. Th17: the third member of the effector T cell trilogy. *Curr Opin Immunol* **19**: 652-7.
- Bird A. 2011. The dinucleotide CG as a genomic signalling module. *J Mol Biol* **409**: 47-53.
- Blank V, Andrews NC. 1997. The Maf transcription factors: regulators of differentiation. *Trends Biochem Sci* **22**: 437-41.

Bopp T, Becker C, Klein M, Klein-Hessling S, Palmetshofer A, Serfling E, Heib V, Becker M, Kubach J, Schmitt S et al. 2007. Cyclic adenosine monophosphate is a key component of regulatory T cell-mediated suppression. *J Exp Med* **204**: 1303-10.

Borsellino G, Kleinewietfeld M, Di Mitri D, Sternjak A, Diamantini A, Giometto R, Hopner S, Centonze D, Bernardi G, Dell'Acqua ML et al. 2007. Expression of ectonucleotidase CD39 by Foxp3+ Treg cells: hydrolysis of extracellular ATP and immune suppression. *Blood* **110**: 1225-32.

Bottcher RT, Pollet N, Delius H, Niehrs C. 2004. The transmembrane protein XFLRT3 forms a complex with FGF receptors and promotes FGF signalling. *Nat Cell Biol* **6**: 38-44.

Bottini N, Firestein GS. 2013. Epigenetics in rheumatoid arthritis: a primer for rheumatologists. *Curr Rheumatol Rep* **15**: 372.

Bradford MM. 1976. A rapid and sensitive method for the quantitation of microgram quantities of protein utilizing the principle of protein-dye binding. *Anal Biochem* **72**: 248-54.

Bultmann I, Conradi A, Kretschmer C, Sterner-Kock A. 2013. Latent transforming growth factor beta-binding protein 4 is downregulated in esophageal cancer via promoter methylation. *PLoS One* **8**: e65614.

Cao D, van Vollenhoven R, Klareskog L, Trollmo C, Malmstrom V. 2004. CD25brightCD4+ regulatory T cells are enriched in inflamed joints of patients with chronic rheumatic disease. *Arthritis Res Ther* **6**: R335-46.

Cartharius K, Frech K, Grote K, Klocke B, Haltmeier M, Klingenhoff A, Frisch M, Bayerlein M, Werner T. 2005. MatInspector and beyond: promoter analysis based on transcription factor binding sites. *Bioinformatics* **21**: 2933-42.

Cervoni N, Szyf M. 2001. Demethylase activity is directed by histone acetylation. *J Biol Chem* **276**: 40778-87.

Chan DV, Somani AK, Young AB, Massari JV, Ohtola J, Sugiyama H, Garaczi E, Babineau D, Cooper KD, McCormick TS. 2011. Signal peptide cleavage is essential for surface expression of a regulatory T cell surface protein, leucine rich repeat containing 32 (LRRC32). *BMC Biochem* **12**: 27.

Chatila TA. 2005. Role of regulatory T cells in human diseases. *J Allergy Clin Immunol* **116**: 949-59.

Chen C, Rowell EA, Thomas RM, Hancock WW, Wells AD. 2006. Transcriptional regulation by Foxp3 is associated with direct promoter occupancy and modulation of histone acetylation. *J Biol Chem* **281**: 36828-34.

Chen ML, Pittet MJ, Gorelik L, Flavell RA, Weissleder R, von Boehmer H, Khazaie K. 2005. Regulatory T cells suppress tumor-specific CD8 T cell cytotoxicity through TGF-beta signals in vivo. *Proc Natl Acad Sci U S A* **102**: 419-24.

- Cheong J, Yamada Y, Yamashita R, Irie T, Kanai A, Wakaguri H, Nakai K, Ito T, Saito I, Sugano S et al. 2006. Diverse DNA methylation statuses at alternative promoters of human genes in various tissues. *DNA Res* **13**: 155-67.
- Choy E. 2012. Understanding the dynamics: pathways involved in the pathogenesis of rheumatoid arthritis. *Rheumatology* **51**: v3-11.
- Chung Y, Chang SH, Martinez GJ, Yang XO, Nurieva R, Kang HS, Ma L, Watowich SS, Jetten AM, Tian Q et al. 2009. Critical regulation of early Th17 cell differentiation by interleukin-1 signaling. *Immunity* **30**: 576-87.
- Chytil M, Verdine GL. 1996. The Rel family of eukaryotic transcription factors. *Curr Opin Struct Biol* **6**: 91-100.
- Cierpicki T, Risner LE, Grembecka J, Lukasik SM, Popovic R, Omonkowska M, Shultis DD, Zeleznik-Le NJ, Bushweller JH. 2010. Structure of the MLL CXXC domain-DNA complex and its functional role in MLL-AF9 leukemia. *Nat Struct Mol Biol* **17**: 62-8.
- Cobb BS, Hertweck A, Smith J, O'Connor E, Graf D, Cook T, Smale ST, Sakaguchi S, Livesey FJ, Fisher AG et al. 2006. A role for Dicer in immune regulation. *J Exp Med* **203**: 2519-27.
- Collison LW, Workman CJ, Kuo TT, Boyd K, Wang Y, Vignali KM, Cross R, Sehy D, Blumberg RS, Vignali DA. 2007. The inhibitory cytokine IL-35 contributes to regulatory T-cell function. *Nature* **450**: 566-9.
- Cribbs AP, Kennedy A, Penn H, Read JE, Amjadi P, Green P, Syed K, Manka SW, Brennan FM, Gregory B et al. 2014. Treg cell function in rheumatoid arthritis is compromised by ctla-4 promoter methylation resulting in a failure to activate the indoleamine 2,3-dioxygenase pathway. *Arthritis Rheumatol* **66**: 2344-54.
- Cuende J, Lienart S, Dedobbeleer O, van der Woning B, De Boeck G, Stockis J, Huygens C, Colau D, Somja J, Delvenne P et al. 2015. Monoclonal antibodies against GARP/TGF-beta1 complexes inhibit the immunosuppressive activity of human regulatory T cells in vivo. *Sci Transl Med* **7**: 284ra56.
- Daniels MA, Teixeira E, Gill J, Hausmann B, Roubaty D, Holmberg K, Werlen G, Hollander GA, Gascoigne NR, Palmer E. 2006. Thymic selection threshold defined by compartmentalization of Ras/MAPK signalling. *Nature* **444**: 724-9.
- Davis MR, Andersson R, Severin J, de Hoon M, Bertin N, Baillie JK, Kawaji H, Sandelin A, Forrest AR, Summers KM. 2014. Transcriptional profiling of the human fibrillin/LTBP gene family, key regulators of mesenchymal cell functions. *Mol Genet Metab* **112**: 73-83.
- Diehl S, Anguita J, Hoffmeyer A, Zapton T, Ihle JN, Fikrig E, Rincon M. 2000. Inhibition of Th1 differentiation by IL-6 is mediated by SOCS1. *Immunity* **13**: 805-15.

- Diehl S, Rincon M. 2002. The two faces of IL-6 on Th1/Th2 differentiation. *Mol Immunol* **39**: 531-6.
- Doig CL, Bashir J, Zielinska AE, Cooper MS, Stewart PM, Lavery GG. 2014. TNFalpha-mediated Hsd11b1 binding of NF-kappaB p65 is associated with suppression of 11beta-HSD1 in muscle. *J Endocrinol* **220**: 389-96.
- Edwards J, Krishna NS, Witton CJ, Bartlett JM. 2003. Gene amplifications associated with the development of hormone-resistant prostate cancer. *Clin Cancer Res* **9**: 5271-81.
- Edwards JP, Fujii H, Zhou AX, Creemers J, Unutmaz D, Shevach EM. 2013. Regulation of the expression of GARP/latent TGF-beta1 complexes on mouse T cells and their role in regulatory T cell and Th17 differentiation. *J Immunol* **190**: 5506-15.
- Ehrenstein MR, Evans JG, Singh A, Moore S, Warnes G, Isenberg DA, Mauri C. 2004. Compromised function of regulatory T cells in rheumatoid arthritis and reversal by anti-TNFalpha therapy. *J Exp Med* **200**: 277-85.
- Farre D, Romà R, Huerta M, Adsuara JE, Rosello L, Alba MM, Messeguer X. 2003. Identification of patterns in biological sequences at the ALGGEN server: PROMO and MALGEN. *Nucl Acids Res* **31**: 3651-53.
- Firestein GS. 2005. Immunologic mechanisms in the pathogenesis of rheumatoid arthritis. *J Clin Rheumatol* **11**: 39-44.
- Firestein GS, Budd RC, Gabriel SE, McInnes IB, O'Dell JR. 2012. Rheumatoid arthritis. Kelley's Textbook of Rheumatology. **9th Edition**, Elsevier Saunders, Philadelphia.
- Flores-Borja F, Jury EC, Mauri C, Ehrenstein MR. 2008. Defects in CTLA-4 are associated with abnormal regulatory T cell function in rheumatoid arthritis. *Proc Natl Acad Sci U S A* **105**: 19396-401.
- Fontenot JD, Gavin MA, Rudensky AY. 2003. Foxp3 programs the development and function of CD4+CD25+ regulatory T cells. *Nat Immunol* **4**: 330-6.
- Fontenot JD, Rasmussen JP, Gavin MA, Rudensky AY. 2005. A function for interleukin 2 in Foxp3-expressing regulatory T cells. *Nat Immunol* **6**: 1142-51.
- Fransen J, van Riel PL. 2006. DAS remission cut points. *Clin Exp Rheumatol* **24**: 29-32.
- Frey O, Petrow PK, Gajda M, Siegmund K, Huehn J, Scheffold A, Hamann A, Radbruch A, Brauer R. 2005. The role of regulatory T cells in antigen-induced arthritis: aggravation of arthritis after depletion and amelioration after transfer of CD4+CD25+ T cells. *Arthritis Res Ther* **7**: R291-301.
- Gavin MA, Rasmussen JP, Fontenot JD, Vasta V, Manganiello VC, Beavo JA, Rudensky AY. 2007. Foxp3-dependent programme of regulatory T-cell differentiation. *Nature* **445**: 771-5.

- Getts MT, Miller SD. 2010. 99th Dahlem conference on infection, inflammation and chronic inflammatory disorders: triggering of autoimmune diseases by infections. *Clin Exp Immunol* **160**: 15-21.
- Girbal-Neuhauser E, Durieux JJ, Arnaud M, Dalbon P, Sebbag M, Vincent C, Simon M, Senshu T, Masson-Bessiere C, Jolivet-Reynaud C et al. 1999. The epitopes targeted by the rheumatoid arthritis-associated antifilaggrin autoantibodies are posttranslationally generated on various sites of (pro)filaggrin by deimination of arginine residues. *J Immunol* **162**: 585-94.
- Gondek DC, Lu LF, Quezada SA, Sakaguchi S, Noelle RJ. 2005. Cutting edge: contact-mediated suppression by CD4+CD25+ regulatory cells involves a granzyme B-dependent, perforin-independent mechanism. *J Immunol* **174**: 1783-6.
- Goode EL, DeRycke M, Kalli KR, Oberg AL, Cunningham JM, Maurer MJ, Fridley BL, Armasu SM, Serie DJ, Ramar P et al. 2013. Inherited variants in regulatory T cell genes and outcome of ovarian cancer. *PLoS One* **8**: e53903.
- Green EA, Gorelik L, McGregor CM, Tran EH, Flavell RA. 2003. CD4+CD25+ T regulatory cells control anti-islet CD8+ T cells through TGF-beta-TGF-beta receptor interactions in type 1 diabetes. *Proc Natl Acad Sci U S A* **100**: 10878-83.
- Green MR. 2005. Eukaryotic transcription activation: right on target. *Mol Cell* **18**: 399-402.
- Gregersen PK, Amos CI, Lee AT, Lu Y, Remmers EF, Kastner DL, Seldin MF, Criswell LA, Plenge RM, Holers VM et al. 2009. REL, encoding a member of the NF-kappaB family of transcription factors, is a newly defined risk locus for rheumatoid arthritis. *Nat Genet* **41**: 820-3.
- Grossman WJ, Verbsky JW, Barchet W, Colonna M, Atkinson JP, Ley TJ. 2004. Human T regulatory cells can use the perforin pathway to cause autologous target cell death. *Immunity* **21**: 589-601.
- Grumont R, Hochrein H, O'Keeffe M, Gugasyan R, White C, Caminschi I, Cook W, Gerondakis S. 2001. c-Rel regulates interleukin 12 p70 expression in CD8(+) dendritic cells by specifically inducing p35 gene transcription. *J Exp Med* **194**: 1021-32.
- Grunstein M. 1997. Histone acetylation in chromatin structure and transcription. *Nature* **389**: 349-52.
- Guthridge JM, Lu R, Sun H, Sun C, Wiley GB, Dominguez N, Macwana SR, Lessard CJ, Kim-Howard X, Cobb BL et al. 2014. Two functional lupus-associated BLK promoter variants control cell-type- and developmental-stage-specific transcription. *Am J Hum Genet* **94**: 586-98.
- Hahn SA, Stahl HF, Becker C, Correll A, Schneider FJ, Tuettenberg A, Jonuleit H. 2013. Soluble GARP has potent antiinflammatory and immunomodulatory impact on human CD4(+) T cells. *Blood* **122**: 1182-91.

- Han Y, Yang Y, Chen Z, Jiang Z, Gu Y, Liu Y, Xu S, Lin C, Pan Z, Zhou W et al. 2014. Human hepatocellular carcinoma-infiltrating CD4(+)CD69(+)Foxp3(-) regulatory T cell suppresses T cell response via membrane-bound TGF-beta1. *J Mol Med* **92**: 539-50.
- Han YJ, Ma SF, Wade MS, Flores C, Garcia JG. 2012. An intronic MYLK variant associated with inflammatory lung disease regulates promoter activity of the smooth muscle myosin light chain kinase isoform. *J Mol Med* **90**: 299-308.
- Hashimoto H, Vertino PM, Cheng X. 2010. Molecular coupling of DNA methylation and histone methylation. *Epigenomics* **2**: 657-69.
- Hogan PG, Chen L, Nardone J, Rao A. 2003. Transcriptional regulation by calcium, calcineurin, and NFAT. *Genes Dev* **17**: 2205-32.
- Hori S, Nomura T, Sakaguchi S. 2003. Control of regulatory T cell development by the transcription factor Foxp3. *Science* **299**: 1057-61.
- Hou J, Wang P, Lin L, Liu X, Ma F, An H, Wang Z, Cao X. 2009. MicroRNA-146a feedback inhibits RIG-I-dependent Type I IFN production in macrophages by targeting TRAF6, IRAK1, and IRAK2. *J Immunol* **183**: 2150-8.
- Hunt R, Sauna ZE, Ambudkar SV, Gottesman MM, Kimchi-Sarfaty C. 2009. Silent (synonymous) SNPs: should we care about them? *Methods Mol Biol* **578**: 23-39.
- Huter EN, Punkosdy GA, Glass DD, Cheng LI, Ward JM, Shevach EM. 2008. TGF-beta-induced Foxp3+ regulatory T cells rescue scurfy mice. *Eur J Immunol* **38**: 1814-21.
- Inman GJ. 2011. Switching TGFbeta from a tumor suppressor to a tumor promoter. *Curr Opin Genet Dev* **21**: 93-9.
- Isomura I, Palmer S, Grumont RJ, Bunting K, Hoyne G, Wilkinson N, Banerjee A, Proietto A, Gugasyan R, Wu L et al. 2009. c-Rel is required for the development of thymic Foxp3+ CD4 regulatory T cells. *J Exp Med* **206**: 3001-14.
- Jadidi-Niaragh F, Mirshafiey A. 2011. Th17 cell, the new player of neuroinflammatory process in multiple sclerosis. *Scand J Immunol* **74**: 1-13.
- Janeway CA, Travers P, Walport M, Shlomchik MJ. 2001. Immunobiology: The Immune System in Health and Disease. Principles of innate and adaptive immunity. Garland Science, New York.
- Jonuleit H, Schmitt E, Stassen M, Tuettenberg A, Knop J, Enk AH. 2001. Identification and functional characterization of human CD4(+)CD25(+) T cells with regulatory properties isolated from peripheral blood. *J Exp Med* **193**: 1285-94.
- Kalathil S, Lugade AA, Miller A, Iyer R, Thanavala Y. 2013. Higher frequencies of GARP(+)CTLA-4(+)Foxp3(+) T regulatory cells and myeloid-derived suppressor cells in hepatocellular carcinoma patients are associated with impaired T-cell functionality. *Cancer Res* **73**: 2435-44.

- Kanber D, Berulava T, Ammerpohl O, Mitter D, Richter J, Siebert R, Horsthemke B, Lohmann D, Buiting K. 2009. The human retinoblastoma gene is imprinted. *PLoS Genet* **5**: e1000790. 10.1371/journal.pgen.90.
- Kaplan MH, Schindler U, Smiley ST, Grusby MJ. 1996. Stat6 is required for mediating responses to IL-4 and for development of Th2 cells. *Immunity* **4**: 313-9.
- Kataoka K, Noda M, Nishizawa M. 1996. Transactivation activity of Maf nuclear oncoprotein is modulated by Jun, Fos and small Maf proteins. *Oncogene* **12**: 53-62.
- Katoh H, Qin ZS, Liu R, Wang L, Li W, Li X, Wu L, Du Z, Lyons R, Liu CG et al. 2011. FOXP3 orchestrates H4K16 acetylation and H3K4 trimethylation for activation of multiple genes by recruiting MOF and causing displacement of PLU-1. *Mol Cell* **44**: 770-84.
- Katsuoka F, Motohashi H, Ishii T, Aburatani H, Engel JD, Yamamoto M. 2005. Genetic evidence that small maf proteins are essential for the activation of antioxidant response element-dependent genes. *Mol Cell Biol* **25**: 8044-51.
- Kelemen O, Convertini P, Zhang Z, Wen Y, Shen M, Falaleeva M, Stamm S. 2013. Function of alternative splicing. *Gene* **514**: 1-30.
- Kimura K, Wakamatsu A, Suzuki Y, Ota T, Nishikawa T, Yamashita R, Yamamoto J, Sekine M, Tsuritani K, Wakaguri H et al. 2006. Diversification of transcriptional modulation: large-scale identification and characterization of putative alternative promoters of human genes. *Genome Res* **16**: 55-65.
- Klareskog L, Padyukov L, Alfredsson L. 2007. Smoking as a trigger for inflammatory rheumatic diseases. *Curr Opin Rheumatol* **19**: 49-54.
- Klein L, Hinterberger M, Wirnsberger G, Kyewski B. 2009. Antigen presentation in the thymus for positive selection and central tolerance induction. *Nat Rev Immunol* **9**: 833-44.
- Klug M, Rehli M. 2006. Functional analysis of promoter CpG methylation using a CpG-free luciferase reporter vector. *Epigenetics* **1**: 127-30.
- Knutson KL, Disis ML, Salazar LG. 2007. CD4 regulatory T cells in human cancer pathogenesis. *Cancer Immunol Immunother* **56**: 271-85.
- Kobie JJ, Shah PR, Yang L, Rebhahn JA, Fowell DJ, Mosmann TR. 2006. T regulatory and primed uncommitted CD4 T cells express CD73, which suppresses effector CD4 T cells by converting 5'-adenosine monophosphate to adenosine. *J Immunol* **177**: 6780-6.
- Kornberg RD. 2007. The molecular basis of eucaryotic transcription. *Cell Death Differ* **14**: 1989-97.
- Kornblihtt AR. 2005. Promoter usage and alternative splicing. *Curr Opin Cell Biol* **17**: 262-8.

- Koski C, Saharinen J, Keski-Oja J. 1999. Independent promoters regulate the expression of two amino terminally distinct forms of latent transforming growth factor-beta binding protein-1 (LTBP-1) in a cell type-specific manner. *J Biol Chem* **274**: 32619-30.
- Kulis M, Queiros AC, Beekman R, Martin-Subero JJ. 2013. Intragenic DNA methylation in transcriptional regulation, normal differentiation and cancer. *Biochim Biophys Acta* **1829**: 1161-74.
- Kurowska-Stolarska M, Alivernini S, Ballantine LE, Asquith DL, Millar NL, Gilchrist DS, Reilly J, Ierna M, Fraser AR, Stolarski B et al. 2011. MicroRNA-155 as a proinflammatory regulator in clinical and experimental arthritis. *Proc Natl Acad Sci U S A* **108**: 11193-8.
- Landry JR, Mager DL, Wilhelm BT. 2003. Complex controls: the role of alternative promoters in mammalian genomes. *Trends Genet* **19**: 640-8.
- Lassmann S, Weis R, Makowicz F, Roth J, Danciu M, Hopt U, Werner M. 2007. Array CGH identifies distinct DNA copy number profiles of oncogenes and tumor suppressor genes in chromosomal- and microsatellite-unstable sporadic colorectal carcinomas. *J Mol Med* **85**: 293-304.
- Laurent L, Wong E, Li G, Huynh T, Tsiganos A, Ong CT, Low HM, Kin Sung KW, Rigoutsos I, Loring J et al. 2010. Dynamic changes in the human methylome during differentiation. *Genome Res* **20**: 320-31.
- Le Dantec C, Vallet S, Brooks WH, Renaudineau Y. 2015. Human endogenous retrovirus group E and its involvement in diseases. *Viruses* **7**: 1238-57.
- Leah E. 2011. Rheumatoid arthritis: miR-155 mediates inflammation. *Nat Rev Rheumatol* **7**: 437.
- Lee YH, Choi SJ, Ji JD, Song GG. 2012. The CTLA-4 +49 A/G and -318 C/T polymorphisms and susceptibility to asthma: a meta-analysis. *Mol Biol Rep* **39**: 8525-32.
- Leipe J, Grunke M, Dechant C, Reindl C, Kerzendorf U, Schulze-Koops H, Skapenko A. 2010. Role of Th17 cells in human autoimmune arthritis. *Arthritis Rheum* **62**: 2876-85.
- Leipe J, Schramm MA, Prots I, Schulze-Koops H, Skapenko A. 2014. Increased Th17 cell frequency and poor clinical outcome in rheumatoid arthritis are associated with a genetic variant in the IL4R gene, rs1805010. *Arthritis Rheumatol* **66**: 1165-75.
- Leng RX, Pan HF, Qin WZ, Chen GM, Ye DQ. 2011. Role of microRNA-155 in autoimmunity. *Cytokine Growth Factor Rev* **22**: 141-7.
- Li LC, Dahiya R. 2002a. MethPrimer: designing primers for methylation PCRs. *Bioinformatics* **18**: 1427-31.
- Li MO, Sanjabi S, Flavell RA. 2006. Transforming growth factor-beta controls development, homeostasis, and tolerance of T cells by regulatory T cell-dependent and -independent mechanisms. *Immunity* **25**: 455-71.

- Li Q, Verma IM. 2002b. NF-kappaB regulation in the immune system. *Nat Rev Immunol* **2**: 725-34.
- Li X, Ye F, Chen H, Lu W, Wan X, Xie X. 2007. Human ovarian carcinoma cells generate CD4(+)CD25(+) regulatory T cells from peripheral CD4(+)CD25(-) T cells through secreting TGF-beta. *Cancer Lett* **253**: 144-53.
- Lighvani AA, Frucht DM, Jankovic D, Yamane H, Aliberti J, Hissong BD, Nguyen BV, Gadina M, Sher A, Paul WE et al. 2001. T-bet is rapidly induced by interferon-gamma in lymphoid and myeloid cells. *Proc Natl Acad Sci U S A* **98**: 15137-42.
- Liston A, Lu LF, O'Carroll D, Tarakhovsky A, Rudensky AY. 2008. Dicer-dependent microRNA pathway safeguards regulatory T cell function. *J Exp Med* **205**: 1993-2004.
- Liu CC, Fang TJ, Ou TT, Wu CC, Li RN, Lin YC, Lin CH, Tsai WC, Liu HW, Yen JH. 2011. Global DNA methylation, DNMT1, and MBD2 in patients with rheumatoid arthritis. *Immunol Lett* **135**: 96-9.
- Liu CJ, Lin SC, Chen YJ, Chang KM, Chang KW. 2006. Array-comparative genomic hybridization to detect genomewide changes in microdissected primary and metastatic oral squamous cell carcinomas. *Mol Carcinog* **45**: 721-31.
- Liu VC, Wong LY, Jang T, Shah AH, Park I, Yang X, Zhang Q, Lonning S, Teicher BA, Lee C. 2007. Tumor evasion of the immune system by converting CD4+CD25- T cells into CD4+CD25+ T regulatory cells: role of tumor-derived TGF-beta. *J Immunol* **178**: 2883-92.
- Loizou L, Andersen KG, Betz AG. 2011. Foxp3 interacts with c-Rel to mediate NF-kappaB repression. *PLoS One* **6**: e18670.
- Long M, Park SG, Strickland I, Hayden MS, Ghosh S. 2009. Nuclear factor-kappaB modulates regulatory T cell development by directly regulating expression of Foxp3 transcription factor. *Immunity* **31**: 921-31.
- Lozano T, Casares N, Lasarte JJ. 2013. Searching for the Achilles Heel of FOXP3. *Front Oncol* **3**: 294.
- Lu LF, Boldin MP, Chaudhry A, Lin LL, Taganov KD, Hanada T, Yoshimura A, Baltimore D, Rudensky AY. 2010. Function of miR-146a in controlling Treg cell-mediated regulation of Th1 responses. *Cell* **142**: 914-29.
- Luckheeram RV, Zhou R, Verma AD, Xia B. 2012. CD4(+)T cells: differentiation and functions. *Clin Dev Immunol* **Vol. 2012**:
- Ma X, Becker Buscaglia LE, Barker JR, Li Y. 2011. MicroRNAs in NF-kappaB signaling. *J Mol Cell Biol* **3**: 159-66.

- Macaulay IC, Tijssen MR, Thijssen-Timmer DC, Gusnanto A, Steward M, Burns P, Langford CF, Ellis PD, Dudbridge F, Zwaginga JJ et al. 2007. Comparative gene expression profiling of in vitro differentiated megakaryocytes and erythroblasts identifies novel activatory and inhibitory platelet membrane proteins. *Blood* **109**: 3260-9.
- Maitra U, Davis S, Reilly CM, Li L. 2009. Differential regulation of Foxp3 and IL-17 expression in CD4 T helper cells by IRAK-1. *J Immunol* **182**: 5763-9.
- Mantel PY, Schmidt-Weber CB. 2011. Transforming growth factor-beta: recent advances on its role in immune tolerance. *Methods Mol Biol* **677**: 303-38.
- Marini MG, Asunis I, Chan K, Chan JY, Kan YW, Porcu L, Cao A, Moi P. 2002. Cloning MafF by recognition site screening with the NFE2 tandem repeat of HS2: analysis of its role in globin and GCSI genes regulation. *Blood Cells Mol Dis* **29**: 145-58.
- Marson A, Kretschmer K, Frampton GM, Jacobsen ES, Polansky JK, MacIsaac KD, Levine SS, Fraenkel E, von Boehmer H, Young RA. 2007. Foxp3 occupancy and regulation of key target genes during T-cell stimulation. *Nature* **445**: 931-5.
- Maruyama T, Li J, Vaque JP, Konkel JE, Wang W, Zhang B, Zhang P, Zamarron BF, Yu D, Wu Y et al. 2011. Control of the differentiation of regulatory T cells and T(H)17 cells by the DNA-binding inhibitor Id3. *Nat Immunol* **12**: 86-95.
- Mason NJ, Liou HC, Hunter CA. 2004. T cell-intrinsic expression of c-Rel regulates Th1 cell responses essential for resistance to *Toxoplasma gondii*. *J Immunol* **172**: 3704-11.
- Massrieh W, Derjuga A, Doualla-Bell F, Ku CY, Sanborn BM, Blank V. 2006. Regulation of the MAFF transcription factor by proinflammatory cytokines in myometrial cells. *Biol Reprod* **74**: 699-705.
- Maunakea AK, Nagarajan RP, Bilenky M, Ballinger TJ, D'Souza C, Fouse SD, Johnson BE, Hong C, Nielsen C, Zhao Y et al. 2010. Conserved role of intragenic DNA methylation in regulating alternative promoters. *Nature* **466**: 253-7.
- Menegazzo L, Albiero M, Avogaro A, Fadini GP. 2012. Endothelial progenitor cells in diabetes mellitus. *Biofactors* **38**: 194-202.
- Messeguer X, Escudero R, Farre D, Nunez O, Martinez J, Alba MM. 2002. PROMO: detection of known transcription regulatory elements using species-tailored searches. *Bioinformatics* **18**: 333-4.
- Milne TA, Briggs SD, Brock HW, Martin ME, Gibbs D, Allis CD, Hess JL. 2002. MLL targets SET domain methyltransferase activity to Hox gene promoters. *Mol Cell* **10**: 1107-17.
- Mise-Omata S, Kuroda E, Niikura J, Yamashita U, Obata Y, Doi TS. 2007. A proximal kappaB site in the IL-23 p19 promoter is responsible for RelA- and c-Rel-dependent transcription. *J Immunol* **179**: 6596-603.

- Miyazaki K, Miyazaki M, Guo Y, Yamasaki N, Kanno M, Honda Z, Oda H, Kawamoto H, Honda H. 2010. The role of the basic helix-loop-helix transcription factor Dec1 in the regulatory T cells. *J Immunol* **185**: 7330-9.
- Moo-Young TA, Larson JW, Belt BA, Tan MC, Hawkins WG, Eberlein TJ, Goedegebuure PS, Linehan DC. 2009. Tumor-derived TGF-beta mediates conversion of CD4+Foxp3+ regulatory T cells in a murine model of pancreas cancer. *J Immunother* **32**: 12-21.
- Morikawa H, Ohkura N Fau - Vandenbon A, Vandenbon A Fau - Itoh M, Itoh M Fau - Nagao-Sato S, Nagao-Sato S Fau - Kawaji H, Kawaji H Fau - Lassmann T, Lassmann T Fau - Carninci P, Carninci P Fau - Hayashizaki Y, Hayashizaki Y Fau - Forrest ARR, Forrest Ar Fau - Standley DM et al. 2014. Differential roles of epigenetic changes and Foxp3 expression in regulatory T cell-specific transcriptional regulation. *Proc Natl Acad Sci U S A* **111**: 5289-94.
- Mosmann TR, Cherwinski H, Bond MW, Giedlin MA, Coffman RL. 1986. Two types of murine helper T cell clone. I. Definition according to profiles of lymphokine activities and secreted proteins. *J Immunol* **136**: 2348-57.
- Motohashi H, Katsuoka F, Shavit JA, Engel JD, Yamamoto M. 2000. Positive or negative MARE-dependent transcriptional regulation is determined by the abundance of small Maf proteins. *Cell* **103**: 865-75.
- Movassagh M, Choy MK, Goddard M, Bennett MR, Down TA, Foo RS. 2010. Differential DNA methylation correlates with differential expression of angiogenic factors in human heart failure. *PLoS One* **5**: e8564.
- Nadkarni S, Mauri C, Ehrenstein MR. 2007. Anti-TNF-alpha therapy induces a distinct regulatory T cell population in patients with rheumatoid arthritis via TGF-beta. *J Exp Med* **204**: 33-9.
- Nakamura K, Kitani A, Fuss I, Pedersen A, Harada N, Nawata H, Strober W. 2004. TGF-beta 1 plays an important role in the mechanism of CD4+CD25+ regulatory T cell activity in both humans and mice. *J Immunol* **172**: 834-42.
- Nakamura K, Kitani A, Strober W. 2001. Cell contact-dependent immunosuppression by CD4(+)CD25(+) regulatory T cells is mediated by cell surface-bound transforming growth factor beta. *J Exp Med* **194**: 629-44.
- Nakasa T, Miyaki S, Okubo A, Hashimoto M, Nishida K, Ochi M, Asahara H. 2008. Expression of microRNA-146 in rheumatoid arthritis synovial tissue. *Arthritis Rheum* **58**: 1284-92.
- Nakasa T, Shibuya H, Nagata Y, Niimoto T, Ochi M. 2011. The inhibitory effect of microRNA-146a expression on bone destruction in collagen-induced arthritis. *Arthritis Rheum* **63**: 1582-90.
- Nie H, Zheng Y, Li R, Guo TB, He D, Fang L, Liu X, Xiao L, Chen X, Wan B et al. 2013. Phosphorylation of FOXP3 controls regulatory T cell function and is inhibited by TNF-alpha in rheumatoid arthritis. *Nat Med* **19**: 322-8.

- Nishibori T, Tanabe Y, Su L, David M. 2004. Impaired development of CD4<sup>+</sup> CD25<sup>+</sup> regulatory T cells in the absence of STAT1: increased susceptibility to autoimmune disease. *J Exp Med* **199**: 25-34.
- Odegaard JI, Ricardo-Gonzalez RR, Goforth MH, Morel CR, Subramanian V, Mukundan L, Red Eagle A, Vats D, Brombacher F, Ferrante AW et al. 2007. Macrophage-specific PPAR $\gamma$  controls alternative activation and improves insulin resistance. *Nature* **447**: 1116-20.
- Ohkura N, Hamaguchi M, Morikawa H, Sugimura K, Tanaka A, Ito Y, Osaki M, Tanaka Y, Yamashita R, Nakano N et al. 2012. T cell receptor stimulation-induced epigenetic changes and Foxp3 expression are independent and complementary events required for Treg cell development. *Immunity* **37**: 785-99.
- Okada Y, Wu D, Trynka G, Raj T, Terao C, Ikari K, Kochi Y, Ohmura K, Suzuki A, Yoshida S et al. 2014. Genetics of rheumatoid arthritis contributes to biology and drug discovery. *Nature* **506**: 376-81.
- Ollendorff V, Noguchi T, deLapeyriere O, Birnbaum D. 1994. The GARP gene encodes a new member of the family of leucine-rich repeat-containing proteins. *Cell Growth Differ* **5**: 213-9.
- Ollendorff V, Szepetowski P, Mattei MG, Gaudray P, Birnbaum D. 1992. New gene in the homologous human 11q13-q14 and mouse 7F chromosomal regions. *Mamm Genome* **2**: 195-200.
- Onodera K, Shavit JA, Motohashi H, Katsuoka F, Akasaka JE, Engel JD, Yamamoto M. 1999. Characterization of the murine mafF gene. *J Biol Chem* **274**: 21162-9.
- Onodera K, Shavit JA, Motohashi H, Yamamoto M, Engel JD. 2000. Perinatal synthetic lethality and hematopoietic defects in compound mafG::mafK mutant mice. *EMBO J* **19**: 1335-45.
- Ooi SK, Qiu C, Bernstein E, Li K, Jia D, Yang Z, Erdjument-Bromage H, Tempst P, Lin SP, Allis CD et al. 2007. DNMT3L connects unmethylated lysine 4 of histone H3 to de novo methylation of DNA. *Nature* **448**: 714-7.
- Pahl HL. 1999. Activators and target genes of Rel/NF-kappaB transcription factors. *Oncogene* **18**: 6853-66.
- Pandiyani P, Zheng L, Ishihara S, Reed J, Lenardo MJ. 2007. CD4<sup>+</sup>CD25<sup>+</sup>Foxp3<sup>+</sup> regulatory T cells induce cytokine deprivation-mediated apoptosis of effector CD4<sup>+</sup> T cells. *Nat Immunol* **8**: 1353-62.
- Pauley KM, Satoh M, Chan AL, Bubb MR, Reeves WH, Chan EK. 2008. Upregulated miR-146a expression in peripheral blood mononuclear cells from rheumatoid arthritis patients. *Arthritis Res Ther* **10**: R101.
- Principe DR, Doll JA, Bauer J, Jung B, Munshi HG, Bartholin L, Pasche B, Lee C, Grippo PJ. 2014. TGF-beta: duality of function between tumor prevention and carcinogenesis. *J Natl Cancer Inst* **106**: djt369.

- Prots I, Skapenko A, Lipsky PE, Schulze-Koops H. 2011. Analysis of the transcriptional program of developing induced regulatory T cells. *PLoS One* **6**: e16913.
- Puccetti P, Grohmann U. 2007. IDO and regulatory T cells: a role for reverse signalling and non-canonical NF-kappaB activation. *Nat Rev Immunol* **7**: 817-23.
- Quandt K, Frech K, Karas H, Wingender E, Werner T. 1995. MatInd and MatInspector: new fast and versatile tools for detection of consensus matches in nucleotide sequence data. *Nucleic Acids Res* **23**: 4878-84.
- Read S, Malmstrom V, Powrie F. 2000. Cytotoxic T lymphocyte-associated antigen 4 plays an essential role in the function of CD25(+)CD4(+) regulatory cells that control intestinal inflammation. *J Exp Med* **192**: 295-302.
- Richardson B, Scheinbart L, Strahler J, Gross L, Hanash S, Johnson M. 1990. Evidence for impaired T cell DNA methylation in systemic lupus erythematosus and rheumatoid arthritis. *Arthritis Rheum* **33**: 1665-73.
- Roeder RG. 2005. Transcriptional regulation and the role of diverse coactivators in animal cells. *FEBS Lett* **579**: 909-15.
- Rosenberg SA, Lipsky PE. 1979. Monocyte dependence of pokeweed mitogen-induced differentiation of immunoglobulin-secreting cells from human peripheral blood mononuclear cells. *J Immunol* **122**: 926-31.
- Roubin R, Pizette S, Ollendorff V, Planche J, Birnbaum D, Delapeyriere O. 1996. Structure and developmental expression of mouse Garp, a gene encoding a new leucine-rich repeat-containing protein. *Int J Dev Biol* **40**: 545-55.
- Rubtsov YP, Rasmussen JP, Chi EY, Fontenot J, Castelli L, Ye X, Treuting P, Siewe L, Roers A, Henderson WR, Jr. et al. 2008. Regulatory T cell-derived interleukin-10 limits inflammation at environmental interfaces. *Immunity* **28**: 546-58.
- Ruthenburg AJ, Allis CD, Wysocka J. 2007. Methylation of lysine 4 on histone H3: intricacy of writing and reading a single epigenetic mark. *Mol Cell* **25**: 15-30.
- Sakaguchi S, Fukuma K, Kuribayashi K, Masuda T. 1985. Organ-specific autoimmune diseases induced in mice by elimination of T cell subset. I. Evidence for the active participation of T cells in natural self-tolerance; deficit of a T cell subset as a possible cause of autoimmune disease. *J Exp Med* **161**: 72-87.
- Sarkar S, Fox DA. 2007. Regulatory T cell defects in rheumatoid arthritis. *Arthritis Rheum* **56**: 710-3.
- Schellekens GA, de Jong BA, van den Hoogen FH, van de Putte LB, van Venrooij WJ. 1998. Citrulline is an essential constituent of antigenic determinants recognized by rheumatoid arthritis-specific autoantibodies. *J Clin Invest* **101**: 273-81.

- Schmidl C, Klug M, Boeld TJ, Andreesen R, Hoffmann P, Edinger M, Rehli M. 2009. Lineage-specific DNA methylation in T cells correlates with histone methylation and enhancer activity. *Genome Res* **19**: 1165-74.
- Schmidt SV, Nino-Castro AC, Schultze JL. 2012. Regulatory dendritic cells: there is more than just immune activation. *Front Immunol* **3**: 274.
- Schmitz ML, Bacher S, Dienz O. 2003. NF-kappaB activation pathways induced by T cell costimulation. *FASEB J* **17**: 2187-93.
- Schuler PJ, Harasymczuk M, Schilling B, Saze Z, Strauss L, Lang S, Johnson JT, Whiteside TL. 2013. Effects of adjuvant chemoradiotherapy on the frequency and function of regulatory T cells in patients with head and neck cancer. *Clin Cancer Res* **19**: 6585-96.
- Schuler PJ, Schilling B, Harasymczuk M, Hoffmann TK, Johnson J, Lang S, Whiteside TL. 2012. Phenotypic and functional characteristics of CD4+ CD39+ FOXP3+ and CD4+ CD39+ FOXP3neg T-cell subsets in cancer patients. *Eur J Immunol* **42**: 1876-85.
- Sebbag M, Simon M, Vincent C, Masson-Bessiere C, Girbal E, Durieux JJ, Serre G. 1995. The antiperinuclear factor and the so-called antikeratin antibodies are the same rheumatoid arthritis-specific autoantibodies. *J Clin Invest* **95**: 2672-9.
- Shavit JA, Motohashi H, Onodera K, Akasaka J, Yamamoto M, Engel JD. 1998. Impaired megakaryopoiesis and behavioral defects in mafG-null mutant mice. *Genes Dev* **12**: 2164-74.
- Shaw JP, Utz PJ, Durand DB, Toole JJ, Emmel EA, Crabtree GR. 1988. Identification of a putative regulator of early T cell activation genes. *Science* **241**: 202-5.
- Shin HM, Kim MH, Kim BH, Jung SH, Kim YS, Park HJ, Hong JT, Min KR, Kim Y. 2004. Inhibitory action of novel aromatic diamine compound on lipopolysaccharide-induced nuclear translocation of NF-kappaB without affecting IkappaB degradation. *FEBS Lett* **571**: 50-4.
- Smigielska-Czepiel K, van den Berg A, Jellema P, van der Lei RJ, Bijzet J, Kluiver J, Boots AM, Brouwer E, Kroesen BJ. 2014. Comprehensive analysis of miRNA expression in T-cell subsets of rheumatoid arthritis patients reveals defined signatures of naive and memory Tregs. *Genes Immun* **15**: 115-25.
- Smolen JS, Aletaha D, Koeller M, Weisman MH, Emery P. 2007. New therapies for treatment of rheumatoid arthritis. *Lancet* **370**: 1861-74.
- Snir O, Widhe M, Hermansson M, von Spee C, Lindberg J, Hensen S, Lundberg K, Engstrom A, Venables PJ, Toes RE et al. 2010. Antibodies to several citrullinated antigens are enriched in the joints of rheumatoid arthritis patients. *Arthritis Rheum* **62**: 44-52.
- Stockis J, Colau D, Coulie PG, Lucas S. 2009a. Membrane protein GARP is a receptor for latent TGF-beta on the surface of activated human Treg. *Eur J Immunol* **39**: 3315-22.

- Stockis J, Fink W, Francois V, Connerotte T, de Smet C, Knoop L, van der Bruggen P, Boon T, Coulie PG, Lucas S. 2009b. Comparison of stable human Treg and Th clones by transcriptional profiling. *Eur J Immunol* **39**: 869-82.
- Strauss L, Bergmann C, Szczepanski M, Gooding W, Johnson JT, Whiteside TL. 2007. A unique subset of CD4<sup>+</sup>CD25<sup>high</sup>Foxp3<sup>+</sup> T cells secreting interleukin-10 and transforming growth factor-beta1 mediates suppression in the tumor microenvironment. *Clin Cancer Res* **13**: 4345-54.
- Taganov KD, Boldin MP, Chang KJ, Baltimore D. 2006. NF-kappaB-dependent induction of microRNA miR-146, an inhibitor targeted to signaling proteins of innate immune responses. *Proc Natl Acad Sci U S A* **103**: 12481-6.
- Takahashi T, Tagami T, Yamazaki S, Uede T, Shimizu J, Sakaguchi N, Mak TW, Sakaguchi S. 2000. Immunologic self-tolerance maintained by CD25(+)CD4(+) regulatory T cells constitutively expressing cytotoxic T lymphocyte-associated antigen 4. *J Exp Med* **192**: 303-10.
- Tang Y, Luo X, Cui H, Ni X, Yuan M, Guo Y, Huang X, Zhou H, de Vries N, Tak PP et al. 2009. MicroRNA-146A contributes to abnormal activation of the type I interferon pathway in human lupus by targeting the key signaling proteins. *Arthritis Rheum* **60**: 1065-75.
- Thaker YR, Schneider H, Rudd CE. 2015. TCR and CD28 activate the transcription factor NF-kappaB in T-cells via distinct adaptor signaling complexes. *Immunol Lett* **163**: 113-9.
- Tiemessen MM, Jagger AL, Evans HG, van Herwijnen MJ, John S, Taams LS. 2007. CD4<sup>+</sup>CD25<sup>+</sup>Foxp3<sup>+</sup> regulatory T cells induce alternative activation of human monocytes/macrophages. *Proc Natl Acad Sci U S A* **104**: 19446-51.
- Tivol EA, Borriello F, Schweitzer AN, Lynch WP, Bluestone JA, Sharpe AH. 1995. Loss of CTLA-4 leads to massive lymphoproliferation and fatal multiorgan tissue destruction, revealing a critical negative regulatory role of CTLA-4. *Immunity* **3**: 541-7.
- Tone Y, Furuuchi K, Kojima Y, Tykocinski ML, Greene MI, Tone M. 2008. Smad3 and NFAT cooperate to induce Foxp3 expression through its enhancer. *Nat Immunol* **9**: 194-202.
- Tran DQ, Andersson J, Wang R, Ramsey H, Unutmaz D, Shevach EM. 2009. GARP (LRRC32) is essential for the surface expression of latent TGF-beta on platelets and activated FOXP3<sup>+</sup> regulatory T cells. *Proc Natl Acad Sci U S A* **106**: 13445-50.
- Valencia X, Stephens G, Goldbach-Mansky R, Wilson M, Shevach EM, Lipsky PE. 2006. TNF downmodulates the function of human CD4<sup>+</sup>CD25<sup>hi</sup> T-regulatory cells. *Blood* **108**: 253-61.
- van Riel PL. 2014. The development of the disease activity score (DAS) and the disease activity score using 28 joint counts (DAS28). *Clin Exp Rheumatol* **32**: S-65-74.
- Vignali DA, Collison LW, Workman CJ. 2008. How regulatory T cells work. *Nat Rev Immunol* **8**: 523-32.

- Volpe E, Touzot M, Servant N, Marloie-Provost MA, Hupe P, Barillot E, Soumelis V. 2009. Multiparametric analysis of cytokine-driven human Th17 differentiation reveals a differential regulation of IL-17 and IL-22 production. *Blood* **114**: 3610-4.
- Wang R, Kozhaya L, Mercer F, Khaitan A, Fujii H, Unutmaz D. 2009. Expression of GARP selectively identifies activated human FOXP3+ regulatory T cells. *Proc Natl Acad Sci U S A* **106**: 13439-44.
- Wang R, Zhu J, Dong X, Shi M, Lu C, Springer TA. 2012a. GARP regulates the bioavailability and activation of TGFbeta. *Mol Biol Cell* **23**: 1129-39.
- Wang X, Zhu K, Li S, Liao Y, Du R, Zhang X, Shu HB, Guo AY, Li L, Wu M. 2012b. MLL1, a H3K4 methyltransferase, regulates the TNFalpha-stimulated activation of genes downstream of NF-kappaB. *J Cell Sci* **125**: 4058-66.
- Wei B, Baker S, Wieckiewicz J, Wood KJ. 2010. IFN-gamma triggered STAT1-PKB/AKT signalling pathway influences the function of alloantigen reactive regulatory T cells. *Am J Transplant* **10**: 69-80.
- Wei G, Wei L, Zhu J, Zang C, Hu-Li J, Yao Z, Cui K, Kanno Y, Roh TY, Watford WT et al. 2009. Global mapping of H3K4me3 and H3K27me3 reveals specificity and plasticity in lineage fate determination of differentiating CD4+ T cells. *Immunity* **30**: 155-67.
- Wei L, Laurence A, Elias KM, O'Shea JJ. 2007. IL-21 is produced by Th17 cells and drives IL-17 production in a STAT3-dependent manner. *J Biol Chem* **282**: 34605-10.
- Wilson NJ, Boniface K, Chan JR, McKenzie BS, Blumenschein WM, Mattson JD, Basham B, Smith K, Chen T, Morel F et al. 2007. Development, cytokine profile and function of human interleukin 17-producing helper T cells. *Nat Immunol* **8**: 950-7.
- Winer S, Chan Y, Paltser G, Truong D, Tsui H, Bahrami J, Dorfman R, Wang Y, Zielenski J, Mastronardi F et al. 2009. Normalization of obesity-associated insulin resistance through immunotherapy. *Nat Med* **15**: 921-9.
- Wing K, Onishi Y, Prieto-Martin P, Yamaguchi T, Miyara M, Fehervari Z, Nomura T, Sakaguchi S. 2008. CTLA-4 control over Foxp3+ regulatory T cell function. *Science* **322**: 271-5.
- Wu Y, Borde M, Heissmeyer V, Feuerer M, Lapan AD, Stroud JC, Bates DL, Guo L, Han A, Ziegler SF et al. 2006. FOXP3 controls regulatory T cell function through cooperation with NFAT. *Cell* **126**: 375-87.
- Yamane K, Tateishi K, Klose RJ, Fang J, Fabrizio LA, Erdjument-Bromage H, Taylor-Papadimitriou J, Tempst P, Zhang Y. 2007. PLU-1 is an H3K4 demethylase involved in transcriptional repression and breast cancer cell proliferation. *Mol Cell* **25**: 801-12.
- Yan Y, Phan L, Yang F, Talpaz M, Yang Y, Xiong Z, Ng B, Timchenko NA, Wu CJ, Ritz J et al. 2004. A novel mechanism of alternative promoter and splicing regulates the epitope generation of tumor antigen CML66-L. *J Immunol* **172**: 651-60.

- Yang L, Anderson DE, Baecher-Allan C, Hastings WD, Bettelli E, Oukka M, Kuchroo VK, Hafler DA. 2008. IL-21 and TGF-beta are required for differentiation of human T(H)17 cells. *Nature* **454**: 350-2.
- Yang M, Ye L, Wang B, Gao J, Liu R, Hong J, Wang W, Gu W, Ning G. 2015. Decreased miR-146 expression in peripheral blood mononuclear cells is correlated with ongoing islet autoimmunity in type 1 diabetes patients 1miR-146. *J Diabetes* **7**: 158-65.
- Ye X, Li Y, Huang Q, Yu Y, Yuan H, Wang P, Wan D, Gu J, Huo K, Li YY et al. 2006. The novel human gene MIP functions as a co-activator of hMafF. *Arch Biochem Biophys* **449**: 87-93.
- Yocum DE, Furst DE, Kaine JL, Baldassare AR, Stevenson JT, Borton MA, Mengle-Gaw LJ, Schwartz BD, Wisemandle W, Mekki QA. 2003. Efficacy and safety of tacrolimus in patients with rheumatoid arthritis: a double-blind trial. *Arthritis Rheum* **48**: 3328-37.
- Yoshimura A, Mori H, Ohishi M, Aki D, Hanada T. 2003. Negative regulation of cytokine signaling influences inflammation. *Curr Opin Immunol* **15**: 704-8.
- Zhang X, Wu M, Xiao H, Lee MT, Levin L, Leung YK, Ho SM. 2010. Methylation of a single intronic CpG mediates expression silencing of the PMP24 gene in prostate cancer. *Prostate* **70**: 765-76.
- Zhang X, Zhou L, Fu G, Sun F, Shi J, Wei J, Lu C, Zhou C, Yuan Q, Yang M. 2014. The identification of an ESCC susceptibility SNP rs920778 that regulates the expression of lncRNA HOTAIR via a novel intronic enhancer. *Carcinogenesis* **35**: 2062-7.
- Zhang Y, Maksimovic J, Naselli G, Qian J, Chopin M, Blewitt ME, Oshlack A, Harrison LC. 2013. Genome-wide DNA methylation analysis identifies hypomethylated genes regulated by FOXP3 in human regulatory T cells. *Blood* **122**: 2823-36.
- Zhao X, Su J, Wang F, Liu D, Ding J, Yang Y, Conaway JW, Conaway RC, Cao L, Wu D et al. 2013. Crosstalk between NSL histone acetyltransferase and MLL/SET complexes: NSL complex functions in promoting histone H3K4 di-methylation activity by MLL/SET complexes. *PLoS Genet* **9**: e1003940.
- Zheng Y, Josefowicz SZ, Kas A, Chu TT, Gavin MA, Rudensky AY. 2007. Genome-wide analysis of Foxp3 target genes in developing and mature regulatory T cells. *Nature* **445**: 936-40.
- Zhou AX, Kozhaya L, Fujii H, Unutmaz D. 2013a. GARP-TGF-beta complexes negatively regulate regulatory T cell development and maintenance of peripheral CD4+ T cells in vivo. *J Immunol* **190**: 5057-64.
- Zhou Q, Haupt S, Kreuzer JT, Hammitzsch A, Proft F, Neumann C, Leipe J, Witt M, Schulze-Koops H, Skapenko A. 2015. Decreased expression of miR-146a and miR-155 contributes to an abnormal Treg phenotype in patients with rheumatoid arthritis. *Ann Rheum Dis* **74**: 1265-74.

---

Zhou Q, Haupt S, Prots I, Thummler K, Kremmer E, Lipsky PE, Schulze-Koops H, Skapenko A. 2013b. miR-142-3p is involved in CD25+ CD4 T cell proliferation by targeting the expression of glycoprotein A repetitions predominant. *J Immunol* **190**: 6579-88.

Zhou X, Jeker LT, Fife BT, Zhu S, Anderson MS, McManus MT, Bluestone JA. 2008. Selective miRNA disruption in T reg cells leads to uncontrolled autoimmunity. *J Exp Med* **205**: 1983-91.

Zhu J, Guo L, Watson CJ, Hu-Li J, Paul WE. 2001. Stat6 is necessary and sufficient for IL-4's role in Th2 differentiation and cell expansion. *J Immunol* **166**: 7276-81.

Zhu J, Yamane H, Paul WE. 2010. Differentiation of effector CD4 T cell populations. *Annu Rev Immunol* **28**: 445-89.

## ACKNOWLEDGEMENTS

PD Dr. Alla Skapenko danke ich für die Vergabe des interessanten Promotionsthemas, die finanzielle Unterstützung und die Möglichkeit im Forschungslabor der Rheumaeinheit am Klinikum der LMU München meine Arbeit durchführen zu können. Außerdem möchte ich mich für die gute Zusammenarbeit und die Hilfe in allen Belangen bedanken. Die Diskussionen während der Lab Meetings, während des Schreibens der Veröffentlichungen und dieser Doktorarbeit waren immer sehr hilfreich. Auch hat sie mich immer bei der Planung, Durchführung und Auswertung meiner Daten unterstützt. Zudem war sie eine große Hilfe bei der Ausarbeitung der Patientendaten. Ich möchte mich außerdem für das Korrekturlesen und die Unterstützung bei der Ausarbeitung dieser Doktorarbeit bedanken. Herzlichen Dank für die unermüdliche Hilfe bei den weiteren Schritten meines wissenschaftlichen Lebensweges.

Auch Prof. Dr. Schulze-Koops danke ich herzlich für die Vergabe des Promotionsthemas, die Ermöglichung der Arbeit durch die finanzielle Unterstützung und die Arbeit im Forschungslabor der Rheumaeinheit. Ich möchte mich auch für die hilfreichen Diskussionen während der Lab Meetings bedanken. Außerdem wäre es ohne seine ständige Unterstützung zur Rekrutierung der RA-Patienten nicht möglich gewesen, so viele Daten so schnell zusammen zu tragen. Des Weiteren danke ich auch ihm für die Bereitschaft meine Referenzperson zu sein und die Hilfe und schnelle Unterstützung bei den weiteren Schritten meiner wissenschaftlichen Laufbahn.

Ich möchte allen aktuellen und ehemaligen Mitgliedern der Rheumaeinheit für die kollegiale Atmosphäre danken. Insbesondere danke ich Viktoria Söntgerath für die tolle Zusammenarbeit und Unterstützung im Rahmen ihrer Doktorarbeit und die gemeinsame Veröffentlichung. Ich habe die netten Diskussionen und Anregungen mit ihr immer sehr geschätzt. Fausto Pirronello und Lena Vockentanz möchte ich außerdem für die schönen Momente außerhalb der Arbeit danken, in denen ich viel und oft gelacht habe. Herzlichen Dank auch an alle, die jederzeit für mich Blut abgenommen haben. Mein Dank gilt ebenso Wenke Barkey, die mir bei der Durchführung sehr vieler SNP-PCRs geholfen hat. Des Weiteren gilt mein Dank Dr. Qihui Zhou und Johannes Kreuzer für die ergebnisreiche Zusammenarbeit an verschiedenen Veröffentlichungen und die Unterstützung dieser Arbeit. Ich möchte mich herzlich bei Dr. Iryna Prots für die Unterstützung, Zusammenarbeit und Einführung ins Labor bedanken. Außerdem

möchte ich den ärztlichen Mitarbeitern der Rheumaeinheit herzlich für die gute Zusammenarbeit und die Rekrutierung der RA-Patienten danken.

Besonders möchte ich zudem Christine Schnabel erwähnen, die mich nicht nur im Labor unterstützt hat, sondern auch viele, gemeinsame Stunden mit mir verbracht hat. Ohne sie wäre so manche Lebensphase sehr einsam und schwer geworden.

Ich möchte außerdem meinen lieben Freunden danken, die mich während der Zeit in München immer tatkräftig unterstützt haben. Ich bedanke mich für die Ausdauer, Ruhe und Geduld mit der sie mir immer zur Seite standen und mich immer wieder aufgemuntert haben. Großen Dank geht an Claudia Roskopf und Saskia Graf, die nicht nur regelmäßig Blut für mich gespendet haben, sondern auch immer ein offenes Ohr für mich hatten. Zudem möchte ich besonders Elke Prade für die schnelle Hilfe beim Korrekturlesen danken.

Ein besonderes Dankeschön geht an meinen lieben Freund, Ludwig Prade. Danke für die Geduld, die lieben aufbauenden Worte und das gute Essen während des Schreibens. Vielen Dank für die tolle und tatkräftige Unterstützung meines weiteren Lebensweges.

Das Beste kommt immer zum Schluss: ich möchte meinen Eltern, Charlotte und Günter Haupt, ganz herzlich danken, dass sie mich immer begleitet haben, auch wenn es mal schwere Phasen gab. Sie haben immer an mich geglaubt und haben erheblich zur Vollendung dieser Arbeit beigetragen. Dank gilt auch meiner Schwester, Claudia Stich, sowie Georg und Franziska Stich, für die netten Stunden, die wir in den letzten Jahren miteinander verbringen durften. Ich hoffe, es werden noch viele weitere folgen.